Studies on functional bio-based polymers from aromatic amine derivatives

KAI KAN

Japan Advanced Institute of Science and Technology

Studies on functional bio-based polymers from aromatic amine derivatives

by

KAI KAN

Submitted to

Japan Advanced Institute of Science and Technology

In partial fulfillment of the requirements

For the degree of

Doctor of Philosophy

Supervisor: Associate Professor Tatsuo Kaneko

School of Materials Science

Japan Advanced Institute of Science and technology

March 2014

CONTENTS

CHAPTER 3

Syntheses of thermotropic liquid crystalline copolyesters derived from wholly aromatic amino acids and their polarized photoluminescence

CHAPTER 4

Syntheses of novel polybenzobisoxazoles from symmetric π-conjugated azine compounds

Chapter 1

General Introduction

CHAPTER 1

1.1 Green chemistry

In 20th century, the world's food supply has met an explosive expansion because of the development of chemicals that protect crops and enhance growth. In virtually every arena and every aspect of material life – transportation, communication, clothing, shelter, etc.- chemistry has resulted in an improvement, not merely in the trappings of life, but also in the quality of the lives of the billions of individuals who now inhabit the planet [1]. However, in another aspects, these almost unbelievable achievements have come at a price, the tool that the manufacture, use, and disposal of synthetic chemicals have taken on human health and the environment. To solve this problem, the new concept of chemistry, *Green chemistry*, was born.

Green chemistry is defined as environmentally benign chemical synthesis, alternative synthetic pathways for pollution prevention, benign by design: these phrases all essentially describe the same concept. Green chemistry is the utilization of a set of principles that reduces or eliminates the use or generation of hazardous substances in the design, manufacture and application of chemical products [1]. From this concept, there is an interest and almost a grand challenge for chemists to develop new products, processes, and services that achieve the necessary social, economical, and environmental objectives [2]. Furthermore, green chemistry and green engineering should bring about changes in the hazard of a product at the most fundamental level, that is, the molecular level [3] and have the power to impact on the entire life cycle of a product or process [4], and make it more environmentally safe and sustainable society [5].

1.2 Environmentally friendly plastics

Plastics are widely used, economical materials characterized by excellent all–round properties, easy molding and manufacturing. The main parts of plastics are coming from petroleum-based polyolefins. These conventional plastics such as polyethylene, polypropylene, polystyrene, poly(vinyl chloride) and poly(ethylene terephthalate) were very stable, and not readily degraded in the ambient environment. As a result, environmental pollution from synthetic plastics has been recognized as a large problem. For example, statistics published by the United States Environmental Protection Agency in 2011 indicated that, before recycling, approximately 250 million tons of municipal solid waste was generated in the United States in that year, of which 12.7% was composed of plastics [6]. This amount will be increasing year by year than the previous report in 2003 [7]. Secondly, disposal non-degradable plastic bags adversely affect sea-life and wild animals. It is widely accepted that the use of long-lasting polymers in products with a short life-span, such as engineering applications, packaging, catering, surgery, and hygiene, is not adequate. Moreover, incineration of plastic waste presents environmental issues as well since it yields toxic emissions (e.g., dioxin), and carbon dioxide effects global warming. Material incineration is also limited due to the difficulties to find accurate and economically viable outlets [8]. In this meaning, built for the long haul, these polymers seem inappropriate for applications in which plastics are used for short time periods and then disposed [9]. Unexpectedly in the near future, however, oil peak will come to our society, and then the research and development of the oil substitution which involved with the plastic development is urgently required.

The good answer to solve these problems is plastics having high degree of degradability in nature. This kind of plastic is called at bio-degradable plastics. Biodegradable plastics are seen by many as a promising solution to this problem because they are environmentally-friendly.

Environmentally-friendly polymers originating from renewable starting materials and recyclable by biodegradation are significant with respect to "carbon minus" which is a next-generation concept of carbon neutral where the carbon concentration in the earth atmosphere is kept constant.

However the author claims that the already warmed earth must be cooled by reducing the carbon dioxide concentration. Here one possible method is proposed; 1) the use of the resources from the biomass containing the carbons immobilized as a result of the photosynthesis, 2) the development of high-performance materials such as aromatic polymers which can be used as a high-performance and functional plastics for a long term, and 3) the recycling of materials by a microbe converting into the original resources. By this method, the immobilized carbons will be cycled in the material systems, differently from biofuel easily throwing back carbons into the atmosphere (Figure 1-1).

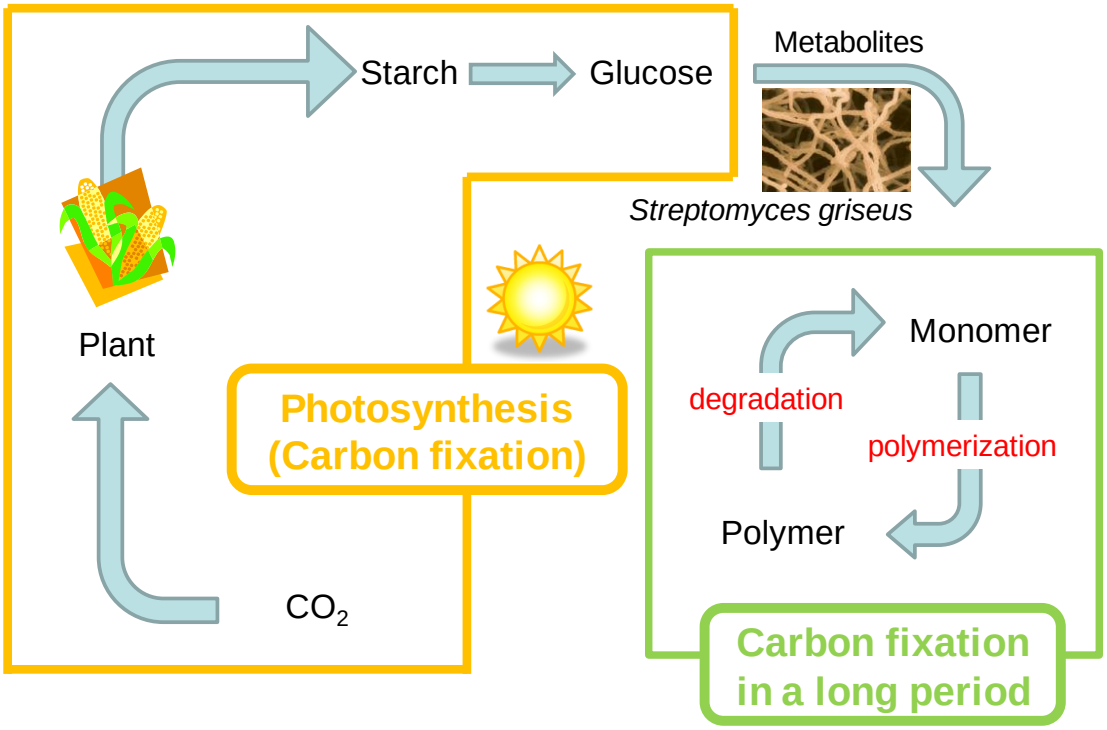

Figure 1-1. The concept of carbon minus system.

For instance, polyhydroxyalkanoates (PHA) and lactic acid, raw materials for poly(lactic acid) (PLA), can be produced by fermentative biotechnological processes using agricultural products and microorganisms [10-12]. Biodegradable plastics offer a lot of advantages such as increased soil fertility, low accumulation of bulky plastic materials in the environment (which invariably will minimize injuries to wild animals), and reduction in the cost of waste management. Furthermore, biodegradable plastics can be recycled to useful metabolites (monomers and oligomers) by microorganisms and enzymes.

However some aliphatic bio-based polyesters, such as poly(hydroxyalkanoate)s [13], poly(butylenes succinate) [14], and so on [15], did not show performances high enough for application in the engineering plastic field. Improvements in durability and performance have been shown by Ecoflex^{TM} (Figure 1-2) [16] and Biomax^{TM} (Figure 1-3) [17], but the environmental toxicity and availability of terephthalic acid are problematic. Poly (lactic acid)s (PLAs) have been remarkably well developed because of their high mechanical strength [18]. However, it was estimated that these polyesters will only replace a small percentage of the non-degradable plastics currently in use, due to their poor level of thermoresistance. As a result, high-performance environmentally friendly polymers originating from and degradable into natural molecules are urgently required to improve human life. Generally, the introduction of an aromatic component into the thermoplastic polymer backbone is an efficient method to intrinsically improve the material performance, because the backbone has strong rigid component and strong interchain interaction. In this meaning, many non-degradable engineering plastics have rigid conjugated rings, such as benzene, benzoxazole, benzimidazole, benzothiazole [19]. For example, poly(*p*-phenylene-2,6-benzobisoxazole) exhibited ultrahigh strength/high modulus properties because they had a rigid-rod structure to exhibit liquid crystal phase [20]. The polymer is able to obtain from 3-amino-4-hydroxybenzoic acid (3,4-AHBA) derived from microorganism

Streptomyces griseus as a precursor for several secondary metabolites [21-24]. 3,4-AHBA is a renewable, functional benzene derivative with three substitutents of amino, carboxyl, and hydroxyl groups. In this research the author prepared a couple of environmentally friendly, functional polymers using a bioderived resource 3,4-AHBA in order to contribute the establishment of carbon-minus society.

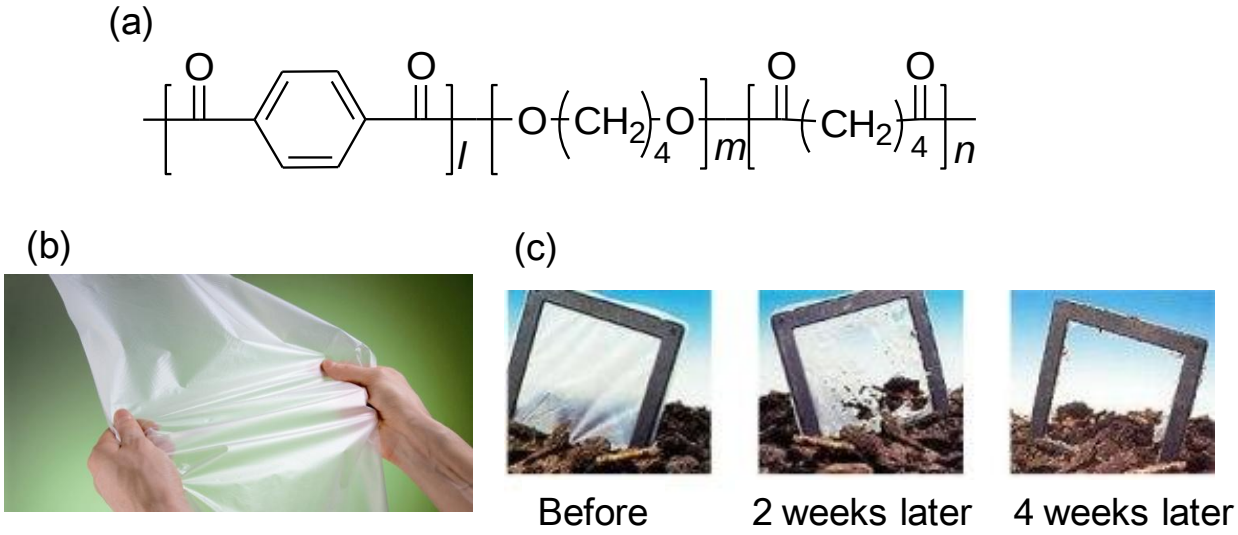

Figure 1-2. Ecoflex® is BASF corporation's product completely biodegradable and compostable plastic. It is ideal for trash bags or disposable packaging as it decomposes in compost within a few weeks or in soil without leaving any residues. (a) The structure of Ecoflex®. Generally, it contained terephthalic acid, 1,4-butanediol, adipic acid to get Aliphatic-Aromatic random copolymer. (b) The picture of Ecoflex®, and (c) The bio-degradation test of Ecoflex® film in soil at 55 ^{o}C compost. After 4 weeks, almost all Ecoflex® film decomposed by nature.

The pictures were cited by http://www.japan.basf.com/apex/Japan/Japan/ja/content/BASF-Japan/1.2_Products_and_Industries/1.2.2_Plastics-JPN/1.2.2.2_Bioplastics.

(a)

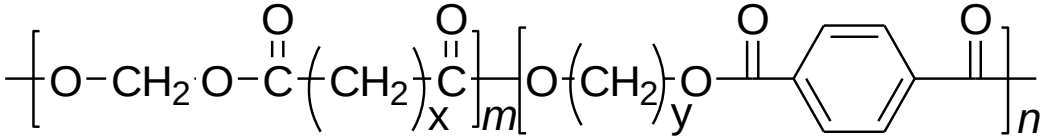

x = 2, y = 4: poly (butylene succinate/terephthalate): PBST
x = y = 4: poly(butylene adipate/terephthalate):PBAT
x = 4, y = 2: poly(ethylene adipate/terephthalate):PEAT

(b)

Figure 1-3. Biomax® is Dupont corporation's product biodegradable and compostable plastic. (a) The structure of Biomax®. Generally, poly(buthylene succinate) could separate three copolymers, in x = 2, y = 4 case, it formed poly(buthylene succinate/terephthalate), x = y = 4 case, it formed poly(butylenes adipate/terephthalate), x = 4, y = 2, it formed poly(ehylenee adipate/terephthalate). (b) The bio-degradation test of Biomax® product in soil. After 27 weeks, some parts of Biomax® product decomposed by nature.

The pictures and information were cited by http://takahara.ifoc.kyushu-u.ac.jp/%E8%AC%9B%E7%BE%A9%E8%B3%87%E6%96%99/%E3%82%B0%E3%83%AA%E3%83%BC%E3%83%B3%E3%82%B1%E3%83%9F%E3%82%B9%E3%83%88%E3%83%AA%E3%83%BC/GCH18.pdf.

1.3 Molecular design of bio-based monomers

1.3.1 Wholly aromatic amino acids

A combination of gene disruption and identification of compounds accumulated in disruptants showed that 3-amino-4-hydroxy benzoic acid (3,4-AHBA) is an intermediate of grixazone. The shikimate pathway, including seven enzymatic steps for production of chorismate via shikimate from phosphoenolpyruvate and erythrose-4-phosphate, is common in various organisms for the biosynthesis not only of aromatic amino acids but also of most biogenic benzene derivatives.

However, 3,4-AHBA turned out to be a benzene derivative that is biosynthesized by a novel, simple enzyme system [21-24]. Two genes, *griI* and *griH*, were found to be responsible for the biosynthesis of 3,4-AHBA; the two genes confer the *in vitro* production of 3,4-AHBA even on *Escherichia coli*. *In vitro* analysis showed that GriI catalyzes aldol condensation between two primary metabolites, L-aspartate-4-semialdehyde and dihydroxyacetone phosphate, to form a C_7 product, 2-amino-4,5-dihydroxy-6-one-heptanoic aicd-7-phosphate, which is subsequently converted to 3,4-AHBA by GriH. This pathway is independent of the shikimate pathway, representing a novel, simple enzyme system responsible for the synthesis of a benzene ring from the C_3 and C_4 primary metabolites. 3,4-AHBA appears to be reduced by the action of GriC and GriD in an ATP-dependent way to form 3,4-AHBAL [25-26].

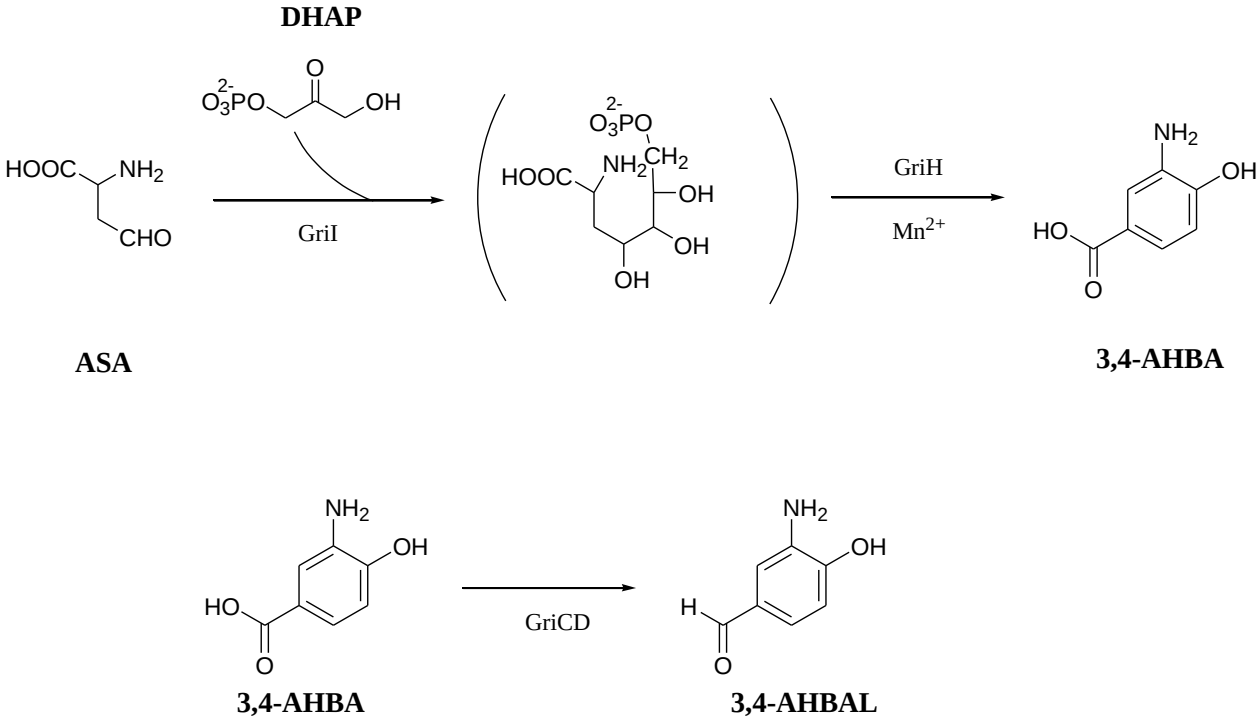

Figure 1-4. The biosynthetic pathway leading to the products, 3,4-AHBA and 3,4-AHBAL.

1.4 Outline of research

The main objective of this PhD study is to synthesize and characterize novel functionality bio-based polymers from 3,4-AHBA derivatives. This thesis included 5 chapters:

CHAPTER 2, "Synthesis of π-conjugated bio-based polymer from bio-aniline and its solvatochromism"

The author synthesized bio-based aniline, poly(3-amino-4-hydroxybenzoic acid) (poly(3,4-AHBA)), by electro-polymerization. The polymer has high solubility in common solvents, compared to polyaniline, due to the polar side groups such as carboxyl and hydroxyl. The

polymers showed various chromic behaviors based on the salvation and ionization of the side groups, and gave a flexible film with a conductivity as high as that of semiconductor.

CHAPTER 3, "Syntheses of thermotropic liquid crystalline copolymers derived from wholly aromatic amino acids and their polarized photoluminescence"

The author synthesized a novel thermotropic liquid crystalline polymers poly{3-benzylidene amino-4-hydroxybenzoic acid (3,4-BAHBA)-*co*-*trans*-4-hydroxycinnamic acid (4HCA: *trans*-coumaric acid)} (P(3,4-BAHBA-*co*-4HCA)), was synthesized by the thermal polycondensation of 4HCA and 3,4-BAHBA, which was synthesized by a reaction of 3,4-AHBA with benzaldehyde. When the 4HCA compositions of P(3,4-BAHBA-*co*-4HCA)s were above 55 mol%, the copolymers showed a nematic, liquid crystalline phase. DSC measurements of the copolymers showed a high glass transition temperature more than 100 °C, sufficient for use as engineering plastics. Furthermore, the copolymers showed photoluminescence in an *N*-methylpyrrolidone (NMP) solution under ultraviolet (UV) light with a wavelength of 365 nm. Oriented film of P(3,4-BAHBA-*co*-4HCA) with a 4HCA composition of 75 mol% emitted polarized light, which was confirmed by fluorescent spectroscopy equipped with parallel and crossed polarizers. Oriented films of the thermotropic liquid-crystalline (LC) polymer P(3,4-BAHBA-*co*-4HCA) with a 4HCA composition of 75 mol% were prepared by shearing the LC melt. X-ray analyses indicated that the main chains were oriented perpendicularly to the shear direction, and the rigid benzylidene amino side chains were parallely oriented. Furthermore, the oriented film showed polarized emission in which the analyzer rotation changed the fluorescent color when the polarizer was set perpendicular to the orientation direction.

CHAPTER 4, "Syntheses of novel polybenzobisoxazoles from symmetric π-conjugated azine compounds"

The author synthesized polybenzobisoxazole (PBO) from 3,4-AHBA derivatives. The preparation of new functional π-conjugated PBO precursors and PBOs was 3,4-AHBZL-TC PHA, 3,4-AHBZL-IC PHA, 3,4-AHBZL-FC PHA and 3,4-AHBZL-TC PBO, 3,4-AHBZL-IC PBO, 3,4-AHBZL-FC PBO from symmetric monomer, *N*,*N'*-Bis-(3-amino-4-hydroxy-benzylidene)-hydrazine (3,4-AHBZL). The new synthesis concept gave soluble PBO precursors having an imine and phenolic OH group. The FT-IR and TGA measurements revealed the conversion of the prePBO to PBO upon heating at 250 ^{o}C for 24h under vacuum in 3,4-AHBZL-IC PHA and 3,4-AHBZL-FC PHA and 300 ^{o}C for 24h under vacuum in 3,4-AHBZL-TC PHA. Especially 3,4-AHBZL-TC PBO film showed thermal resistivity of T_{10} 552 ^{o}C under nitrogen. Furthermore, 3,4-AHBZL-TC PBO, 3,4-AHBZL-IC PBO, and 3,4-AHBZL-FC PBO showed photoluminescence in a concentrated sulfuric acid under ultraviolet (UV) light with a wavelength of 365 nm.

The author synthesized and developed photofunctional, thermalstable polymers from bio monomer 3,4-AHBA.

CHAPTER 2

Synthesis of π-conjugated bio-based polymer from bio-aniline and its solvatochromism

CHAPTER 2

2.1 Introduction

High-functional bio-based polymers attract researchers' attention in the field of low-carbonization in materials development [27]. 3-Amino-4-hydroxybenzoic acid (3,4-AHBA), which is produced by a microorganism *Streptomyces griseus* as a precursor for several secondary metabolites [21-24], is a renewable, functional benzene derivative with three substitutents of amino, carboxyl, and hydroxyl groups. 3,4-AHBA is noteworthy in terms of not only the chemical structure but also possible mass-availability from *S. griseus* that has mass-produced a wide variety of materials such as antibiotics (streptomycin), parasiticides, herbicides, and pharmacologically active substances including antitumor agents and immunosuppressants [28]. Then a patent on the syntheses of polybenzoxazole from 3,4-AHBA extracted from *S. griseus* claimed the usefulness of its renewable resources for the bio-based polymer [29]. Here the author propose a new application of 3,4-AHBA as a functional aniline derivative with two acidic groups. Polyaniline (PANI) is a family of π-conjugated polymers that represents one of the oldest electroconductive synthetic materials [30-32]. The applications of the π-conjugated polymers are getting wider and wider in fields such as electrode materials [33,34], light emitting diodes [35], supercapacitors [36], biosensors [37], optical sensors [38,39], rechargeable batteries [40-43], microelectronics [44-46], optical displays [47,48], electrochromic devices [49], recordable optical disks [50], electrochemical actuator [51-54], antistatic coatings, and electromagnetic shielding materials [55,56].

However, PANI application is limited due to poor solubility and processability and intractable nature [57]. To overcome these problems, the author focused on PANI analogue poly(3,4-

AHBA) which is expected to show high solubility in polar solvents such as water due to its two polar groups, and might show conductivity and solvatochromism. Then 3,4-AHBA can be used in terms of not only a novel resource for soluble π-conjugated polymers but also a renewable monomer for high-functional bio-based polymers.

2.2 Experimental Section

2.2.1 Materials

3,4-AHBA (Kanto chemical, Co. Inc.) and HCl (Kanto chemical, Co. Inc.) were used as received. All other chemicals were used as procured.

2.2.2 Synthesis of poly(3,4-AHBA)

The synthetic method of poly(3,4-AHBA) is shown below. 3,4-AHBA 0.65 mmol (Kanto chemical, Co. Inc.) was stirred to dissolve in 1 M HCl (10 ml; Kanto chemical, Co. Inc.) at 30 ^{o}C (Figure 1). The reaction solution was soaked by two platinum plates, and carried out at a voltage of 1.5 V by using dc bench supply (KIKUSUI PMC 35-1). The author confirmed the electrodeposition of poly(3,4-AHBA) on anode platinum.

2.2.3 Structural analysis

Fourier transform infrared spectrum (FT-IR) of the 3,4-AHBA and its polymer were recorded on a Perkin-Elmer Spectrum One spectrometer using a diamond-attenuated total reflection (ATR) accessory.

2.2.4 Molecular weight measurement

The weight and number average molecular weight (M_w and M_n) of the polymer was analyzed by gel permeation chromatography (GPC) in *N*,*N*-dimethylformamide (DMF) at 40 ^oC using a Shodex GPC-101 system with two TSK gel columns KD-803 and KD-807 (pullulan standard; Shodex-P82).

2.2.5 Ultraviolet-visible (UV-vis) spectroscopy

UV-vis spectra of the polymer solutions were recorded by UV-vis spectroscopy (Perkin Elmer Lambda 25 UV/VIS Spectrometer). For the sample preparation of halochromic measurement, electrodeposited film was washed in distilled water, and dissolved using ultrasonic bath. However, a small amount of the insoluble substance appeared in this solution and was removed by filtration to obtain clear polymer solutions. The solutions of the polymer were first added to HCl aq of pH 2, and then the author adjusted pH by NaOH aq using a digital pH meter (HM-25R; DKK-TOA CORPORATION).

2.3 Results and discussion

2.3.1 Synthesis

The polymer synthesis of poly(3,4-AHBA) was carried out by the electro-polymerization method according to a similar procedure detailed in the preparation of PANI [58]. From this method, the author observed the dark green polymer film electrodeposited on anode platinum (Inset picture; Figure 2-1). In solubility test, poly(3,4-AHBA) had higher solubility in various solvents such as distilled water (D.W.), ethanol, acetone, DMF, dimethyl sulfoxide (DMSO) and *N*-methylpyrrolidone (NMP) (Table 2-1). When compared with PANI [59], it was soluble in only

DMF, DMSO, and NMP. Then the solubility studies indicated that hydroxyl and carboxyl groups in 3,4-AHBA units in the polymers imparted good solubility into the PANI backbone.

The average molecular weight of poly(3,4-AHBA) was measured in DMF by GPC. Poly(3,4-AHBA) showed high molecular weight such as M_w values of 11000 (M_w/M_n = ca. 1.0).

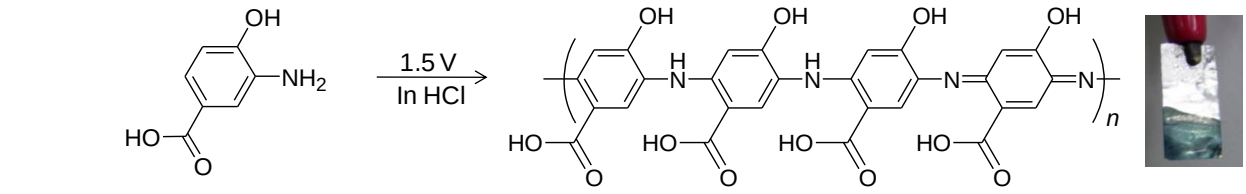

3-amino-4-hydroxybenzoic acid
(3,4-AHBA)

Poly(3-amino-4-hydroxybenzoic acid)
Poly(3,4-AHBA)

Figure 2-1. The electropolymerization scheme of 3,4-AHBA. The inset picture is the deposited film of poly(3,4-AHBA).

Table 2-1. Solubility of polymers with various compositions

3,4-AHBA/PANI (mol%)	D.W.	Ethanol	Acetone	DMSO	DMF	NMP
PANI	-	-	-	++	++	++
Poly(3,4-AHBA)	++	++	++	++	++	++

++: soluble, -: insoluble

D.W.: Distilled water, DMF: *N*,*N*-Dimethyl formamide, DMSO: Dimethyl sulfoxide,

NMP: *N*-methylpyrrolidone

The PANI is also used same polymerization condition as shown in poly(3,4-AHBA) above.

2.3.2 FT-IR spectrum

The FT-IR spectrum of the polymer is shown in Figure 2-2. The assignment was confirmed from the literature [60-62]. The characteristic peak of the stretching vibrations of C=C (quinoid rings) and C=C (benzenoid rings) are observed at 1598 cm^{-1} and 1550 cm^{-1}, respectively. In addition the band observed at 3018 $cm^{-1}$and 1696 cm^{-1} can be assigned to the O-H and C=O stretching vibrations.

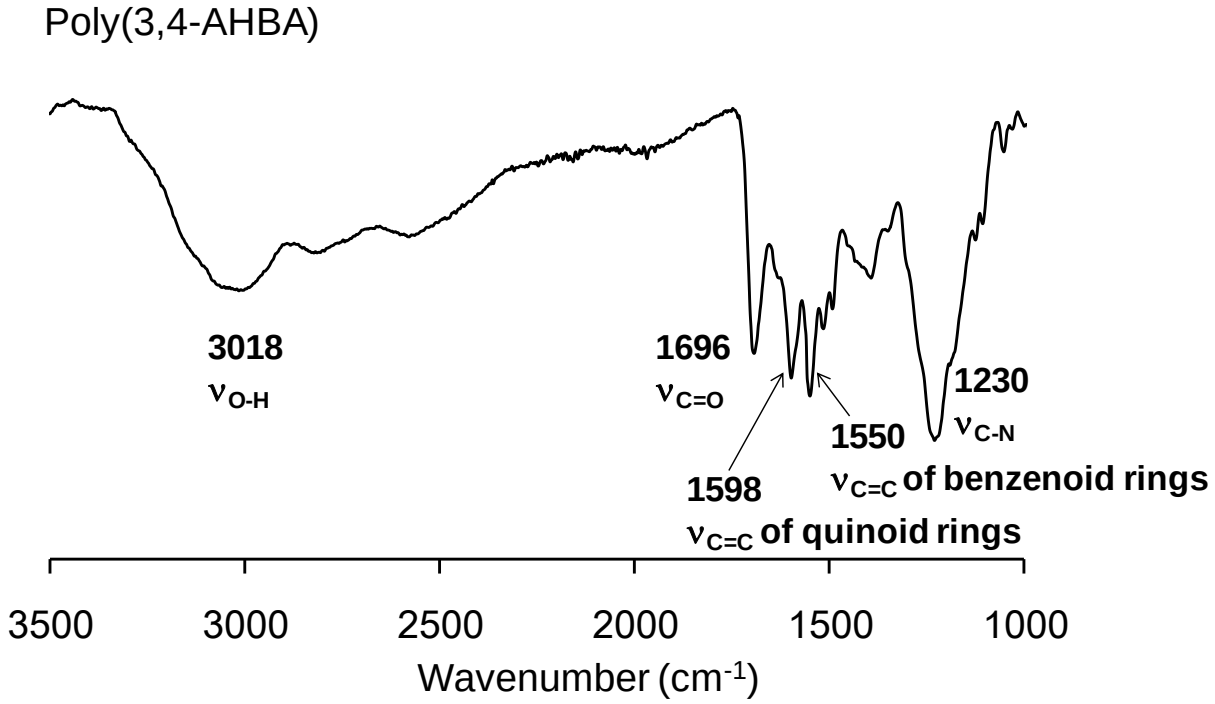

Figure 2-2. FT-IR spectrum of poly(3,4-AHBA).

2.3.3 Halochromism

Since poly(3,4-AHBA) was soluble in various polar solvents and has pH-responsive groups, the halochromic behavior of the poly(3,4-AHBA) was investigated. Poly(3,4-AHBA) solution showed a halochromic pattern different from that of PANI [63-65]. Poly(3,4-AHBA) solution showed brown in pH 3-6, but became almost black around pH 6-7 and gradually changed into dark brown in pH 7-12 (Figrue 2-3). Quinoid absorption appeared at 550 nm in UV-vis spectrum of poly(3,4-AHBA) in acidic solutions, which may indicate that the polaron structure was hardly formed in HCl function presumably due to the steric hindrance of side chains. However the spectrum remarkably changed at pH 7 and polaron band appeared (Figure 2-3b). The polaron peak was gradually broadened with increasing from pH 7 to pH 12. Then the author can consider the self-doping of the polymer by carboxylate anion occurred around pH 6-7 (Figure 2-3c). The self-doping phenomenon was also shown in another polyaniline having sulfonates in polaron band transitions [66].

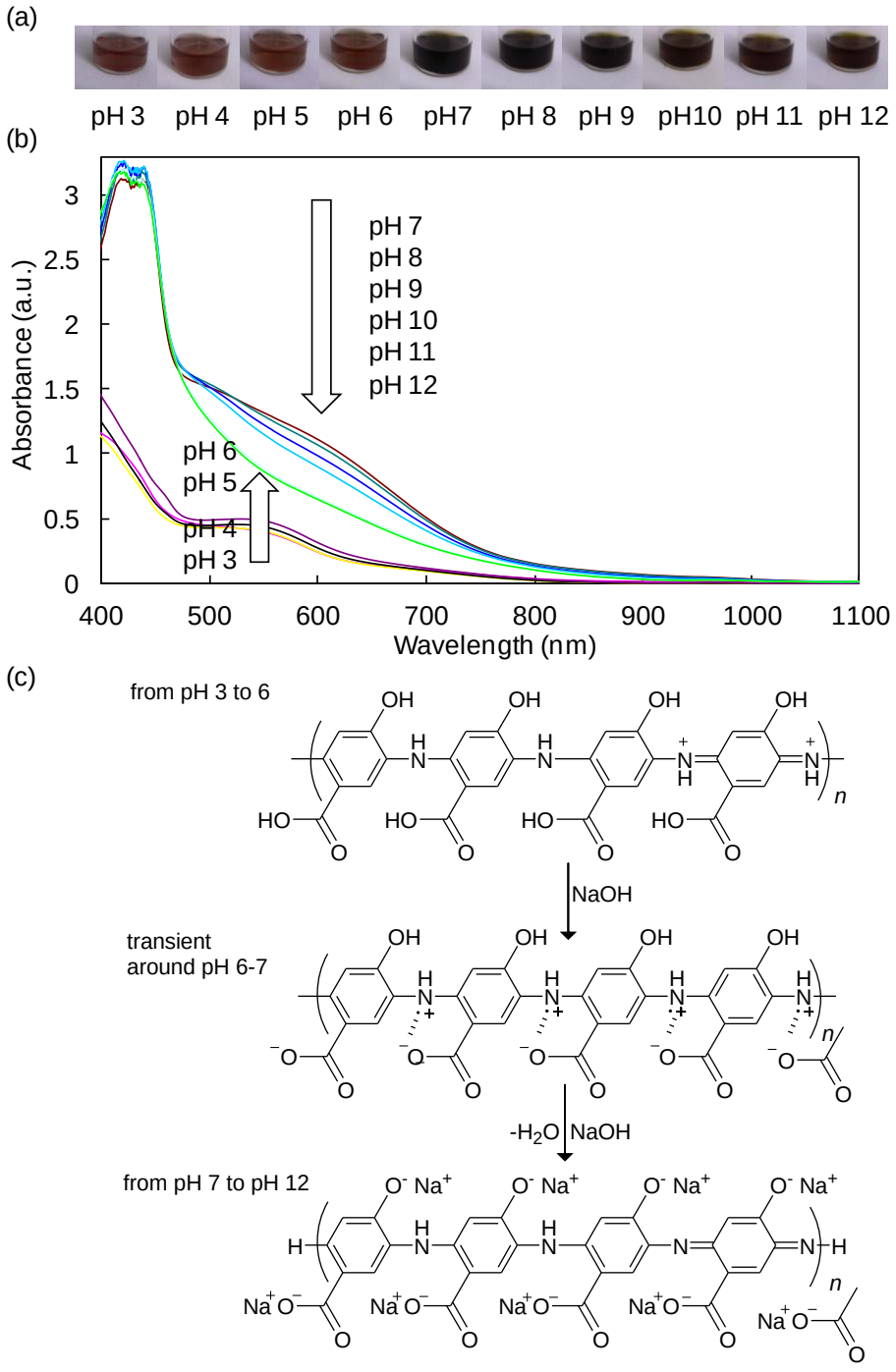

Figure 2-3. Halochromism of poly(3,4-AHBA) solution. (a) Pictures showing halochromic behaviors of poly(3,4-AHBA) solution. (b) UV-vis spectra of poly(3,4-AHBA) solution at different pH. (c) Schematic chemical structure change of poly(3,4-AHBA) with halochromism in the solution.

2.3.4 Solvatochromism

Solvatochromic behavior of poly(3,4-AHBA) electrodeposition film was studied as wrote below. When the film was dissolved in HCl aq/ethanol, the solution was brown but 10 min later changed into green. When solvents such as acetone, DMF, NMP, DMSO, and distilled water (5 ml) were added into this green solution (5 ml), the solution kept green in acetone, but changed into brown in DMF and DMSO while into pink in NMP and distilled water as shown in Figure 2-4. The UV-vis spectra of the poly(3,4-AHBA) in the prepared solutions the author measured (Figure 2-4), showing quinoid and polaron absorption at about 520 nm and 660 nm, respectively. When DMF, NMP, DMSO, and distilled water were used, polaron band became weak but quinoid band became strong. This is a solvatochromic behavior [62,66]. That is to say self-doped conducting poly(3,4-AHBA) induced polaron band transitions by solvent addition and the polaron band disappear after de-doping. From the fact that no dedoping occurred by acetone addition with the lowest polarity of the solvents used in this experiment, the author considered that interaction of the polar solvents with carboxylate groups of 3,4-AHBA units may induce the dedoping.

Finally the author tried to make a film of doped poly(3,4-AHBA) but the self-supporting film was not prepared. Then author used hydroxypropylcellulose as a supporter which is mixed with poly(3,4-AHBA) in acetone. The cast film was prepared by drying the acetone solution. The film was green and transparent (Figure 2-5), and showed a conductivity (2.3×10^{-4} S/cm) as high as that of semiconductors.

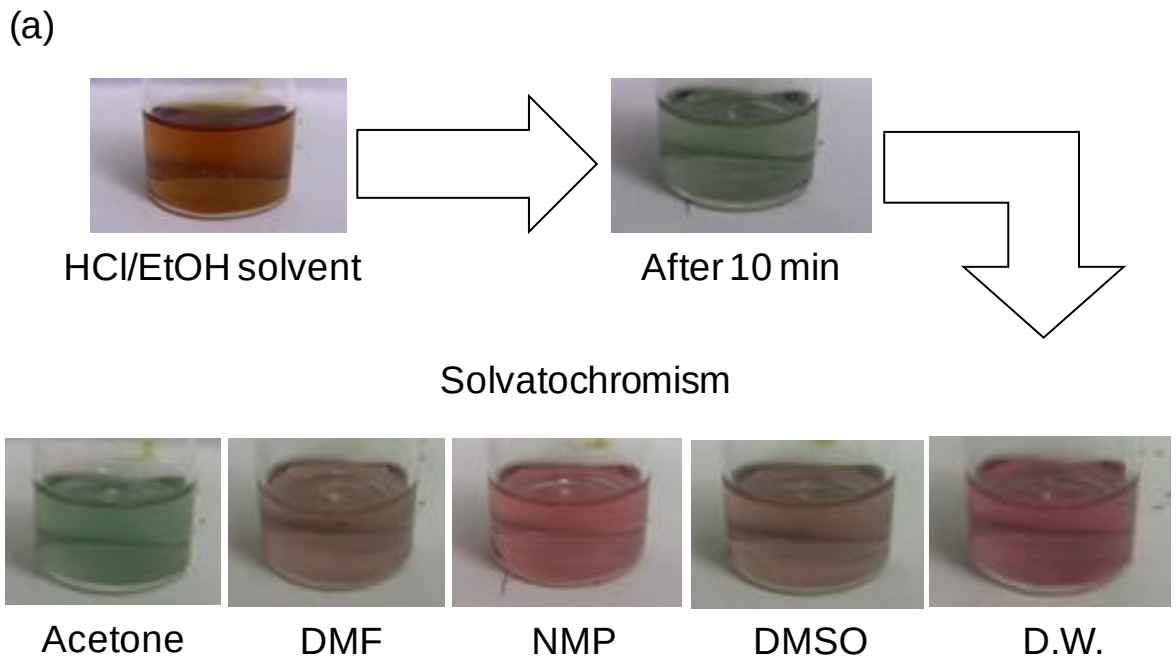

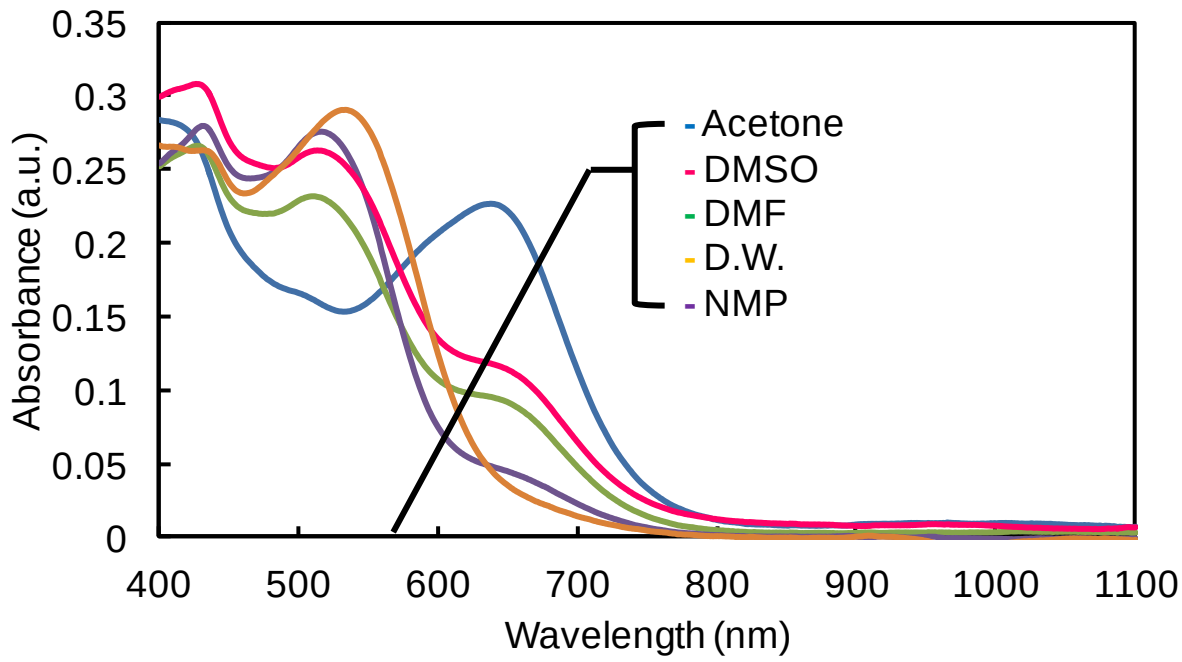

Figure 2-4. Solvatochromic behavior of poly(3,4-AHBA). (a) Photos of various solutions. (b) UV-vis spectra of various solutions (D.W. means distilled water).

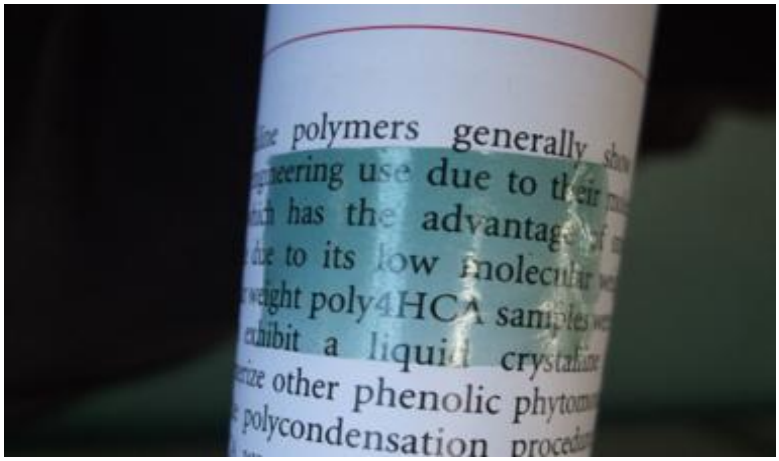

Figure 2-5. Semiconductor bio-based film prepared by casting acetone solution containing poly(3,4-AHBA) and hydroxypropylcellulose (supporter).

2.4 Conclusion

Poly(3,4-AHBA) showed higher solubility than PANI. Halochromism of poly(3,4-AHBA) showed different patterns from that of PANI. Especially, poly(3,4-AHBA) indicated noticeable color changes around pH 5-7. From the results of UV-vis spectra of the polymer solutions, it was suggested that the polymers including 3,4-AHBA units show self-doping effects by carboxylic acids. Further the polar solvent addition rendered the polymers undoped accompanying by the chromism. Thus the author first prepared novel functional bio-based polymers with chromism based on the π-conjugation structure change.

CHAPTER 3

Syntheses of thermotropic liquid crystalline copolyesters derived from wholly aromatic amino acids and their polarized photoluminescence

CHAPTER 3

3.1 Introduction

The development of bio-based polymers is significant for the establishment of a low-carbon society. Although various bio-based polymers have been developed, almost all of them were aliphatic polyesters which generally have no specific function [27]. These aliphatic bio-based polyesters can be used in the category of commodity plastics, but the widespread use of bio-based polymers is very difficult to achieve given the severe competition with the commodity plastics currently in use. The functionalization of bio-based polymers is very important for applications in advanced fields. For example, liquid crystalline polymers, which consist of aromatic component, have been used in several fields [67-69] because the molecular arrangement can be regulated by altering the temperature, concentration, electric field, magnetic field, and other factors [70-76]. Because liquid crystalline (LC) polymers are easily oriented at the molecular level to create materials with ultrahigh-strength, a high modulus, and other orientation-related functions [77,78]. However wholly aromatic LC polymers have rarely been synthesized from bio-derived monomers, but have gained recognition in the field of sustainability science for many natural LC polymers such as DNA [79,80], RNA [81], hemoglobin S (HbS) [82], F-actin [83], and polysaccharides [84,85]. We have already reported the polymerization of *trans*-4-hydroxycinnamic acid (4HCA: *p*-coumaric acid) as a phytomonomer, which exists in plant cell walls as an intermediate metabolite of lignin and is produced by photosynthetic bacteria [86]. Furthermore, 4HCA can also be synthesized by the enzymatic conversion of tyrosine via direct deamination [87]. The 4HCA homopolymer (P4HCA) is a main chain type of rigid homopolymer without a side chain, and showed thermotropic LC properties, whereas conventional polymers did not show thermotropic properties without the copolymerization of more than two monomers [88]. Therefore, 4HCA is expected to show strong mesogenicity to give its copolymers thermotropic properties, and

thus far the author investigated the copolymer characteristics such as LC behavior, LC-induced photoreactivity, oriented cell extension on their LC fibers, and various bio-based copolymers with a liquid crystalline nature [88-94]. If 4HCA is copolymerized with a biomonomer containing a chromophore, then new bio-based materials showing LC-related photoemission may be prepared. In this study, the author reports the synthesis and characterization of the copolymer poly{3-benzylidene amino-4-hydroxybenzoic acid (3,4-BAHBA)-*co*-*trans*-4-hydroxycinnamic acid (4HCA: *trans*-coumaric acid)} (P(3,4-BAHBA-*co*-4HCA)). 3,4-BAHBA is a functional biomonomer synthesized by the reaction of benzaldehyde (a biochemical) with 3-amino-4-hydroxybenzoic acid (3,4-AHBA), which can be extracted from *Streptomyces griseus*, a microorganism suitable for the mass-production of various biomolecules [21-24]. 3,4-BAHBA has a Schiff-based moiety showing visible light absorption and rigid components, and the LC copolymers derived from 4HCA and 3,4-BAHBA had a polarized fluorescence function [95]. The polarized fluorescence is due to the orientation of fluorescent molecules with thermotropic LC properties [77,78] and is attractive in the various fields of not only photonics, but also photosynthetic biology [96-99] and astronomy [100-102].

In this chapter, the author reports the relationship between the structural ordering and the photoreaction of P(3,4-BAHBA-*co*-4HCA)s of various compositions. Second the author further investigated the polarized fluorescence properties of oriented films of P(3,4-BAHBA-*co*-4HCA), and discovered unique properties, i.e., the fluorescent color change of the oriented films by changing the analyzer direction.

3.2 Experimental section

3.2.1 Materials

3,4-AHBA (Kanto chemical, Co. Inc.) and 4HCA (Kitamura Chemicals, Co. Ltd.) monomers were used as received. Acetic anhydride (Kanto chemical, Co. Inc.) was used as an acetylation agent and disodium hydrogen phosphate (Kanto chemical, Co. Inc.) as a polymerization catalyst were used as received. DMSO-d_6 (Sigma-Aldrich Co.) used as an NMR solvent was also used as received.

3.2.2 Synthesis of 3,4-BAHBA

A mixture of 3,4-AHBA (3.0 g) and benzaldehyde (30 ml) was heated at 150 ^{o}C to create a homogeneous liquid, which was stirred for 1 hour under nitrogen in an oil bath. After this reaction, the mixture was cooled to room temperature, and the yellow crystals were filtered, washed with ethanol, and vacuum-dried overnight at room temperature. Yield: 2.6 g (55 %), mp: 237 ^{o}C. IR (in cm^{-1}): 1664 ($\nu_{C=O}$), 1625 ($\nu_{C=N}$) (Figure 3-4). ^{1}H-NMR (400 MHz, DMSO-d_6, δ, ppm, TMS): 12.59 (s, 1H, COOH, H^{e}), 9.88 (s, 1H, OH, H^{d}), 8.75 (s, 1H, CH=N, H^{f}), 8.06 (dd, J = 7.4, 1.6 Hz, 2H, aryl, H^{g}), 7.73 (d, J = 2.0 Hz, 1H, aryl, H^{a}), 7.70 (dd, J = 8.4, 2.0 Hz, 1H, aryl, H^{c}), 7.57-7.50 (m, 3H, aryl, H^{h} and H^{i}), 6.97 (d, J = 8.0 Hz, 1H, aryl, H^{b}) (Figure 3-1). ^{13}C-NMR (100 MHz, DMSO-d_6, δ, ppm, TMS): 167.3 (COOH, C^{a}), 160.7 (CN, C^{h}), 155.3 (aryl, C^{e}), 138.1 (aryl, C^{d}), 136.2 (aryl, C^{i}), 131.6 (aryl, C^{l}), 129.1 (aryl, C^{j}), 129.1 (aryl, C^{g}), 128.7 (aryl, C^{k}), 122.1 (aryl, C^{b}), 120.6 (aryl, C^{c}), 116.0 (aryl, C^{f}) (Figure 3-2). ESI FT-ICR MS $[M+H]^{+}$: 242.08133, Calcd. for $C_{14}H_{12}NO_3$: 242.08117. $[M+Na]^{+}$: 264.06324, Calcd. for $C_{14}H_{11}NO_3Na$: 264.06311.

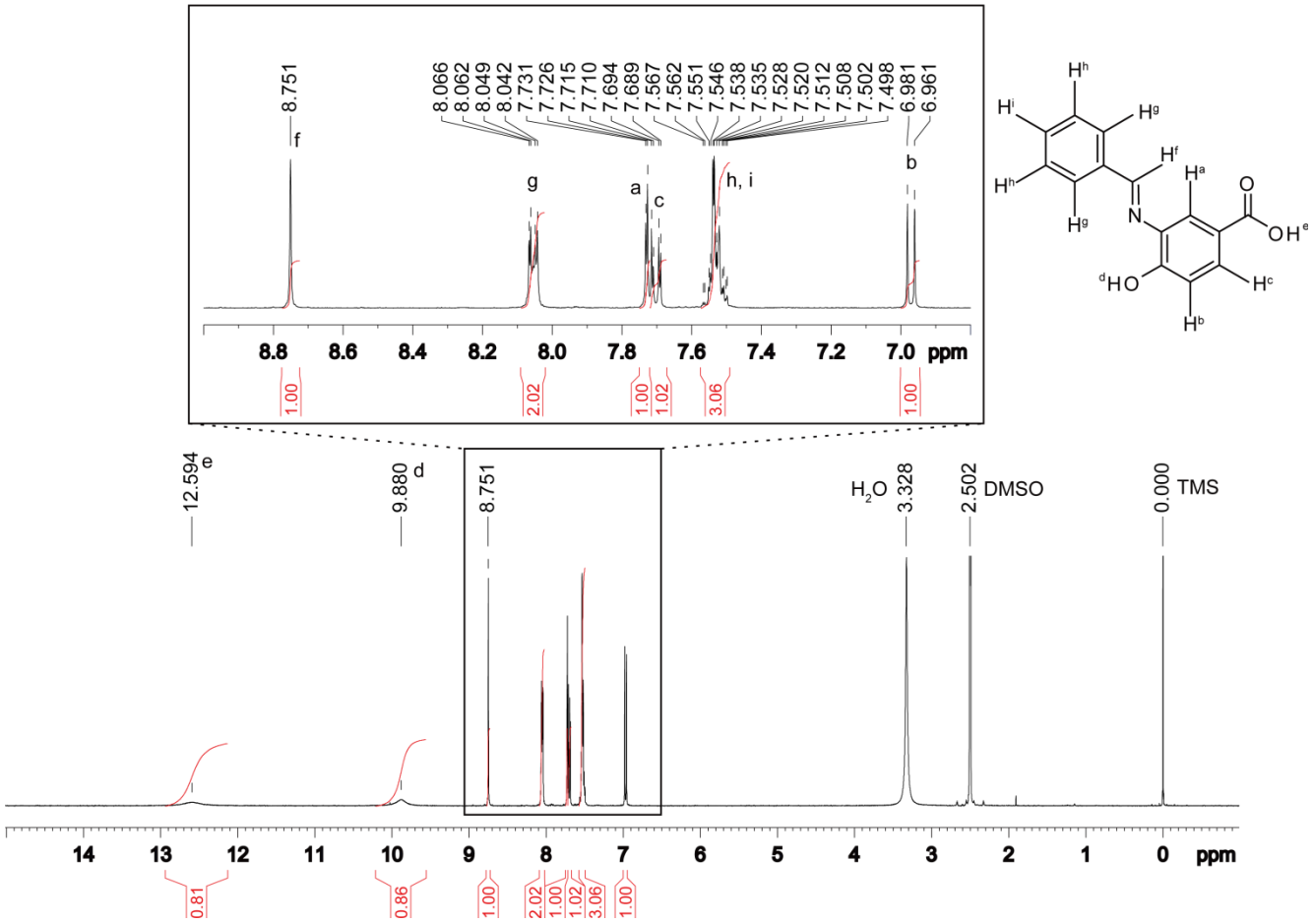

Figure 3-1. ^{1}H-NMR spectrum of 3,4-BAHBA.

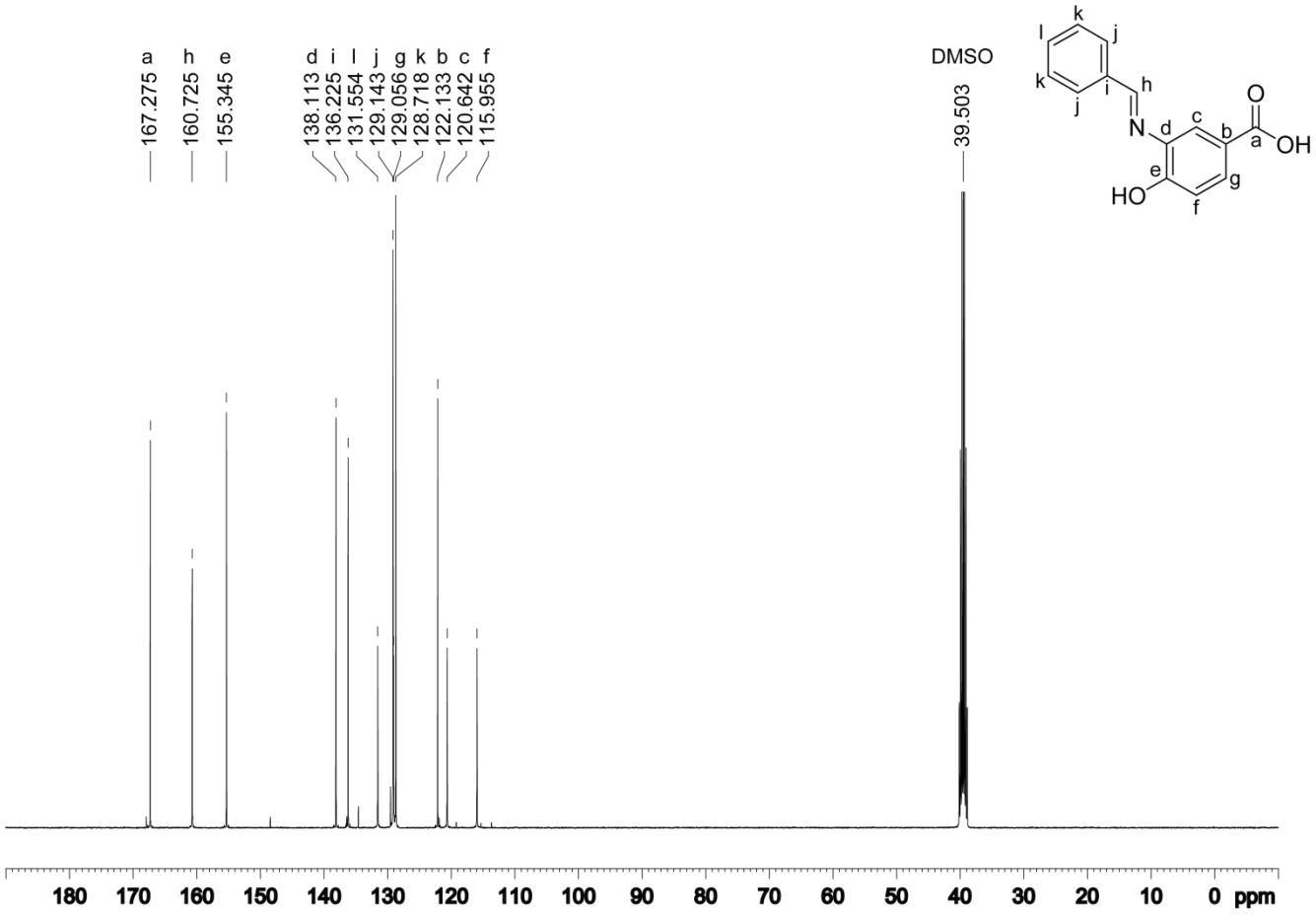

Figure 3-2. ^{13}C-NMR spectrum of 3,4-BAHBA.

3.2.3 Syntheses of P(3,4-BAHBA-*co*-4HCA)s

The copolymer with a 4HCA in-feed composition of 50 mol% was prepared as follows. Monomers of 3,4-BAHBA (2.1 mmol) and 4HCA (2.1 mmol) were stirred at 150 ^{o}C for 3 hours in the presence of 5 ml acetic anhydride as a condensation reagent and disodium hydrogen phosphate as a catalyst for the transesterfication. After 3 hours, the reactants were stirred at an elevated temperature of 180-200 ^{o}C for 30 min to distill acetic acid, and then vacuumed at 1.7 Torr at 200 ^{o}C for 15 min until the reaction mixture became too viscous to stir further. After this reaction, the product was dissolved in DMF and purified by reprecipitation over methanol, filtered, washed with methanol and vacuum-dried overnight at 80 ^{o}C. The yield was 59%. The copolymers with other 4HCA compositions were prepared by an analogous procedure.

3.2.4 Structural analyses

Fourier transform infrared spectra (FT-IR) of 3,4-BAHBA, 4HCA, and its polymer were recorded on a Perkin-Elmer Spectrum One spectrometer using a diamond-attenuated total reflection (ATR) accessory. ^{1}H and ^{13}C NMR spectra were measured in a DMSO-d_6 solution by an NMR spectrometer (Bruker, Avance III) at 400MHz. ^{1}H and ^{13}C NMR spectra chemical shifts in parts per million (ppm) were recorded downfield from 2.5 ppm and 39.5 ppm using DMSO as an internal reference.

Fourier transform ion cyclotron resonance mass spectra (FT-ICR MS) with an electrospray ionization system (ESI) were recorded on a Solari X, Bruker Daltonics Inc. A methanol solution of 3,4-BAHBA was prepared as a specimen by a 50-fold dilution of a saturated solution.

3.2.5 Molecular weight measurement

Number- and weight-average molecular weights (M_n and M_w) were determined by gel permeation chromatography at 40 ^oC (GPC JASCO GULLIVER SERIES UV-970; column, Shodex GPC KF-801 and KF-802; eluant, DMF), and calibrated with polystyrene standards at a flow rate of 1.0 ml/min.

3.2.6 Observation of thermotropic properties by crossed polarizing microscope

The phase transition of P(3,4-BAHBA-*co*-4HCA)s was observed by crossed-polarizing microscopy. The samples were sandwiched between two glass plates, and heated at a rate of 10 ^oC/min by a METTLER TOLEDO FP82HT Hot Stage (Greifensee, Switzerland). The melting temperature (T_m) and the liquid crystalline phase were observed directly by microscopy. The thermotropic behavior was also confirmed by differential scanning calorimetry (DSC) measurements (EXSTAE6100; Seiko Instruments Inc, Chiba, Japan) at a scanning ratio of 10 ^oC/min from 50 to 250 ^oC in a nitrogen atmosphere. The T_m of the new compound 3,4-BAHBA was measured by DSC. The T_g and T_m of the copolymers were obtained from the DSC curves of the second heating cycle. Thermal degradation was also analyzed by thermogravimetric analysis (TGA; SSC/5200 SII Seiko Instruments Inc.) by heating from 50 to 750 ^oC at a rate of 10 ^oC/min under a nitrogen atmosphere.

3.2.7 Wide angle X-ray diffraction (WAXD) measurement

The relationship between the molecular orientation and crystal structure of P(3,4-BAHBA-*co*-4HCA)s with 4HCA composition of 75 mol% was analyzed by WAXD with a graphite monochromatized CuKα radiation beam focused via a 0.3 mm pinhole collimator with a flat 20×20 cm^2 imaging plate (IP) detector of 1900×1900 pixels (Rigaku, R-AXIS IIc). The orientation of the fibers was established from the LC melt state. The fiber was set in its axis perpendicularly in front of a X-ray beam collimator.

3.2.8 Photoluminescence of solutions

Photoluminescence excitation and emission spectra of the polymer solutions were obtained with a spectrophotometer. The polymer concentration in NMP was 0.1 g/l. P(3,4-BAHBA-*co*-4HCA)s solutions with 4HCA compositions of 75 and 100 mol% were filtered because they were partially soluble in NMP.

3.2.9 Photoluminescence of oriented film

Figure 3-3 illustrates the optical train used for the photoluminescence dichroism measurements, which was performed using a fluorophotometer (FP-6500; Jasco Instruments Inc, Japan). The samples were mounted on a glass slide, and were heated by a Hot Stage. Just above the T_m, glass plates were used to sandwich the sample on the arrowed direction, and they were super-cooled to room temperature to create an oriented film coating the glass. The author then inserted the film between the polarizer and the analyzer.

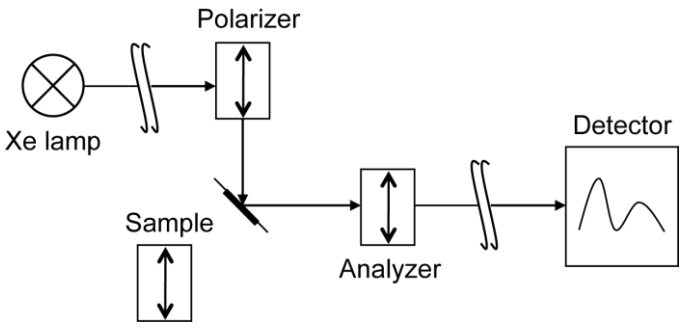

Figure 3-3. Optical train used for the photoluminescence experiments. The polarizer was placed behind the excitation shutter into the light path, and the analyzer was placed in front of the emission shutter, where the arrows indicate the polarizing and analyzing directions. Although the picture shows a parallel direction of the arrows, the polarizer and analyzer both could be rotated. The polarizer and analyzer can rotate.

3.3 Results and discussion

3.3.1 Syntheses

The monomer 3,4-BAHBA was synthesized by the reaction of 3,4-AHBA with benzaldehyde. The preparation of the copolymer P(3,4-BAHBA-*co*-4HCA)s was performed according to Jin's method [103]. Table 3-1 shows the synthetic conditions and copolymer compositions of the P(3,4-BAHBA-*co*-4HCA)s. A mixture of 3,4-BAHBA and 4HCA was stirred at 150 ^{o}C. The solution was yellow and transparent initially, but when the temperature increased to 180-200 ^{o}C to evaporate the acetic acid, the solution changed to a slightly brown color and began to show increased viscosity. The author stopped the reaction when the reaction mixture became too viscous to stir further. The purified products were obtained as an ocher powder, which was dissolved in concentrated sulfuric acid (H_2SO_4) and pentafluorophenol. When the 4HCA ratio was 50 mol% or lower, the copolymers were dissolved in various solvents such as tetrahydrofuran (THF), *N*,*N*-dimethylformamide (DMF), dimethyl sulfoxide (DMSO), *N*-methylpyrrolidone (NMP), and chloroform (Table 3-2). The incorporation of 3,4-BAHBA into the P4HCA increased the solubility of the copolymers.

Scheme 3-1. Synthesis of 3,4-BAHBA

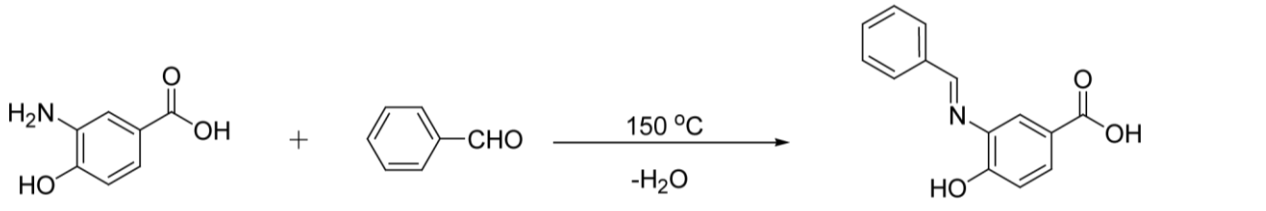

3-amino-4-hydroxybenzoic acid (3,4-AHBA) + benzaldehyde → 3-benzylidene amino-4-hydroxybenzoic acid (3,4-BAHBA)

Scheme 3-2. Synthesis of P(3,4-BAHBA-*co*-4HCA)

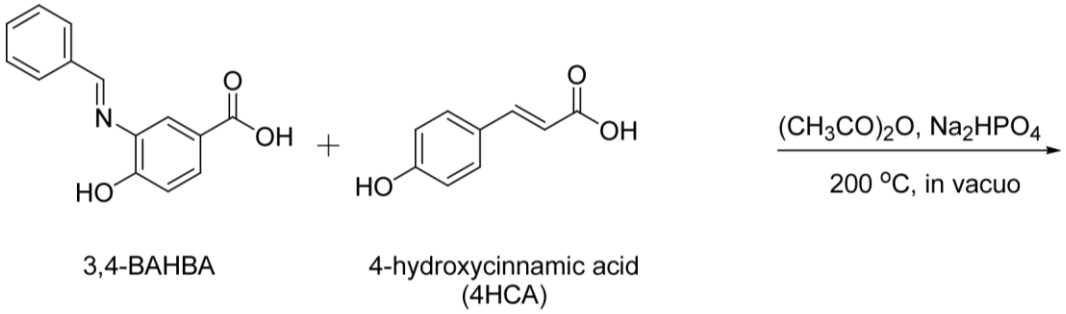

3,4-BAHBA

4-hydroxycinnamic acid (4HCA)

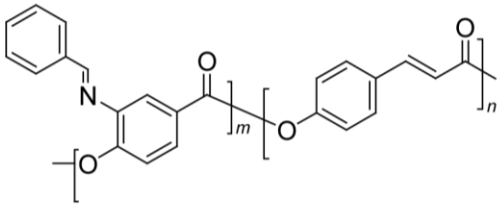

Poly(3-benzylidene amino-4-hydroxybenzoic acid-*co*-4-hydroxycinnamic acid)
P(3,4-BAHBA-*co*-4HCA)

Table 3-1. Synthesis conditions of P(3,4-BAHBA-*co*-4HCA)

3,4-BAHBA/4HCA[a] (mol%)	3,4-BAHBA (mmol)	4HCA (mmol)	3,4-BAHBA/4HCA[b] (mol%)	Yield (%)
100/0	2.1	0	100/0	37
75/25	2.1	0.69	66/34	55
50/50	2.1	2.1	53/47	59
25/75	2.1	6.2	38/62	73
0/100	0	3.0	0/100	85

[a] The numbers refer to the molar percentage of in-feed composition.

[b] Molar ratios were estimated by ^{1}H-NMR spectra.

Table 3-2. Solubility of monomers and copolymers

Solvents	3,4-BAHBA	4HCA	P(3,4-BAHBA-*co*-4HCA) 3,4-BAHBA/4HCA (mol%)				
			100/0	75/25	50/50	25/75	0/100
Methanol	+	++	-	-	-	-	-
Ethanol	+	++	-	-	-	-	-
Acetone	+	++	+-	+-	+-	+-	+-
THF	++	++	++	++	++	+-	+-
DMF	++	++	++	++	++	+-	+-
DMAc	++	++	++	++	++	+-	+-
NMP	++	++	++	++	++	+-	+-
DMSO	++	++	++	++	++	+-	+-
TFA	++	+	++	++	++	+-	+-
H_2SO_4	++	++	++	++	++	++	++
Pentafluorophenol	++	++	++	++	++	++	++
H_2O	-	-	-	-	-	-	-
Chloroform	-	-	++	++	++	-	-
Toluene	-	-	-	-	-	-	-
Hexane	-	-	-	-	-	-	-

++: soluble at r.t., +-: partly soluble, -: insoluble, +: soluble only by heating.
THF: Tetrahydrofuran, DMF: *N*,*N*-Dimethylformamide, DMAc: *N*,*N*-Dimethylacetamide, NMP: *N*-methylpyrrolidone, DMSO: Dimethyl sulfoxide, TFA: Trifluoroacetic acid.

Figure 3-4 shows the FT-IR spectra of the monomers and copolymers. IR peaks assigned to the double bonds ($\nu_{C=C}$: 1626, 1633, and 1635 cm^{-1}), azomethine ($\nu_{C=N}$: 1625, 1632, 1633 cm^{-1}), and aromatic ring ($\nu_{p\text{-}\varphi}$: 1599, 1600, and 1601 cm^{-1}) appeared in the spectra for the monomers of 3,4-BAHBA and 4HCA and for the polymers of P(3,4-BAHBA), P4HCA, and P(3,4-BAHBA-*co*-4HCA). On the other hand, the carboxyl IR peaks observed in the spectra of the monomers of 3,4-BAHBA ($\nu_{C=O}$: 1664 cm^{-1}) and 4HCA ($\nu_{C=O}$: 1668 cm^{-1}) disappeared in those copolymers. Instead, the IR peaks assigned to the ester groups ($\nu_{C=O}$: 1733, 1736, and 1737 cm^{-1}) appeared, indicating the conversion of the carboxylic acids to esters. The shoulders of P(3,4-BAHBA) (1676 cm^{-1}) and P(3,4-BAHBA-*co*-4HCA) (1672 cm^{-1}) would be

assigned to the terminal carboxyl groups. Figure 3-5 shows a representative ^{1}H-NMR spectrum of P(3,4-BAHBA-*co*-4HCA) with a 4HCA composition of 50 mol% in DMSO-d_6. Multiple peaks in the region of the chemical shift of δ = 8.74 ppm (azomethine proton), δ = 8.12-8.13 ppm (aromatic protons), δ = 7.83-7.95 ppm (aromatic protons and β-CH), δ = 7.12-7.67 ppm (aromatic protons), and δ = 6.85-6.94 ppm (α-CH) were assigned. Additionally, the author note that the vicinity of the attributed "c" proton in the ^{1}H-NMR was the NH peak at the end of P(3,4-BAHBA-*co*-4HCA) chains whose molecular weights were not so high according to the results of GPC study. The compositions of 4HCA in the copolymers were calculated by the integral ratios for peak area of (a) and (b) (Table 3-1). ^{1}H-NMR spectroscopy in DMSO-d_6 demonstrated the incorporation of both monomers into the polymer backbone, and the 4HCA composition in copolymer can be estimated by the integration ratio of the aromatic proton signals of the individual units. The results are summarized in Table 3-1. The monomer composition in the feed was close to the monomeric unit composition in the copolymers, indicating the successful formation of the copolymers.

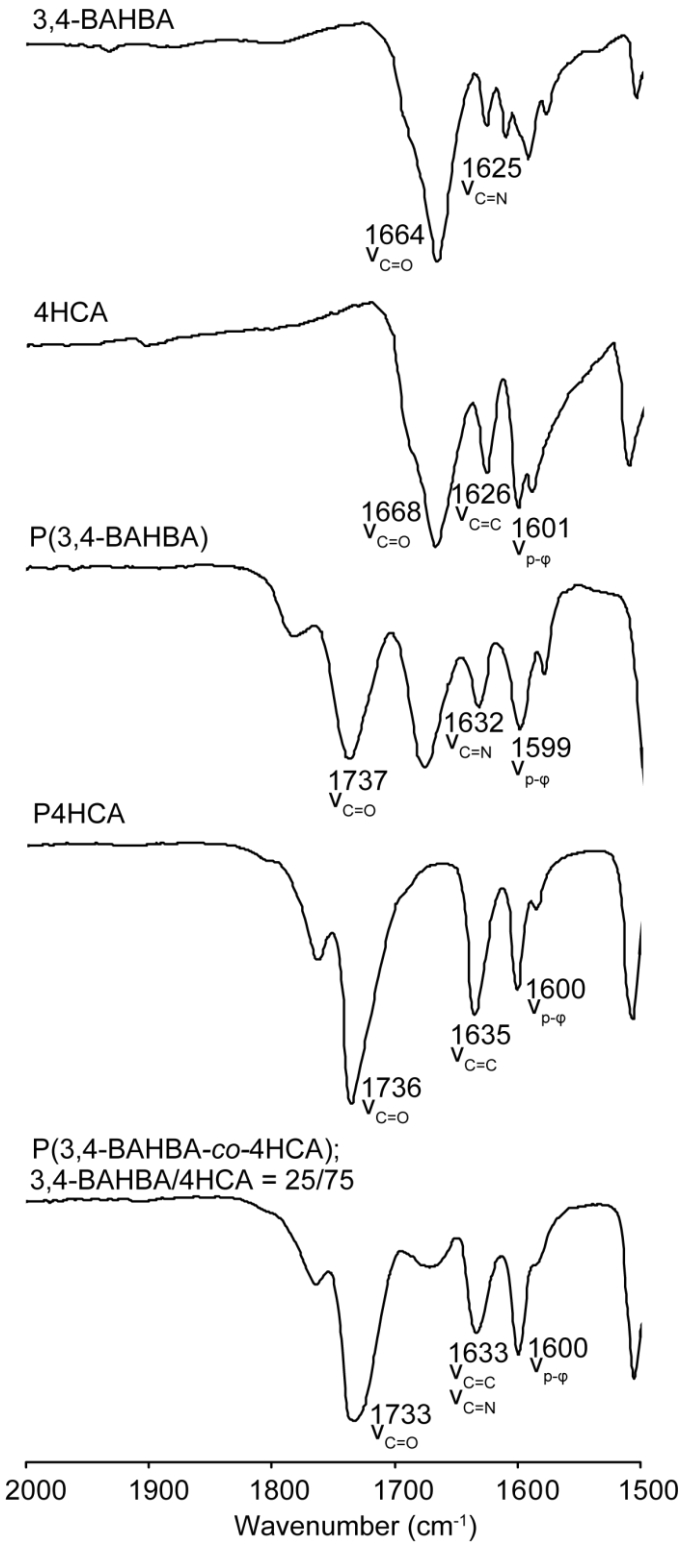

Figure 3-4. FT-IR spectra of the monomers and polymers.

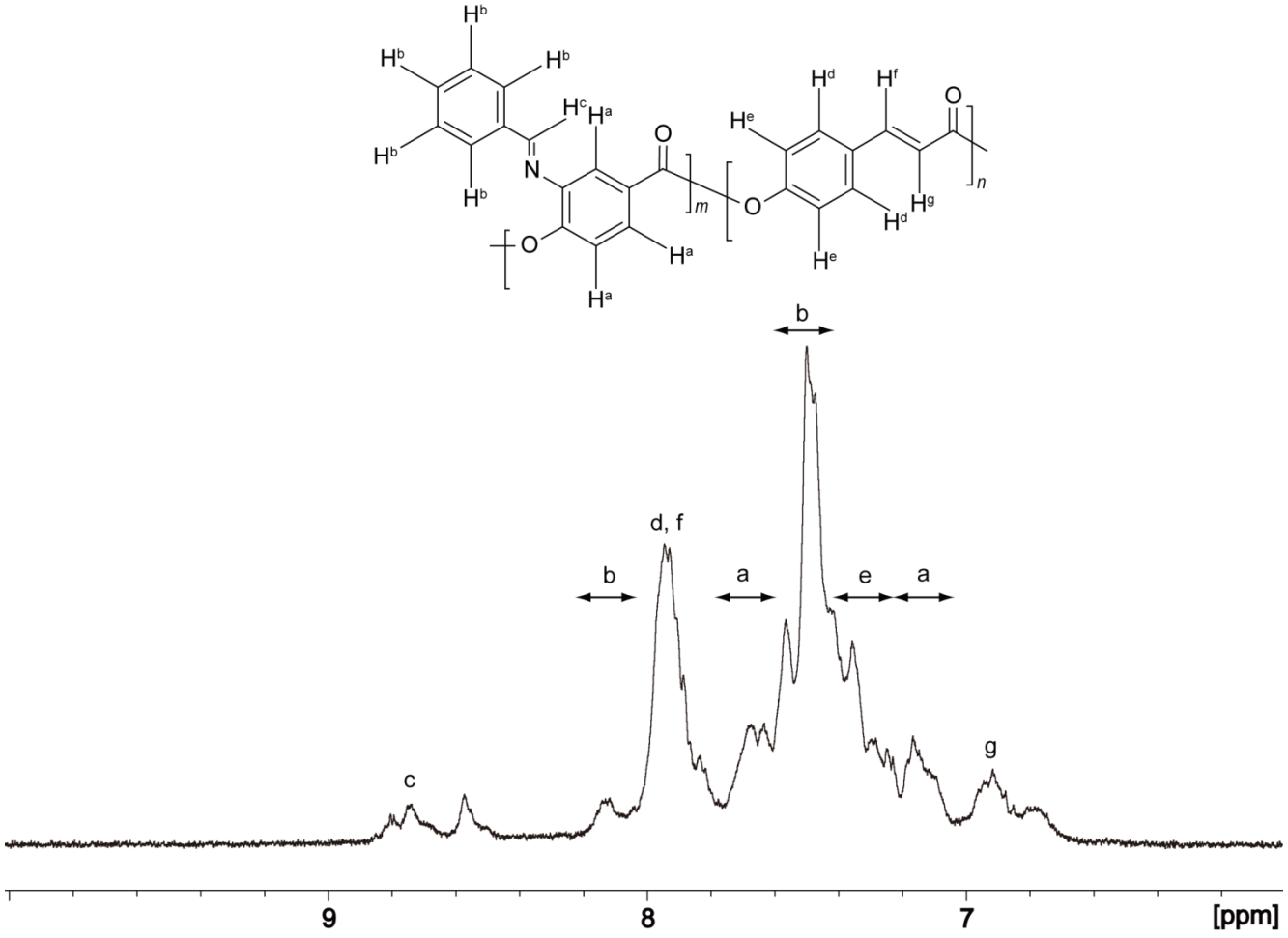

Figure 3-5. ^{1}H-NMR spectrum of P(3,4-BAHBA-*co*-4HCA) with a 4HCA composition of 50 mol% 4HCA in DMSO-d_6.

The average molecular weights of the P(3,4-BAHBA-*co*-4HCA)s were measured in DMF by GPC (Table 3-3). P(3,4-BAHBA) and P(3,4-BAHBA-*co*-4HCA)s with in-feed 4HCA compositions of 25 and 50 mol% showed a single peak in the GPC on indicating M_w values of 6900, 7900, and 7200, respectively (M_w/M_n = ca. 1.5). The molecular weights of the other copolymers with higher 4HCA compositions were not measured because of their low solubility in DMF. However, the author expected their molecular weights to be similar to those of P(3,4-BAHBA) and P(3,4-BAHBA-*co*-4HCA)s with in-feed 4HCA compositions of 25 and 50 mol%, because the viscosity of their concentrated H_2SO_4 solution was similar.

Table 3-3. Monomer composition and molecular weight of P(3,4-BAHBA-*co*-4HCA)s

3,4-BAHBA/4HCA (mol%)	M_n	M_w	M_w/M_n
100/0	4500	6900	1.5
75/25	4800	7900	1.6
50/50	4900	7200	1.5

3.3.2 Liquid crystalline properties

The thermotropic properties were investigated by crossed-polarizing microscopic observation and TGA/DSC measurements (Figure 3-6, Table 3-4). The glass transition temperatures, T_g, of the copolymers ranged between 125 ^oC and 135 ^oC whereas the melting temperature, T_m, ranged between 215 ^oC and 220 ^oC. The 10% weight-loss temperature, T_{10}, ranged between 300 ^oC and 350 ^oC. The T_g values of the copolymers were higher than that of the values of degradable bio-based polymers reported thus far [104]. Moreover the P(3,4-BAHBA-*co*-4HCA)s have good heat resistance properties for using as engineering thermoplastics.

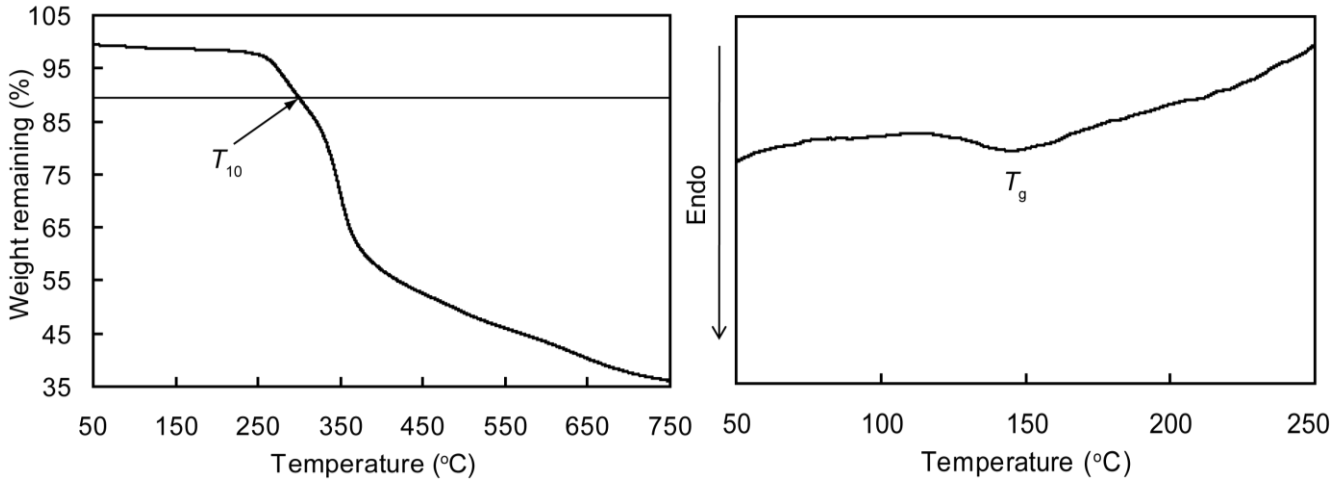

Figure 3-6. TGA and DSA thermogram of P(3,4-BAHBA).

Table 3-4. Thermal analysis data of P(3,4-BAHBA-*co*-4HCA)s

3,4-BAHBA/4HCA (mol%)	T_g [a] (°C)	T_m [a] (°C)	T_m [b] (°C)	T_{rc} [b] (°C)	T_{10} [c] (°C)
100/0	135	N[d]	184	-	300
75/25	130	N[d]	212	-	315
50/50	125	220	217	-	315
25/75	N[d]	215	204	298	345
0/100	N[d]	220	215	280	350

[a] T_g and T_m were measured by DSC upon a second heating under nitrogen (10 °C/min). [b] T_m and T_{rc} were measured by polarizing microscope (10 °C/min). [c] T_{10} were measured by TGA under nitrogen (10 °C/min). [d] N = transition did not occur.

T_g: glass transition temperature, T_m: melting temperature, T_{rc}: recrystallization temperature, T_{10}: 10% weight-loss temperature.

Figure 3-7 shows the phase diagram of P(3,4-BAHBA-*co*-4HCA)s of various compositions. These results indicated that in P(3,4-BAHBA-*co*-4HCA)s with the 4HCA compositions of 55 mol% and higher, a schlieren texture with two and four brushes could be observed (inset picture). Since the brush lines were accompanied by point defects, the LC was identified as the nematic phase. Unexpectedly, the nematic fluid also solidified at 300 °C on average, showing a transformation of its microscopic texture from the schlieren to crystalline needles. This phenomenon was also found in our previous study on P4HCA homopolymer [88], and the author thought that the crystallization was caused by a post-reaction such as acetyl group additions to double-bonds. As a whole, the phase diagram showed that the melting point of the copolymers can be controlled by a change in the composition, while retaining their liquid

crystalline properties. In addition, one can see that the high percentage of 4HCA (low percentage of 3,4-BAHBA) in the composition resulted in liquid crystalline copolymers, although P(3,4-BAHBA) is not a liquid crystalline homopolymer.

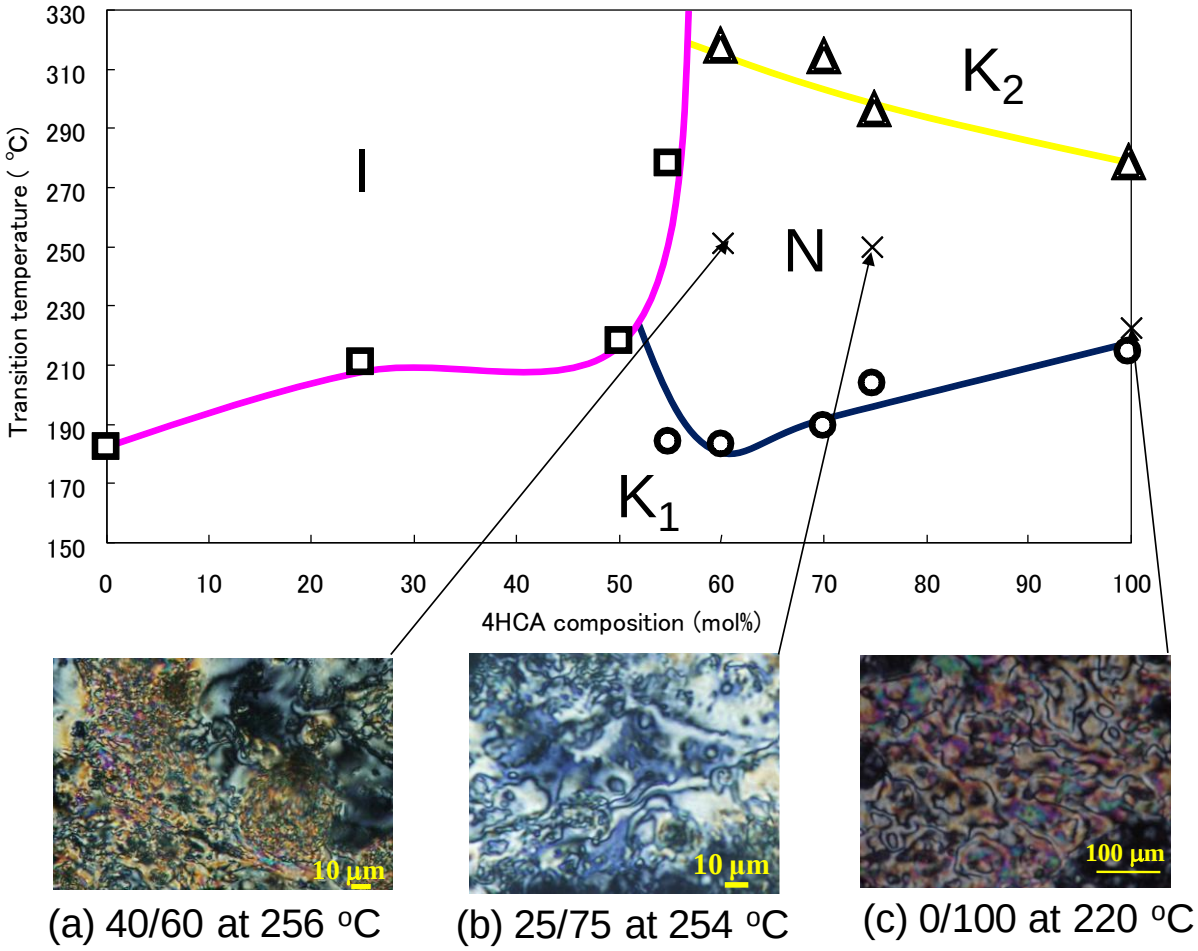

Figure 3-7. Phase diagram of P(3,4-BAHBA-*co*-4HCA)s of various compositions. The inset pictures are crossed-polarizing photomicrographs of P(3,4-BAHBA-*co*-4HCA) with a 4HCA composition of (a) 60 mol% at 256 °C, (b) 75 mol% at 254 °C, and (c) 100 mol% at 220 °C [88] .

To elucidate the molecular orientation effects on the fluorescence of the polymer oriented film and fiber were investigated. An oriented film of the copolymer was prepared by following procedure: the polymer was sandwiched between two glass plates, and the cover at

250 °C, mechanical orientation of the sample was demonstrated by shearing [72,105]. After that supercooled to room temperature to fix the orientation state of the film on the glass. The orientation of the fiber was established from the melt state at 250 °C. Right photos of Figures 3-8a and 3-8b show crossed-polarizing microscopic images taken under cross-nicol. The transmitting light through the samples demonstrate the clear orientation of the films and fibers. If a first-order retardation plate (λ = 530 nm) was inserted into the light path, left photos of Figure 3-8a and 3-8b were obtained. The birefringence was positive, as evidenced by both the subtractive birefringence (orange color) in the film running from the upper left to the lower right, and by the additive birefringence (blue color) in the shearing direction from the upper right to the lower left. These results indicated the orientation direction of polymer chains in the fibers should be same with that in the films.

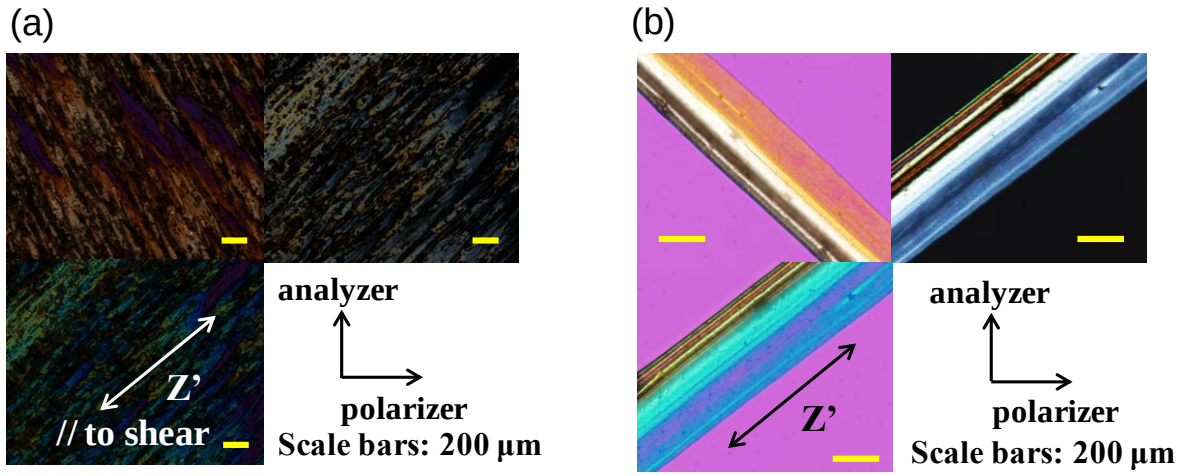

Figure 3-8. Crossed-polarizing optical microscope images of P(3,4-BAHBA-*co*-4HCA) with a 4HCA composition of 75 mol% in the image taken at 250 °C. (a) An image of the oriented film prepared by shearing at 250 °C and super cooling to room temperature. (b) An image of the fiber of P(3,4-BAHBA-*co*-4HCA) with a 4HCA composition of 50 mol% at 250 °C. The left images were taken under a first-order retardation plate (530 nm), and the right image without the plate. The Z'-axis means the direction of first-order retardation plate which is parallel to the shear direction.

3.3.3 WAXD study

To investigate the molecular orientation and crystalline structure, the author performed wide-angle X-ray diffraction (WAXD) studies on the copolymer. Although the author tried to take WAXD image of the oriented film, it was pretty difficult because the sample was too thin. Then the oriented fibers were used for WAXD study (Figure 3-9a). As illustrated below the image, four diffraction arcs marked as d1, d2, d3, and ds at diffraction angles (2θ) of 18.4, 23.9, 27.8, and 28.8^o corresponding to d-spacings of 0.48, 0.37, 0.32, and 0.31 nm were observed. As discussed in the previous paper of P4HCA crystals, the diffractions of $2\theta = 10.3^o$ (d0) [88], d1 and d3 were assigned to the hexagonal arrangement and the spacing of d2 approximates to one half of the length (0.40 nm) of the 4HCA unit [88]. Unexpectedly, however, the satellite diffractions of d0 were absent. In these reasons, the reciprocal spacings of diffractions of d0, d1, and d3 for the copolymer with a 4HCA composition of 75 mol% were 0.116 [88], 0.208, and 0.313 nm^{-1}, respectively, with an approximate relation of 1:√3:√7, respectively $1/d_{100}$:$1/d_{110}$:$1/d_{210}$. Thus these diffractions could be assigned to the main chain, presumably arranging hexagonally with a distance of 0.96 nm [88-90]. As for ds, the diffraction arcs did not locate on the equatorial or meridian line, or correspond with any diffraction of the 4HCA homopolymer crystal, suggesting that the diffraction may be related with 3,4-BHABA residues whose side chains protrude out almost perpendicularly to the polymer backbones. As a consequence, the polymer main-chains aligned perpendicularly to the fiber axis whereas the 3,4-BHABA side-chains arranged almost parallely, as illustrated in Figure 3-9(c). Figure 3-9(b) shows the azimuthal scanning diagrams in which d2 gave a distinct diffraction peak around 90^o (0^o is indicated in the illustration below the WAXD image in Figure 3-9(a). From this diagram, the orientation degree was estimated as 0.64 using the equation (180-β)/180, where β (= 65^o) refers to the summation of the azimuthal angles of the full width at half of the maximum of diffraction arc [72]. This value is in the range typical of nematic liquid crystals, meaning the formation of the film with a good orientation which was

unable in the previously-prepared lower M_w polymers. The crystalline degree was estimated as 14% from the area ratio of the crystalline peaks to the entire area in the 2θ range between 10-40^o (Figure 3-10). Since oriented crystalline domains were formed from the nematic melt, the non-crystalline ones should be in the oriented nematic glass state. Thus the WAXD analyses suggest the positive birefringence of the film as well as the fiber confirmed in polarized microscopy (Figure 3-8b) suggests that the copolymer adopted a perpendicular orientation to the shear direction (fiber direction of Figure 3-9c).

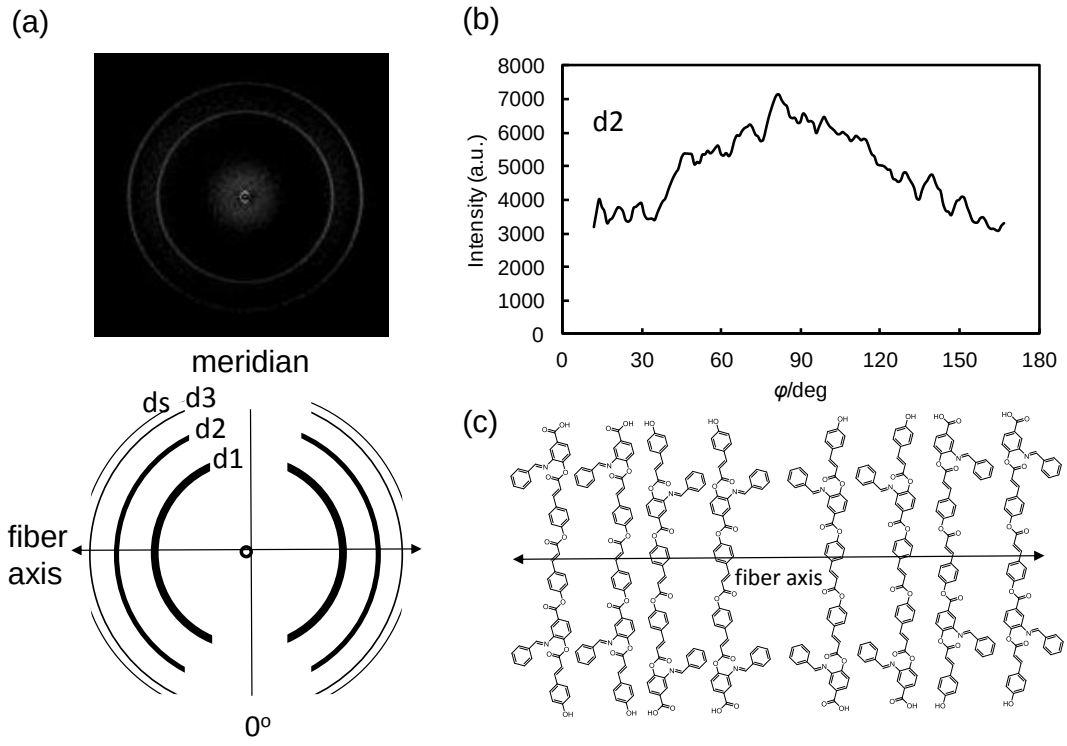

Figure 3-9. Structural analysis of P(3,4-BAHBA-*co*-4HCA) fiber with a 4HCA composition of 75 mol%. (a) Wide angle X-ray diffraction (WAXD) image of an oriented fiber of the copolymer, which was spun from the nematic state. The schematic illustration below the image is shown in order to clarify the location of the diffraction arcs, since the resolution of the image shown here became too low. (b) WAXD diagram of the azimuthal scanning around diffraction arcs of d2 with a 2θ = 23.9^o of the illustration **a**. (c) Schematic illustration of the copolymer chain arrangement in the fiber.

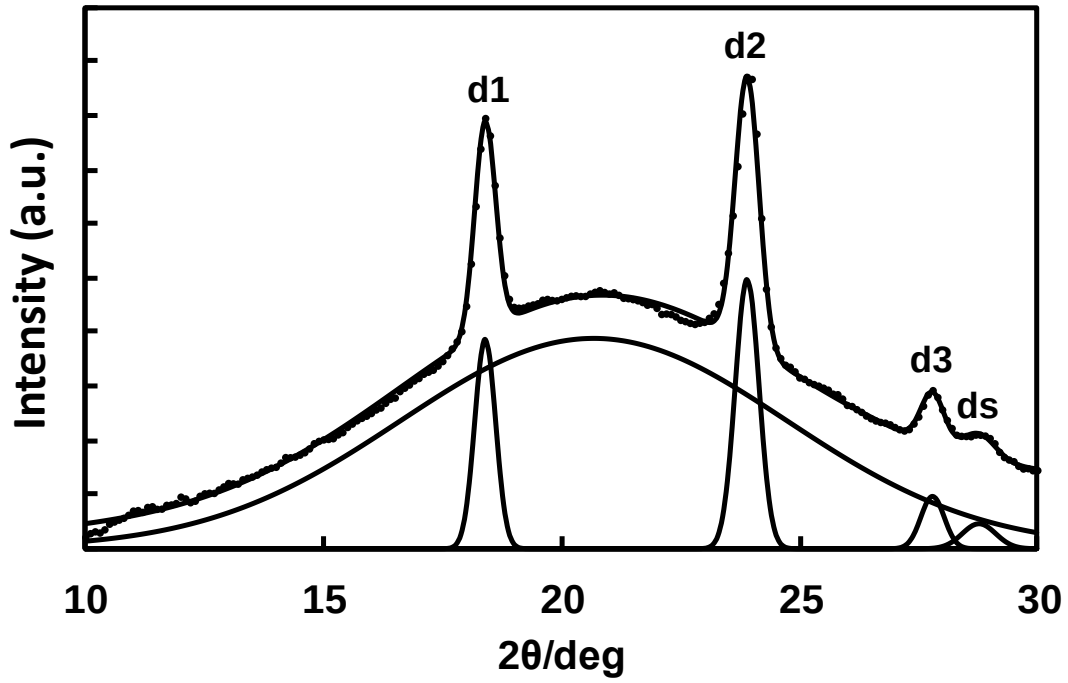

Figure 3-10. Peak deconvolution analysis to determine the degree of crystallization. The peaks correspond with Figure 3-9.

3.3.4 Photoluminescence of solutions

The photograph shown in Figure 3-11 demonstrated the visual photoluminescence of the P(3,4-BAHBA-*co*-4HCA)s in an NMP solution at a concentration of 0.1 g/L. Those solutions were transparent and faint yellow, but emitted various colors depending on the copolymer composition when ultraviolet (UV) light (λ = 365 nm) was irradiated. In order to quantify these colors, the author recorded the photoluminescence spectra. Figure 3-12 shows the photoluminescence excitation spectra (left), and emission spectra (right), and Table 3-5 shows the photoluminescence excitation λ_{max} (ex), and emission λ_{max} (em) of P(3,4-BAHBA-*co*-4HCA)s of various molar ratios. From Figure 3-12, one can see that the P(3,4-BAHBA-*co*-4HCA) with a 4HCA composition of 75 mol% showed the highest intensity of all of the

samples prepared here. The wavelength of the excitation peaks of the P(3,4-BAHBA-*co*-4HCA) with a 4HCA composition of 75 mol% ranged between those of both homopolymers, whereas the wavelength of the emission peak was almost the same as the P4HCA homopolymers. This phenomenon implies that the 3,4-BAHBA units play the role of an antenna for light energy with a wide wavelength range, and transmit this energy into the 4HCA units to emit strongly. As a consequence, the P(3,4-BAHBA-*co*-4HCA)s have photoluminescence properties.

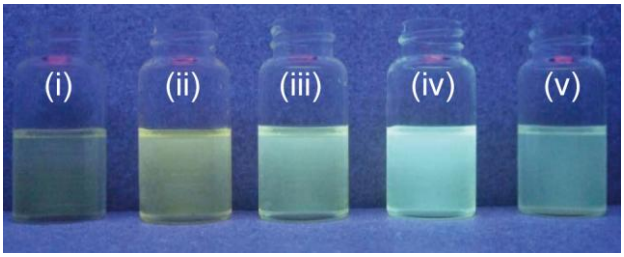

Figure 3-11. Digital photograph of an NMP solution of P(3,4-BAHBA-*co*-4HCA)s under 365 nm UV light excitation. (**i**) 100/0, (**ii**) 75/25, (**iii**) 50/50, (**iv**) 25/75, (**v**) 0/100 in molar ratios.

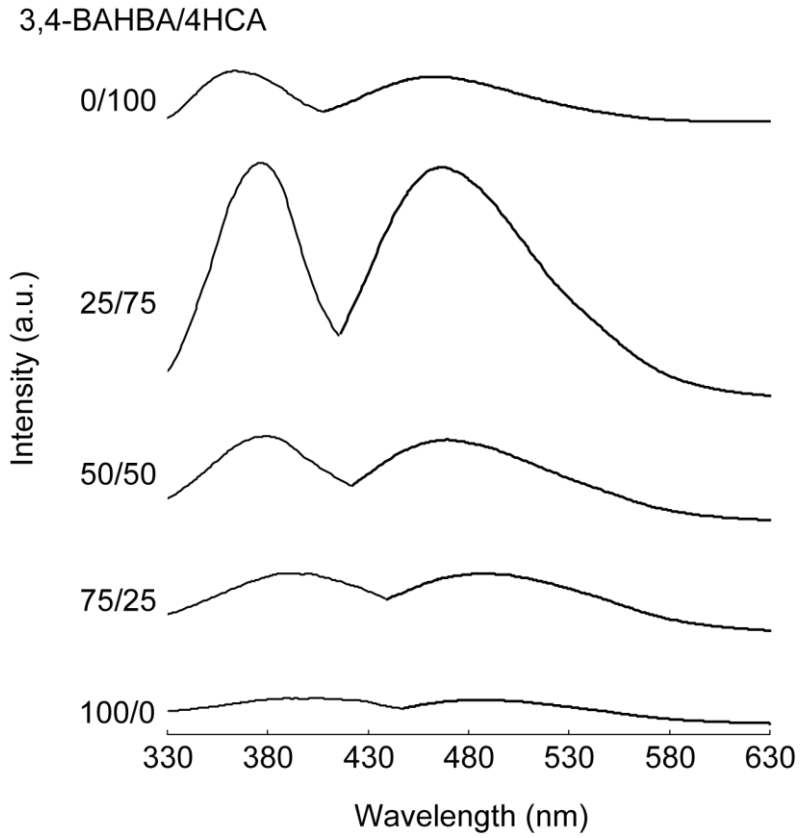

Figure 3-12. Photoluminescence excitation spectra (left), and emission spectra (right) of P(3,4-BAHBA-*co*-4HCA)s of various molar ratios.

Table 3-5. Photoluminescence excitation λ_{max} (ex), and emission λ_{max} (em) of P(3,4-BAHBA-*co*-4HCA)s

3,4-BAHBA/4HCA	λ_{max} (ex) (nm)	λ_{max} (em) (nm)
100/0	402	484
75/25	388	487
50/50	378	468
25/75	374	466
0/100	362	459

3.3.5 Photoluminescence of films

The fluorescence spectra of orientation films of P(3,4-BAHBA-*co*-4HCA)s with the 4HCA compositions of 75 and 100 mol% were measured while changing the directions of the polarizer and analyzer [Figure 3-13(a-b)]. When the polarizer and analyzer directions are both parallel to the film orientation, the emission intensity is the highest. Otherwise, if one of the polarizers or analyzers was perpendicular to the sample orientation, then the intensities were very low. It is noteworthy that even if the polarizer and analyzer direction was parallel, the intensity was low in the film orientation direction perpendicular to either unit. This result supports simple reflection based on a mirror effect of the sample would be insufficient. The emission intensities at 469 nm in the copolymers with the 4HCA compositions of 75 and 100 mol% were 23 and 30, respectively. From these intensity data, The author normalized the emission intensity per 4HCA unit to 0.31 and 0.30, suggesting that the 3,4-BAHBA units slightly enhanced the intensity of polarized light from the 4HCA units, even a shortened 4HCA continuous segment.

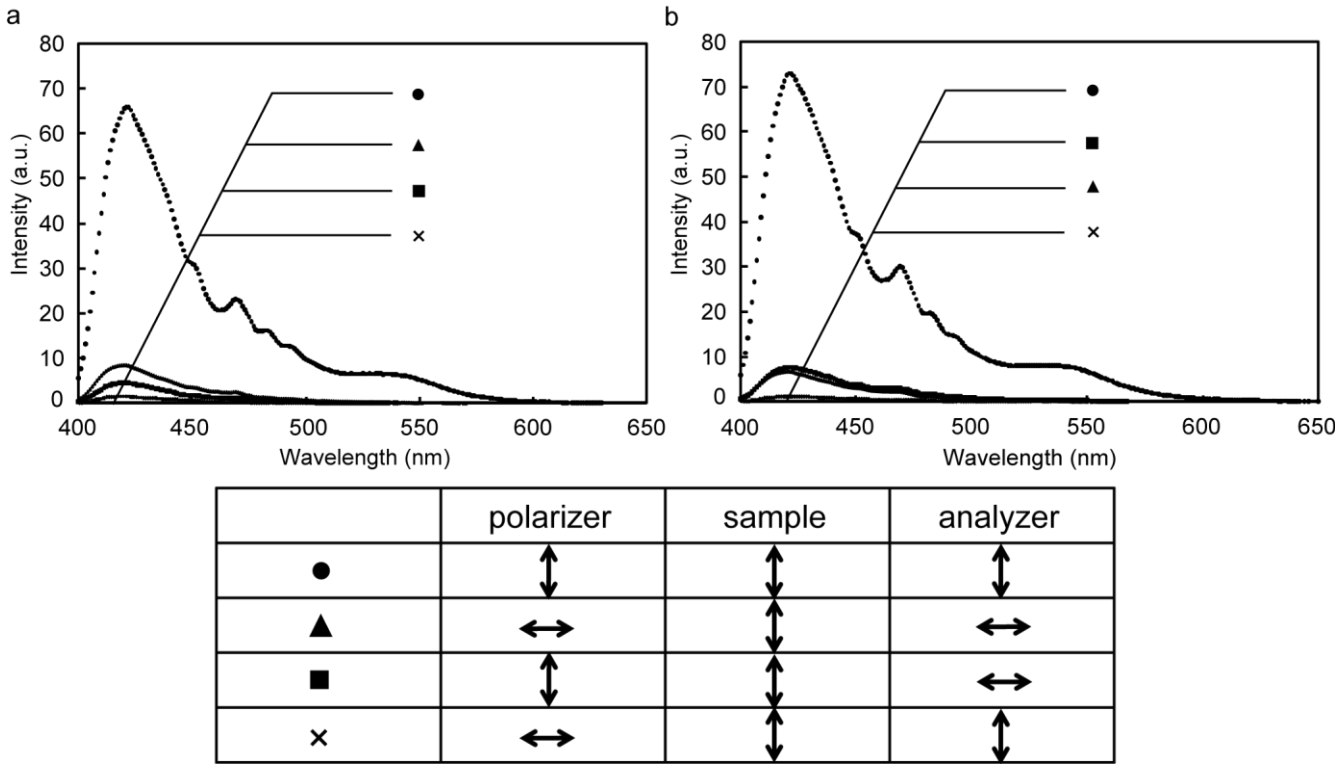

Figure 3-13. Photoluminescence spectra of P(3,4-BAHBA-*co*-4HCA) orientation films with the 4HCA compositions of (**a**) 75 mol% and (**b**) 100 mol% under a polarizer and analyzer irradiated at 374 nm with excited light. The table at the bottom shows direction of the polarizer, sample and analyzer.

Prior to the polarized emission study, we analyzed the photoluminescence spectrum for the representative sheared film P(3,4-BAHBA-*co*-4HCA) with a 4HCA composition of 75% without the polarizer or analyzer. Figure 3-14a shows a spectrogram including two broad peaks around 470 nm and 530 nm on the downward-sloping base line. The peak around 530 nm was assigned to emission of 3,4-BAHBA units because the 3,4-BAHBA homopolymer film showed emission peaks around 530 nm. On the other hand, the peak around 470 nm might be assigned to overlapped emission of both units of 4HCA and 3,4-BAHBA because both homopolymers showed emission peaks around 470 nm. Figure 3-14b and 3-14c show the photoluminescence spectra of the sheared film recorded with the analyzer and polarizer. The polarizer was placed in the light path before the sample, and the analyzer was placed in the

light path between the sample and the detector. The polarizer direction was changed from 0^o to 90^o, where 0^o refers to a direction parallel to the shear direction of the film, and 90^o is perpendicular. In both results of Figure 3-14b and 3-14c, the fluorescence intensity decreased with an increase in the angle (Figure 3-19a and Figure 3-20a, respectively), and showed its maximum at 0^o, which was parallel to the orientation direction of the polymer side chains. This result means that the emissions from oriented films of the copolymer were efficient when the π-electrons of the 3,4-BAHBA side chains were efficiently excited by the light polarized parallel to the side chains (to the shear direction).

Next, both the polarizer and analyzer were placed together. Figure 3-15a shows the photoluminescence spectra recorded under the condition of a 0^o analyzer while rotating the polarizer. Similar to the abovementioned Figure 3-14b and 3-14c results, the photoluminescence intensity decreased with increasing the angles from 0^o to 90^o (Figure 3-19c). However, as shown in Figure 3-15b, the photoluminescence spectra recorded under the condition of a 90^o analyzer showed low intensities almost independent on polarizer angles regardless of the polarizer angle (Figure 3-19e). This phenomenon indicates that the fluorescent light from the 3,4-BAHBA side groups was polarized to be blocked by the 90^o analyzer.

Finally, the polarized emission behavior of the copolymer film was studied under the conditions of the polarizer being fixed at 0^o or 90^o, and the analyzer being rotated. When the polarizer was fixed at 0^o, similar results to Figure 3-15a were obtained as shown in Figure 3-16a and Figure 3-20c. On the other hand, the unique results were obtained when the polarizer was fixed at 90^o (Figure 3-16b). While the luminescent emission around 470 nm increased its intensity after changing the analyzer direction from 0^o (crossed nicol) to 90^o (parallel nicol), the emission around 530 nm decreased. The emission around 470 nm was derived from 4HCA and 3,4-BAHBA emissions in the main chains, whereas the emission around 530 nm was derived from the 3,4-BAHBA side groups as mentioned above. After the π-electrons of

main chains excited by the polarized light in the direction of 90^{o}, the 3,4-BAHBA side groups emitted around 530 nm most efficiently under cross-nicol condition, which suggests that energy transfer from polymer main chains to the 3,4-BAHBA side groups occurred (Figure 3-17). It is noted that the glass substrate showed no fluorescence under these polarimetric condition.

To confirm the generality of such a unique phenomenon, we used homopolymers and other copolymers with 4HCA compositions of 25 and 50 mol%. Figure 3-19b and 3-19d show that the emission wavelength (3,4-BAHBA) was almost constant around 530 nm even when the polarizer was rotated. This phenomenon indicates that the 3,4-BAHBA emission in side groups was more efficient than that of 4HCA and 3,4-BAHBA in main chains. Besides the 3,4-BAHBA emission was controlled by the analyzer direction 0^{o} or 90^{o}.

As shown in Figure 3-20, the emission wavelength became shorter by changing the analyzer direction from parallel to perpendicular to the 3,4-BAHBA side chain, regardless of the polarizer condition and 3,4-BAHBA composition in copolymers. This phenomenon suggests that 3,4-BAHBA emission intensity was lowered by changing the analyzer direction and main chain emission became effective to overlap with 3,4-BAHBA emission. As shown in Figures 3-18b, 3-18c, and 3-18d, 3,4-BAHBA homopolymer and the copolymers showed similar unique tendency to Figure 3-16b and the energy transfer in oriented films occurred. However 4HCA homopolymer showed only negligible fluorescence (Figure 3-18e) and 3,4-BAHBA could play an important role in the polarized emission. Owing to higher composition of 3,4-BAHBA, the intensity change of the 530 nm peak was clearer than Figure 3-16b, and then isosbestic point was clearly detected at 510 nm, indicating that the phenomenon occurred as a result of opposite intensity change of two peaks from main chains and 3,4-BAHBA side chains emissions. In another point of view, the peak red-shift by polarizer direction change from perpendicular to parallel to the sheared direction. Thus, the fluorescent color was changed by changing the analyzer rotation from 0^{o} to 90^{o}.

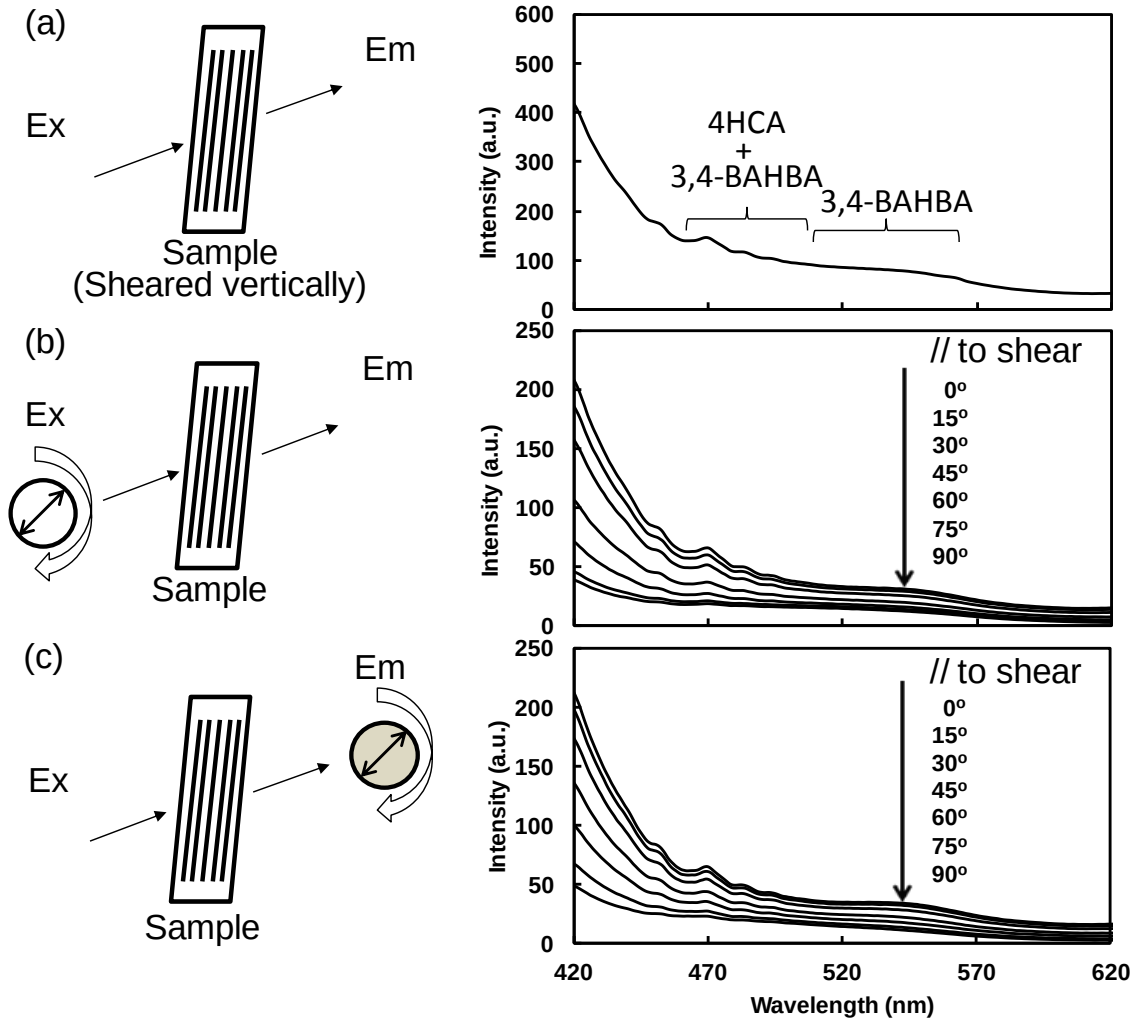

Figure 3-14. (a) Photoluminescence spectra of the sheared film P(3,4-BAHBA-*co*-4HCA) with a 4HCA composition of 75 mol%, recorded a) without polarizer or analyzer, b) under polarizer which was placed into the light path before the sample, but no analyzer was used, and c) under analyzer which was placed into the light path between the sample and a fluorescence detector, but no polarizer was used. The polarizer and analyzer direction changed from an angle of 0^o to 90^o, where 0^o refers to a direction parallel to the shear direction, whereas 90^o refers to the perpendicular.

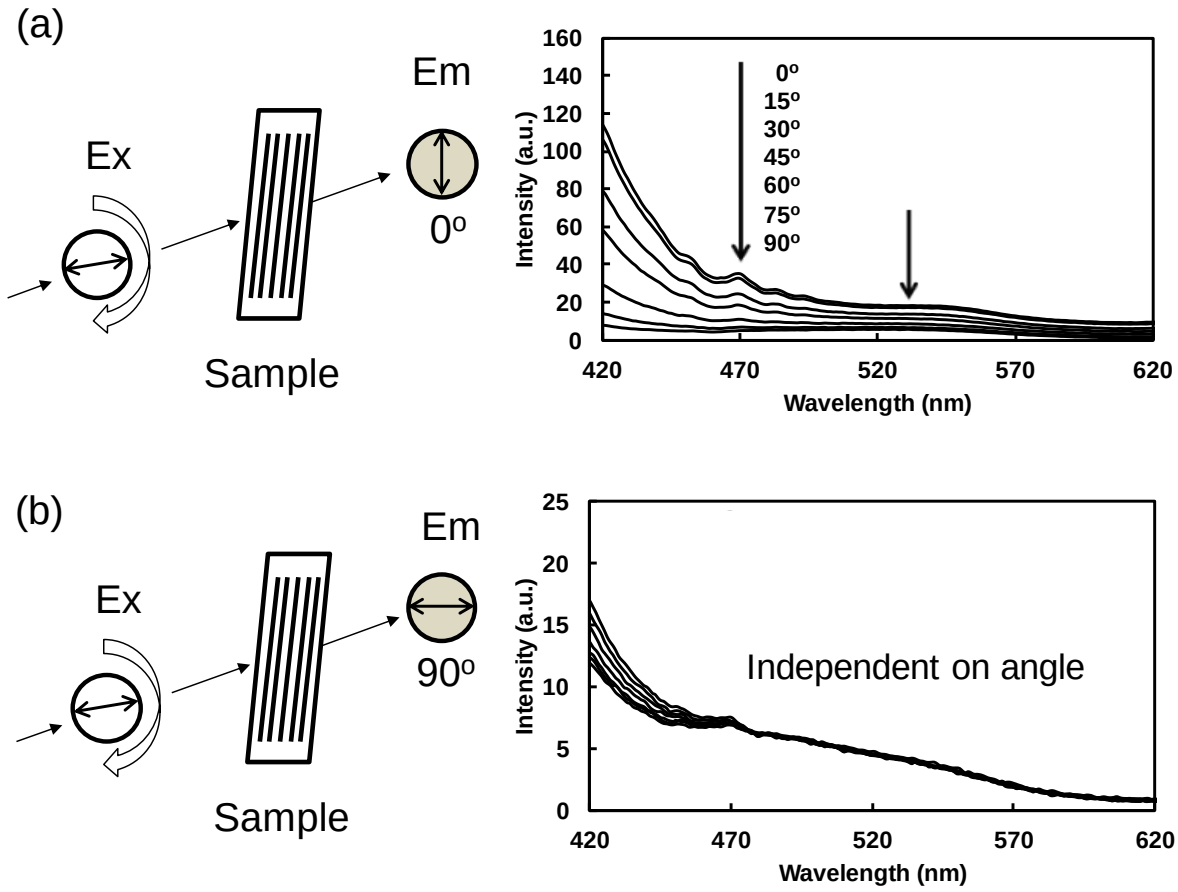

Figure 3-15. Photoluminescence spectra of the sheared film P(3,4-BAHBA-*co*-4HCA) with a 4HCA composition of 75% under both a polarizer and an analyzer, where the polarizer direction changed from 0^o to 90^o while the analyzer direction was fixed at an angle of a) 0^o, and b) 90^o. The positions of polarizer and analyzer, and the angle standard of them were the same with those in Figure 3-14.

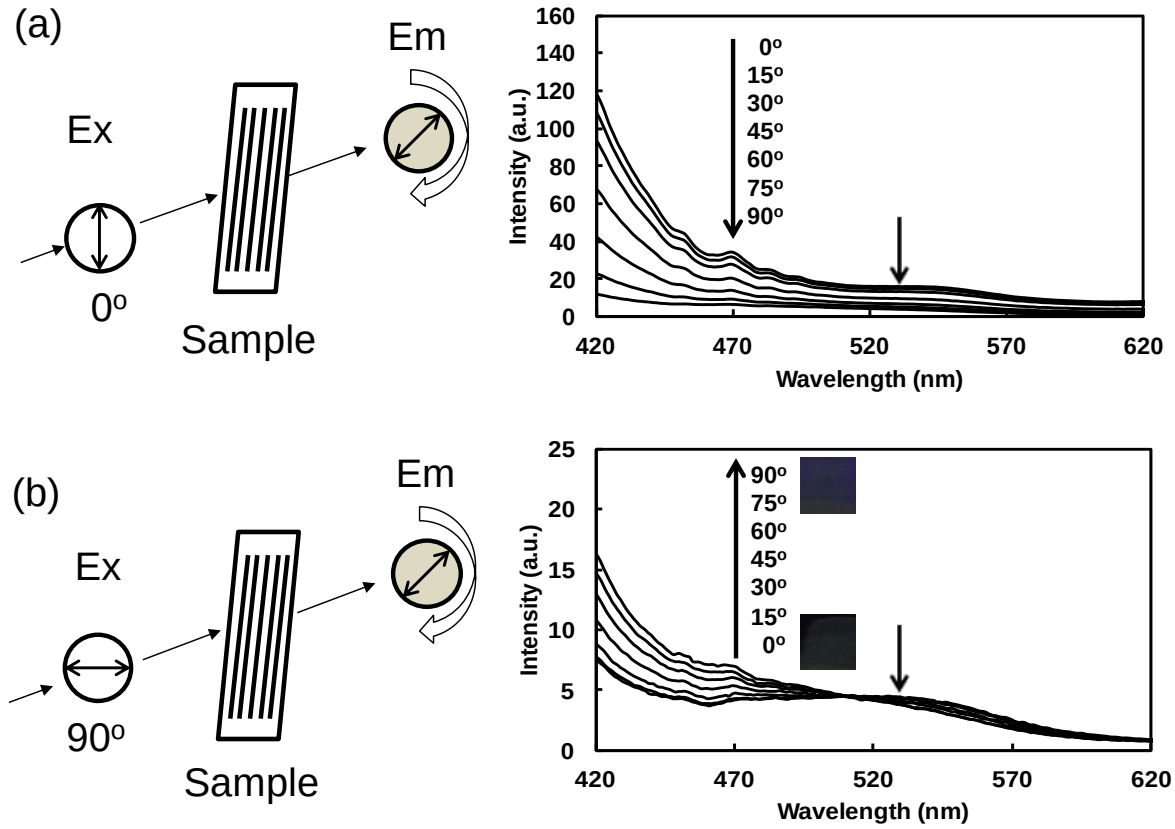

Figure 3-16. Photoluminescence spectra of the sheared film P(3,4-BAHBA-*co*-4HCA) with a 4HCA composition of 75% using both the polarizer and analyzer. (a) The polarizer was fixed at 0^o, and the analyzer rotated from 0^o to 90^o. (b) The polarizer was fixed at 90^o and the analyzer rotated from 0^o to 90^o. Inset pictures of (b) indicated the emission color at 90^o and at 0^o. The positions of polarizer and analyzer, and the angle standard of them were the same with those in Figure 3-14.

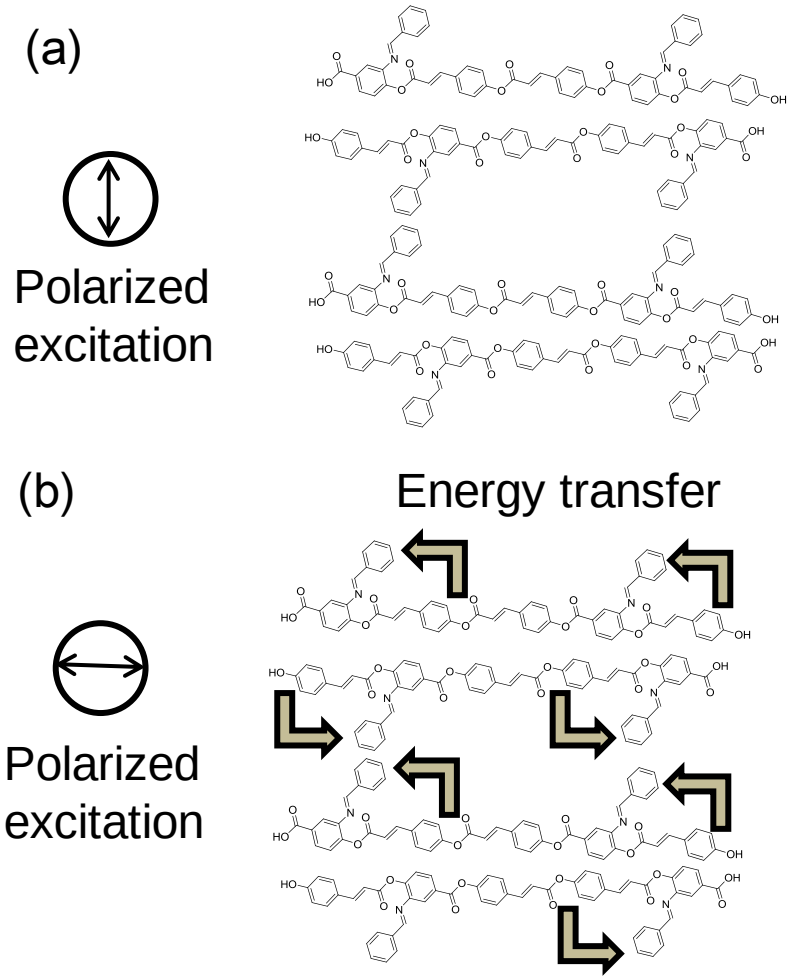

Figure 3-17. Schematic illustration of polarized emission behavior when the polarizer was fixed but the analyzer was rotated under the condition of Figure 5. a) 3,4-BAHBA side groups emitted more efficiently than 4HCA main chain by 0^o excitation. b) 4HCA main chain was efficiently excited by 90^o irradiation but 3,4-BAHBA side chain emitted under 0^o analyzer, presumably due to the energy transfer from 4HCA to 3,4-BAHBA.

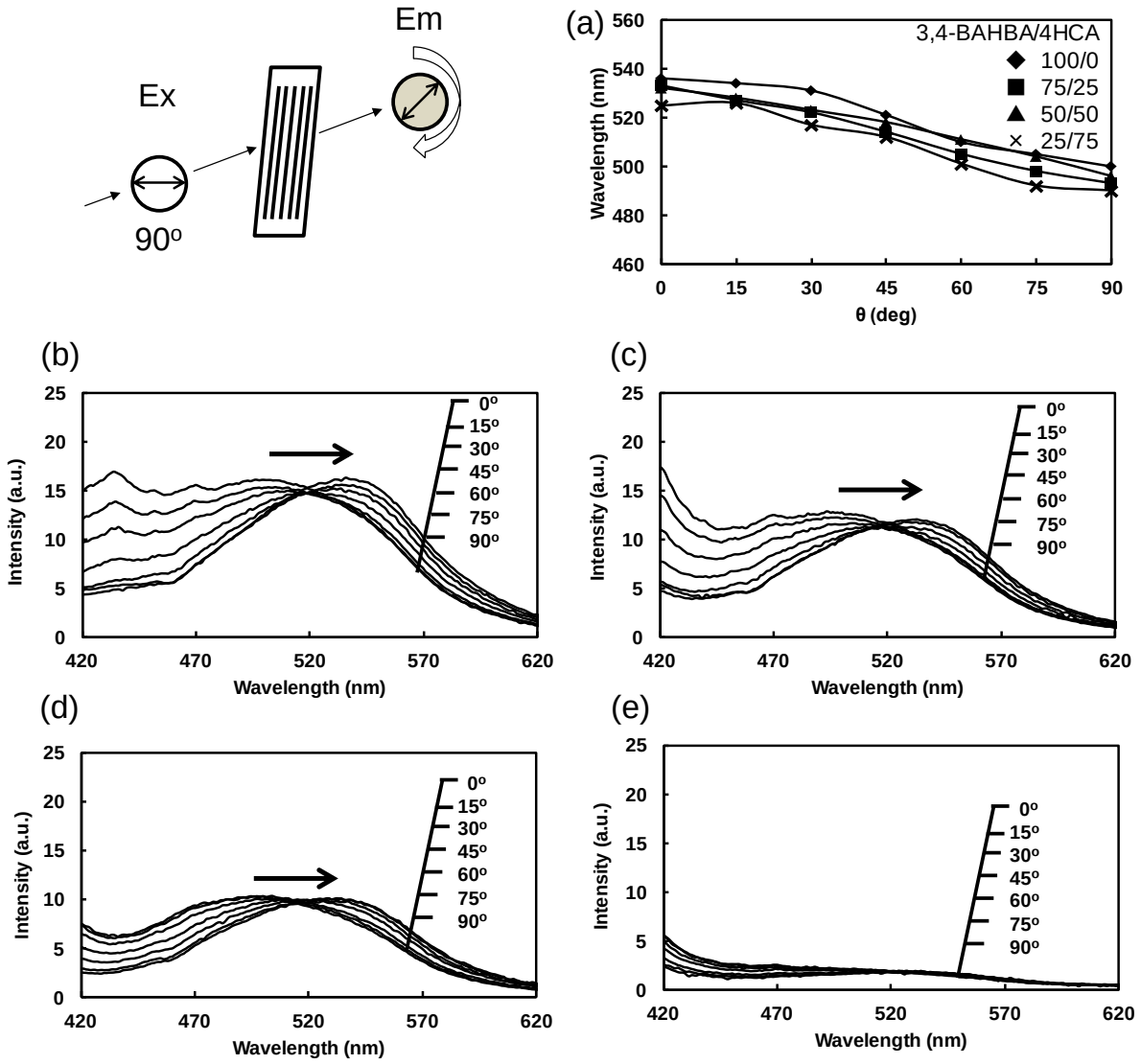

Figure 3-18. (a) The plots of photoluminescence emission λ_{max} of polymers against analyzer angle (θ). (b-e) Photoluminescence spectra of the sheared films of (b) P(3,4-BAHBA), P(3,4-BAHBA-*co*-4HCA) with a 4HCA composition of (c) 25 mol%, (d) 50 mol%, and (e) P4HCA recorded under the same polarimetry condition with Figure 3-16.

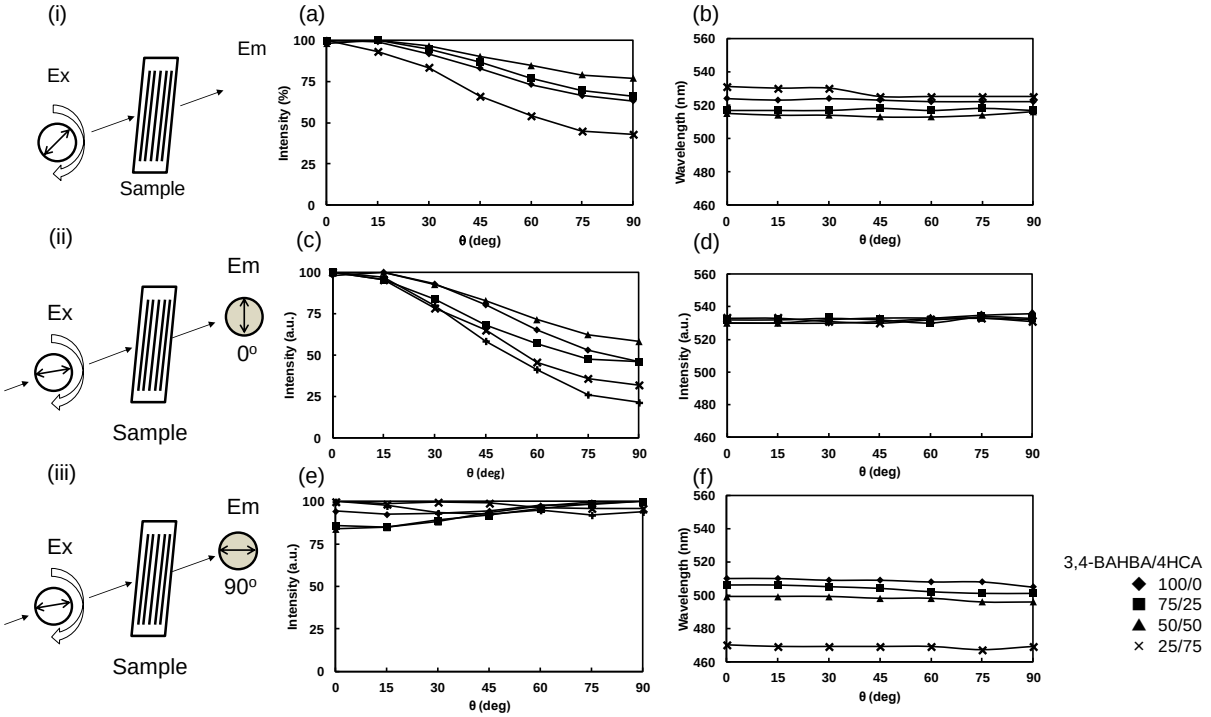

Figure 3-19. Change in photoluminescence intensity and emission wavelength of the sheared film of P(3,4-BAHBA), P(3,4-BAHBA-*co*-4HCA)s with 4HCA compositions of 25 mol%, 50 mol%, and 75 mol% when the polarizer was rotated from 0^o to 90^o. The polarizer was placed into the light path before the sample. The polarizer direction changed from 0^o to 90^o, where 0^o refers to a direction parallel to the shear direction, whereas 90^o refers to the perpendicular. In (i), no analyzer was used. In (ii), the analyzer was fixed at 0^o (parallel to the shear direction). In (iii), the analyzer was fixed at 90^o (perpendicular to the shear direction). The emission intensities at 530 nm normalized as percentage of the intensity at a 0^o analyzer (a, c, e). The emission λ_{max} values (b,d,f).

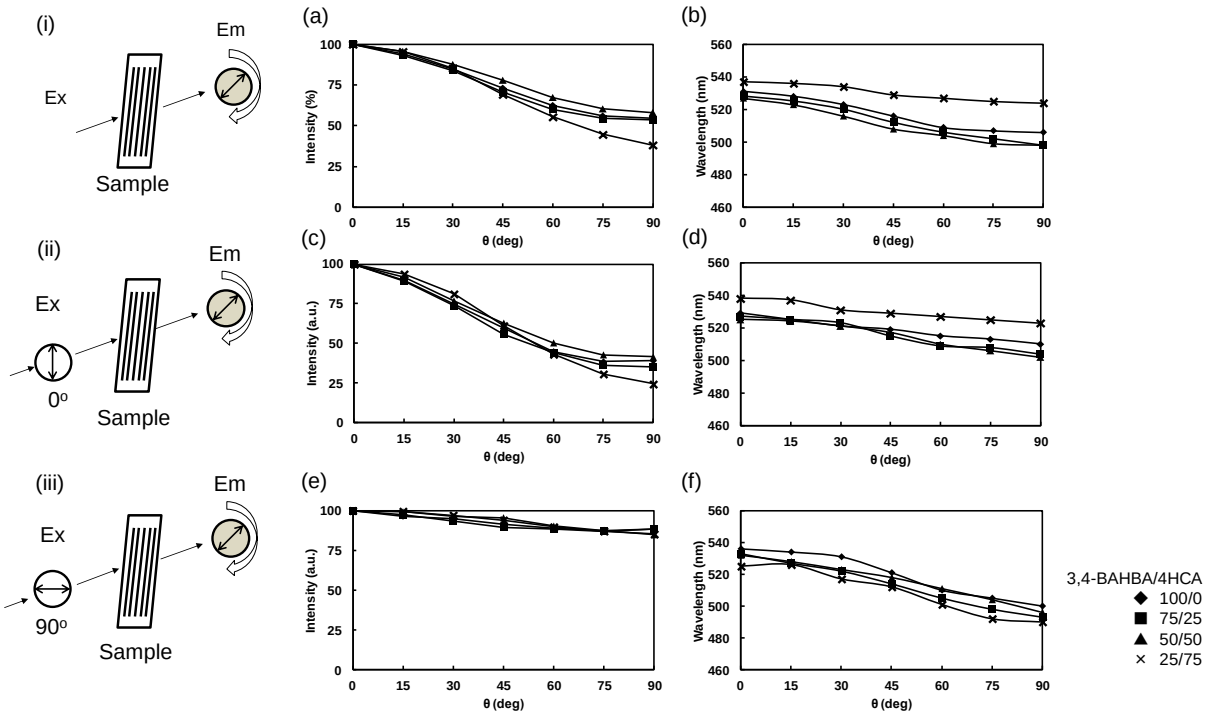

Figure 3-20. Change in photoluminescence intensity and emission wavelength of the sheared film of P(3,4-BAHBA), P(3,4-BAHBA-*co*-4HCA)s with 4HCA compositions of 25 mol%, 50 mol%, and 75 mol% when the analyzer was rotated from 0^o to 90^o. The analyzer was placed into the light path between the sample and a fluorescence detector. The analyzer direction changed from 0^o to 90^o, where 0^o refers to a direction parallel to the shear direction, whereas 90^o refers to the perpendicular. In (i), no polarizer was used. In (ii), the polarizer was fixed at 0^o (parallel to the shear direction). In (iii), the polarizer was fixed at 90^o (perpendicular to the shear direction). The emission intensities at 530 nm normalized as percentage of the intensity at a 0^o analyzer (a, c, e). The emission λ_{max} values (b,d,f).

3.4 Conclusion

In order to prepare new functional bio-based polymers with LC properties, poly{3-benzylidene amino-4-hydroxybenzoic acid (3,4-BAHBA)-*co*-*trans*-4-hydroxycinnamic acid (4HCA: *trans*-coumaric acid)} (P(3,4-BAHBA-*co*-4HCA)) was synthesized by a thermal polycondensation of 4HCA and 3,4-BAHBA, which was synthesized by a reaction of 3-amino-4-hydroxybenzoic acid (3,4-AHBA) with benzaldehyde. When the 4HCA compositions of P(3,4-BAHBA-*co*-4HCA)s were above 55 mol%, the copolymers showed a nematic liquid crystalline phase due to the mesogenic effects of the continuous 4HCA units. The oriented samples of fibers and films were successfully processed, which both showed positive birefringence. The fiber of the copolymer with a 4HCA composition of 75 mol% showed a clear X-ray image, indicating that the main chains were oriented perpendicularly to the fiber axis. These results of birefringence and XRD study suggest the main chains in the films also oriented perpendicularly to the shear direction. The copolymers in an NMP solution showed photoluminescence under 365 nm, and the corresponding oriented films of P(3,4-BAHBA-*co*-4HCA)s with a 4HCA composition of 75 mol% emitted polarized light, as confirmed by fluorescent spectroscopy equipped with paralleled and crossed polarizers. Furthermore, the oriented film showed polarized emissions and color change dependent on the angle of the analyzer rotation with the polarizer perpendicular to the shear direction. This phenomenon is very important for developing advanced photonic devices using light emitting diodes [106-116], organic lasers [117-121], and could be exhibited from LC oriented polymers with fluorescent moieties in both the main-chain and the side-chains. In addition, the fluorescent color change exhibited by liquid crystalline moieties is useful for potential applications such as memory devices, fluorescent sensors, security materials, and information displays [122-131]. Thus, the author prepared new, rigid-rod oligomers with LC-related photoemission properties derived from aromatic structures in biomolecules available from microorganisms.

Chapter 4

Syntheses of novel polybenzobisoxazoles from symmetric π-conjugated azine compounds

CHAPTER 4

4.1 Introduction

Conjugated polymers attracted considerable attention from the scientific field such as electronic and optoelectronics [132-134]. Their structure consists of alternating single and double bonds. (Figure 4-1) In this system, on giving external stimuli such as doping reactions, it showed conductivity or luminescent properties, i.e. poly(acetylene) [135]. In this meaning, conjugated polymer system could be applied for light-emitting diodes and thin film transistors [136,137]. Compared with the traditional inorganic LEDs, the conjugated polymer-based LEDs have many advantages such as color-controllability, bendability, and easy-fabrication. Among all the existing conjugated polymers, polybenzoxazole family, "poly(*p*-phenylene benzobisoxazole) (PBO) and poly(2,5-benzoxazole) (ABPBO)" have been studied since the early 1980s (Figure 4-2) [20, 138-143]. PBOs showed higher modulus and strength than DuPont's Kevlar, [poly(*p*-phenyleneterephthalamide) (PPTA)] [144], and excellent mechanical properties, thermo-stability and environmental stability. This is because the π-conjugated and rigid structure of PBOs brings about many outstanding optical properties as well as mechanical properties and thermal stability. Recently, many conjugated polybenzoxazoles have been synthesized and their optical and electronic properties have been investigated in detail [145-149].

Typically, PBOs are prepared by condensation polymerization using a strong acid such as poly(phosphoric acid) (PPA) [138,139], which formed liquid crystalline phases during polymerization at concentrations above 5 wt% [20]. After condensation, PBO films were fabricated from a PPA solution. However, it has difficultly of removal of the residual PPA, only acid by using as the solvent for PBO, and deterioration of the mechanical property [150].

To overcome this problem, the fabrication of PBO films is the fabrication of precursor films followed by conversation to PBO films [151-155]. In this approach, PBO is made by two steps by soluble in an organic solvent PBO precursor, poly(hydroxyl amide), is required, and followed by thermal cyclodehydration reaction. It is similar to the fabrication of polyimide films from a polyamic acid solution [156].

In this chapter, the author reports the synthesis of the novel aromatic symmetric precursor polymer by starting from 3,4-AHBA derivatives and the stepwise cyclization from precursor to PBO under different thermal conditions. The author further investigated the Fourier transform infrared (FT-IR) spectroscopy, nuclear magnetic resonance (NMR), and thermogravimetric analysis.

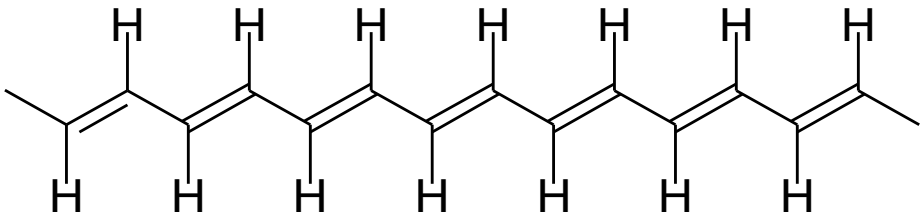

Figure 4-1. The structure of π-conjugated polymer, polyacetylene.

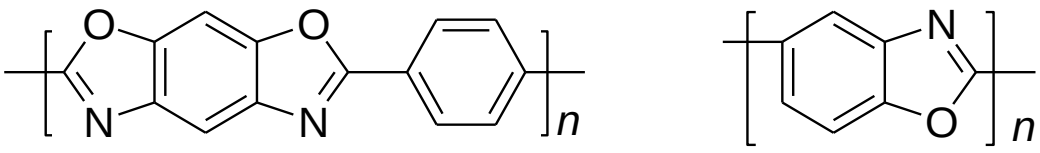

Figure 4-2. The typical structure of poly(*p*-phenylene benzobisoxazole) (PBO) and poly(2,5-benzoxazole) (ABPBO).

4.2 Experimental section

4.2.1 Materials

3-nitro-4-hydroxybenzaldehyde (3,4-NHBAL), terephthaloyl dichloride (TC), isophthaloyl dichloride (IC), 2,5-furandicarboxylic acid (FA) were purchased from TCI. TC and IC were purified by recrystallization from *n*-hexane and the 3,4-NHBAL and FA were used as received. Methanol (MeOH), dichloromethane (DCM), hydrazine monohydrate, thionyl chloride ($SOCl_2$), *N*,*N*-dimethylacetamide, dehydrated (DMAc) were purchased from Kanto chemicals, and used as received. Palladium-activated carbon (Pd 5%) was purchased from Kanto chemicals, and used as received. DMSO-d_6 (Sigma-Aldrich Co.) used as an NMR solvent was also used as received.

4.2.2 Synthesis of *N,N'*-Bis-(3-nitro-4-hydroxy-benzylidene)-hydrazine (3,4-NHBZL)

3,4-NHBAL (5.0 g) was dissolved in 150 ml DCM to create a homogeneous liquid, which was stirred at room temperature under nitrogen. In this homogeneous solution, hydrazine monohydrate (0.8 ml, 16 mmol) was slowly added one drop by syringe. A yellow solid of compound was getting when adding hydrazine monohydrate. After 3 hours, the product was filtered and washed with dichloromethane. The resultant solid was dried under vacuum, yield: 4.4 g (89%), mp: 275 ^{o}C. IR (in cm^{-1}):3268 (ν_{O-H}) 1664 ($\nu_{C=O}$), 1626 ($\nu_{C=N}$), 1533, 1372, 1327(ν_{C-NO2}) (Figure 4-4). ^{1}H-NMR (500 MHz, DMSO-d_6, δ, ppm): 11.67 (s, 1H, OH, H^e), 8.68 (s, 2H, CH=N, H^d), 8.35 (d, J = 2.0 Hz, 2H, aryl H^a), 8.03 (dd, J = 8.7, 2.0 Hz, 2H, aryl H^b), 7.23 (d, J = 8.7 Hz, 2H, aryl, H^c) (Figure 4-5). ^{13}C-NMR (125 MHz, DMSO-d_6, δ, ppm): 159.7 (CN, C^a), 154.4 (aryl, C^e), 137.1 (aryl, C^d), 133.8 (aryl, C^g), 125.8 (aryl, C^c), 125.2 (aryl, C^b), 119.8 (aryl, C^f) (Figure 4-6). The results of HSQC and HMBC are shown in Figure 4-7 and Figure 4-8.

Scheme 4-1. Synthesis of 3,4-NHBZL

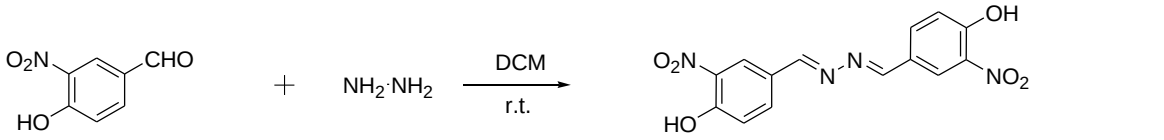

3-nitro-4-hydroxybenzaldehyde (3,4-NHBAL) | Hydrazine | *N,N'*-Bis-(3-nitro-4-hydroxy-benzylidene)-hydrazine (3,4-NHBZL)

Figure 4-3. The image of 3,4-NHBZL.

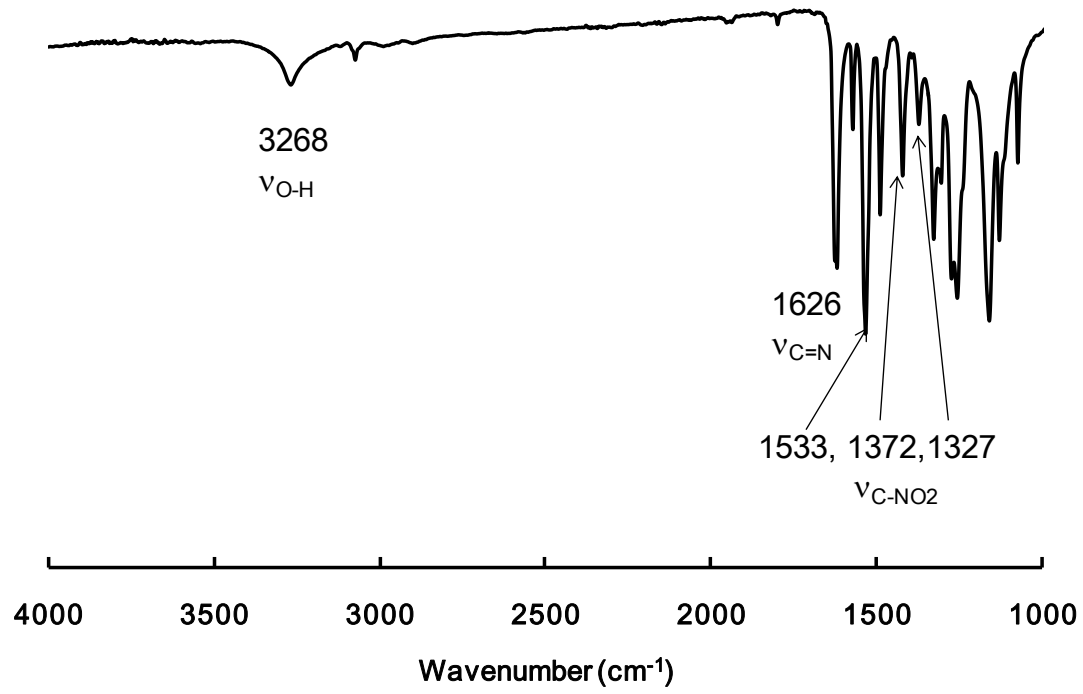

Figure 4-4. The FT-IR spectrum of 3,4-NHBZL.

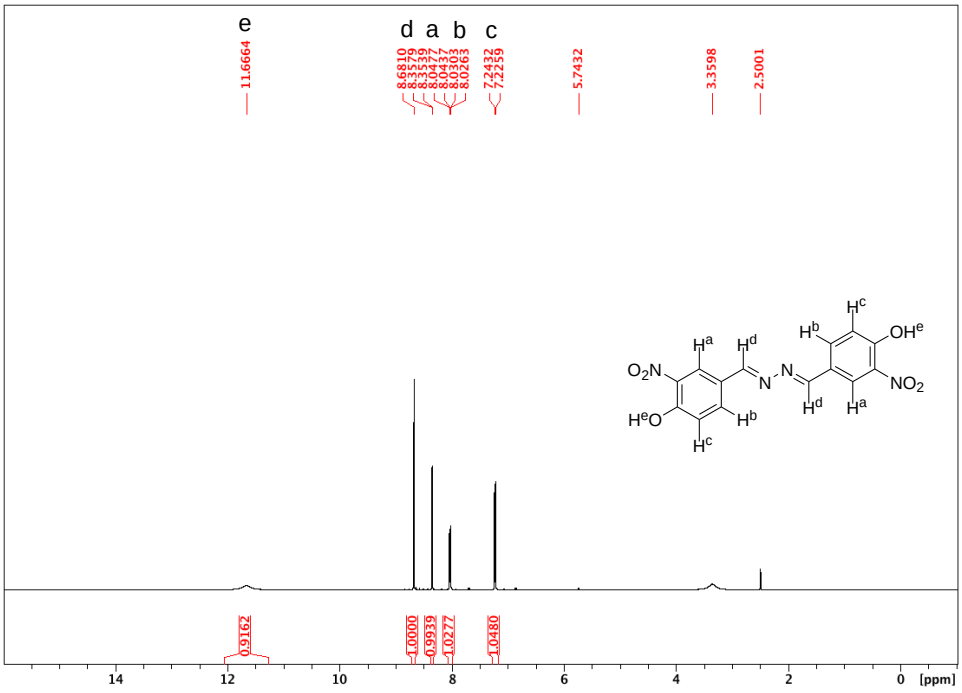

Figure 4-5. ^{1}H-NMR spectrum of 3,4-NHBZL.

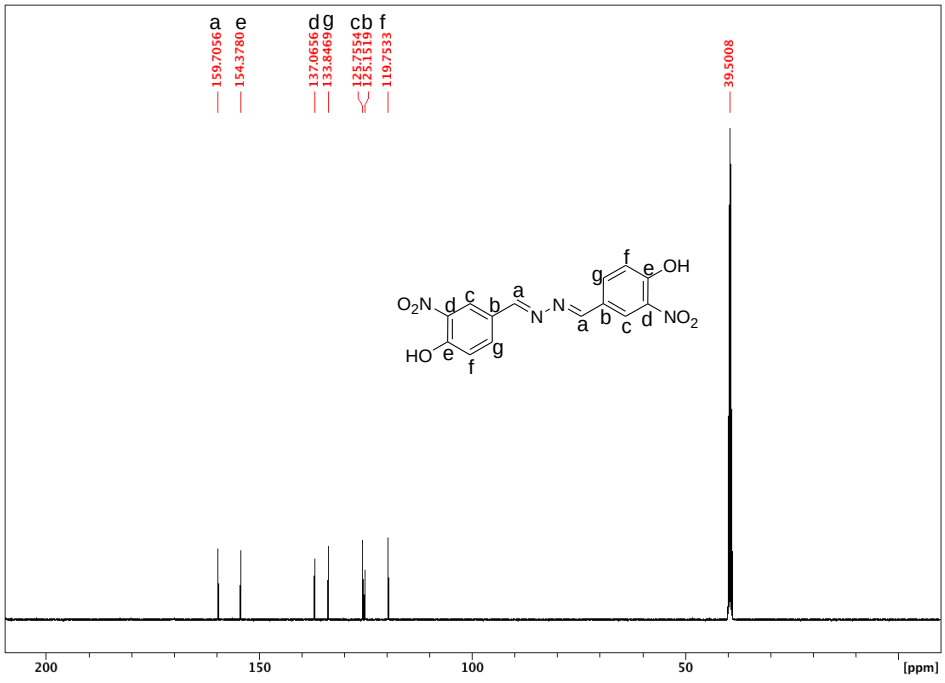

Figure 4-6. ^{13}C-NMR spectrum of 3,4-NHBZL.

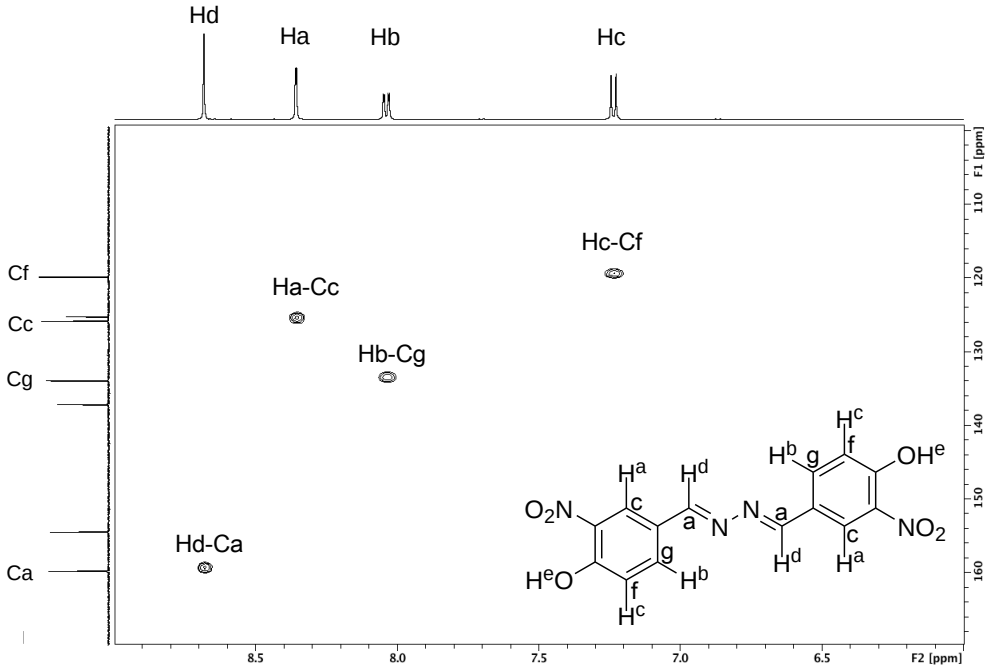

Figure 4-7. HSQC spectrum of 3,4-NHBZL.

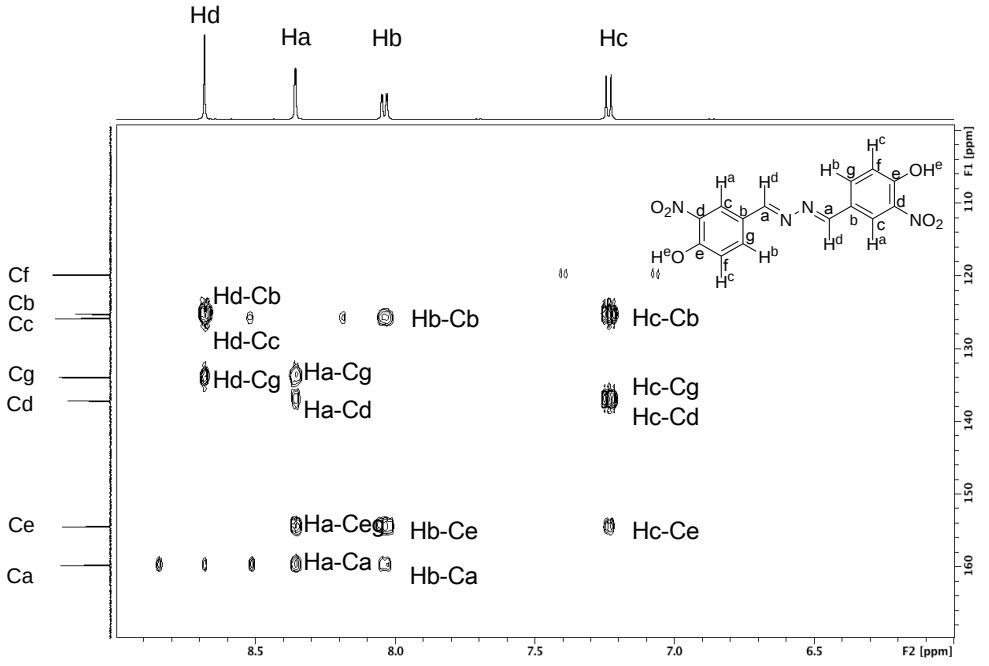

Figure 4-8. HMBC spectrum of 3,4-NHBZL.

4.2.3 Synthesis of *N,N'*-Bis-(3-amino-4-hydroxy-benzylidene)-hydrazine (3,4-AHBZL)

3,4-NHBZL (4 g) and Pd/C were suspended in 400 ml MeOH. H_2 gas was passed into the mixture. After 5h the reaction mixture dissolved in methanol. The mixture was filtered, washed with methanol to separate Pd/C and filtrate was evaporated to get occur color powder. The resultant solid was dried under vacuum, yield: 1.7 g (55%), mp: 259 ^{o}C. IR (in cm^{-1}): 3376 (ν_{NH2}), 3294 (ν_{O-H}), 1664 ($\nu_{C=O}$), 1625 ($\nu_{C=N}$) (Figure 4-10). ^{1}H-NMR (500 MHz, DMSO-d_6, δ, ppm): 9.64 (s, 1H, OH, H^e), 8.38 (s, 2H, CH=N, H^d), 7.17 (d, J = 1.8 Hz, 2H, aryl H^a), 6.86 (dd, J = 8.1, 1.9 Hz, 2H, aryl H^b), 6.72 (d, J = 8.0 Hz, 2H, aryl, H^c) (Figure 4-11). ^{13}C-NMR (125 MHz, DMSO-d_6, δ, ppm): 160.6 (CN, C^a), 147.4 (aryl, C^e), 137.0 (aryl, C^d), 125.7 (aryl, C^b), 119.3 (aryl, C^g), 114.0 (aryl, C^f), 112.0 (aryl, C^c) (Figure 4-12). The results of DEPT 45, DEPT 90, DEPT135, HSQC, HMBC are shown in Figure 4-13, Figure 4-14, Figure 4-15, Figure 4-16, Figure 4-17. ESI FT-ICR MS $[M+H]^+$: 271.11578, Calcd. for $C_{14}H_{11}N_4O_6$: 271.11168.

Scheme 4-2. Synthesis of 3,4-AHBZL

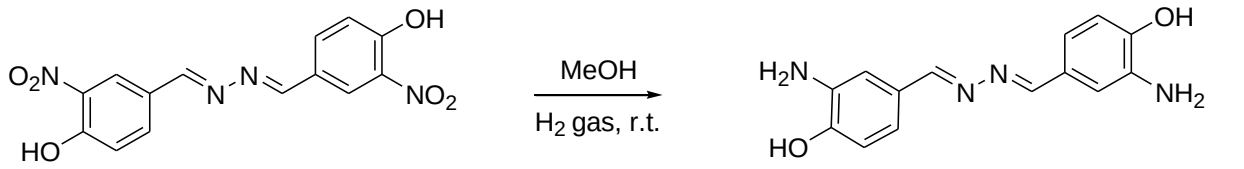

N,N'-Bis-(3-nitro-4-hydroxy-benzylidene)-hydrazine (3,4-NHBZL)

N,N'-Bis-(3-amino-4-hydroxy-benzylidene)-hydrazine (3,4-AHBZL)

Figure 4-9. The image of 3,4-AHBZL.

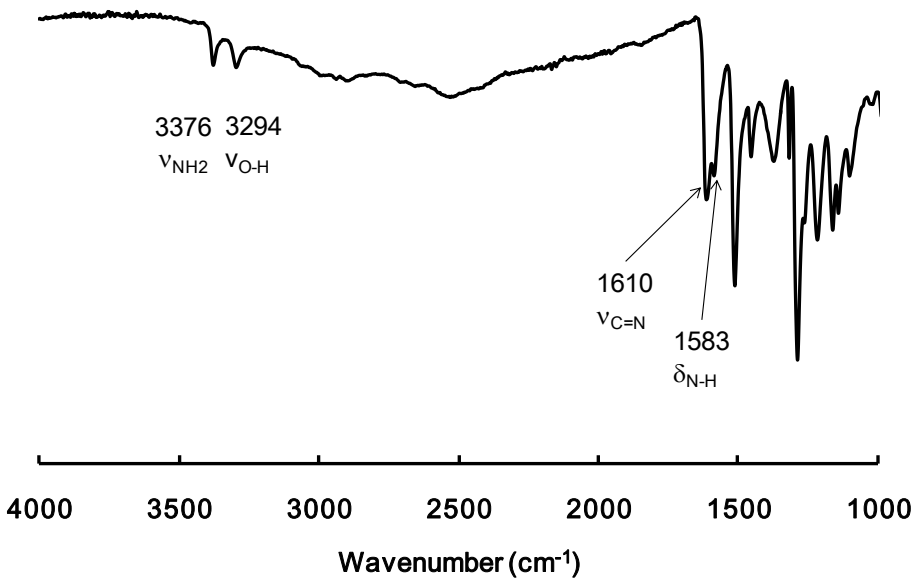

Figure 4-10. The FT-IR spectrum of 3,4-AHBZL.

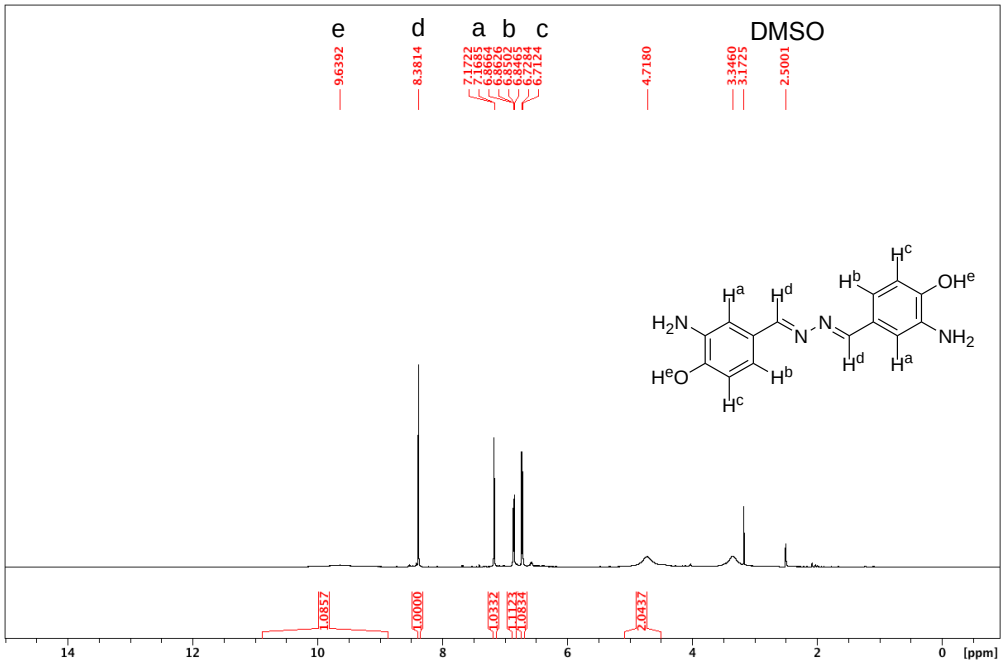

Figure 4-11. ^{1}H-NMR spectrum of 3,4-AHBZL.

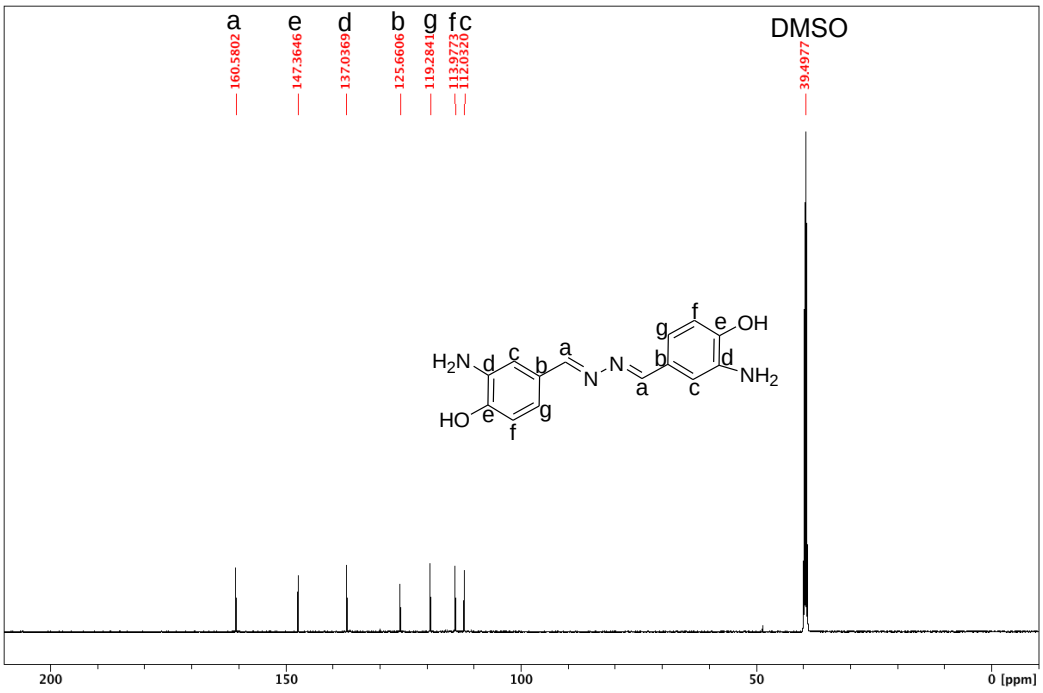

Figure 4-12. ^{13}C-NMR spectrum of 3,4-AHBZL.

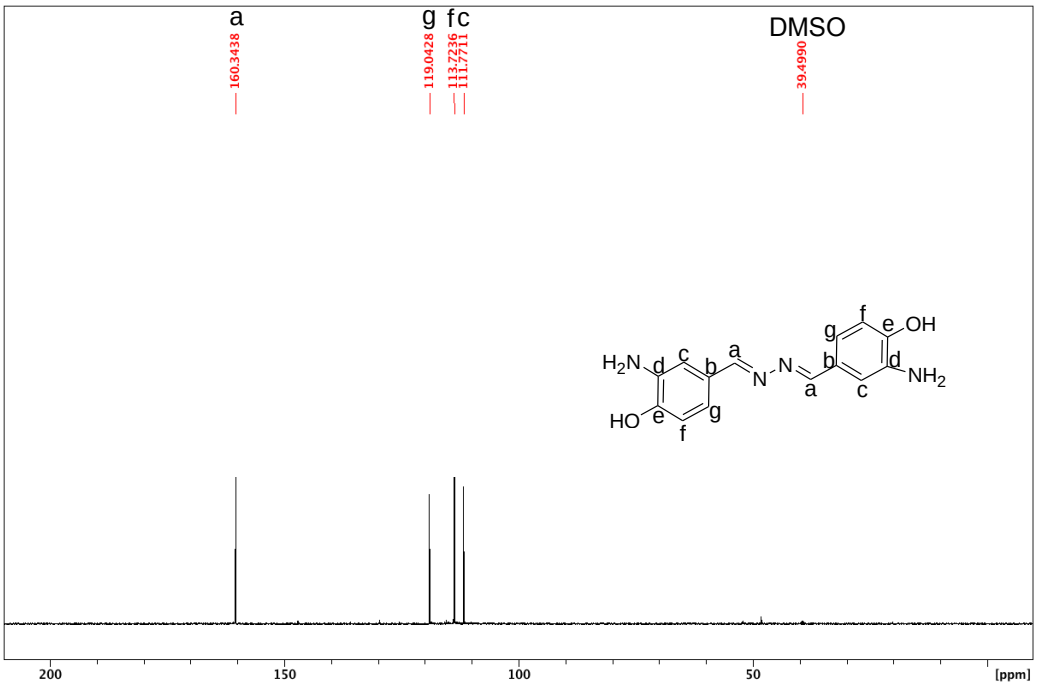

Figure 4-13. 45^{o}-DEPT NMR spectrum of 3,4-AHBZL.

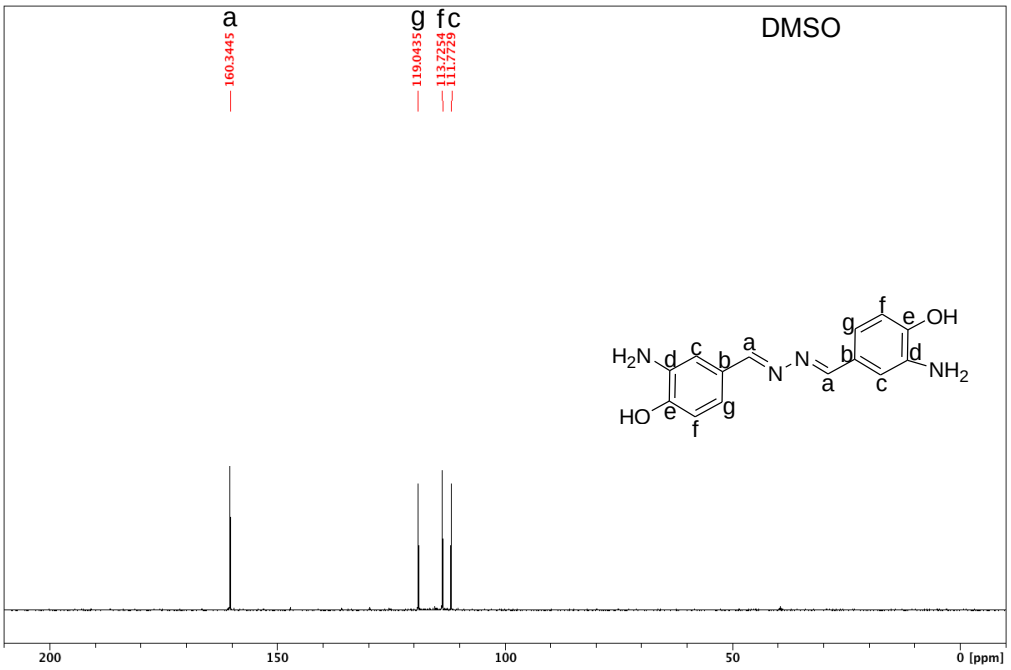

Figure 4-14. 90°-DEPT NMR spectrum of 3,4-AHBZL.

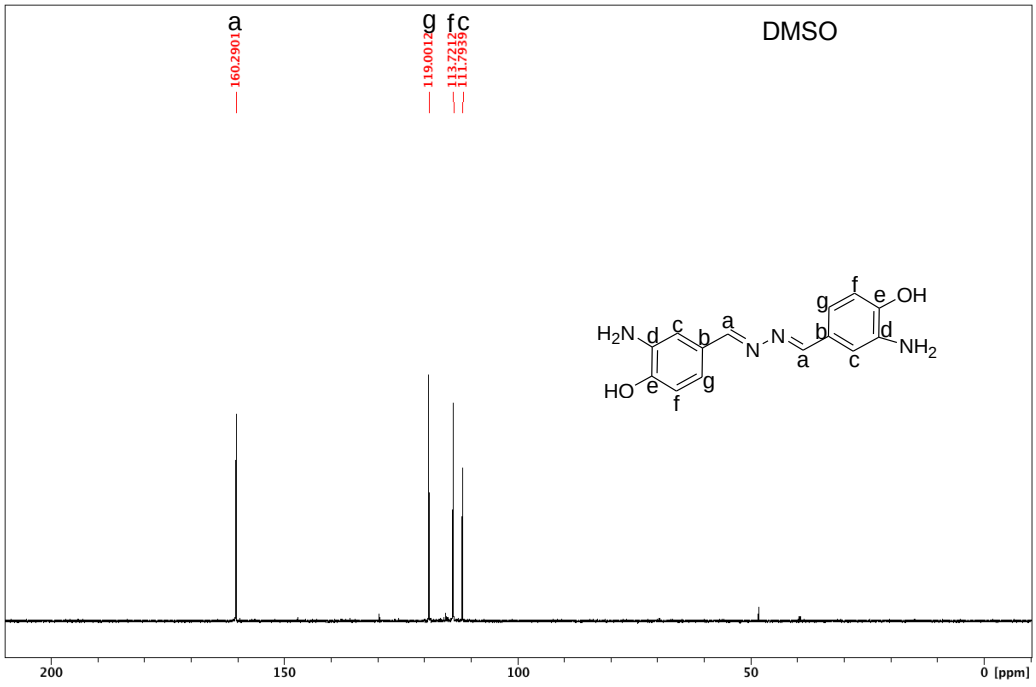

Figure 4-15. 135°-DEPT NMR spectrum of 3,4-AHBZL.

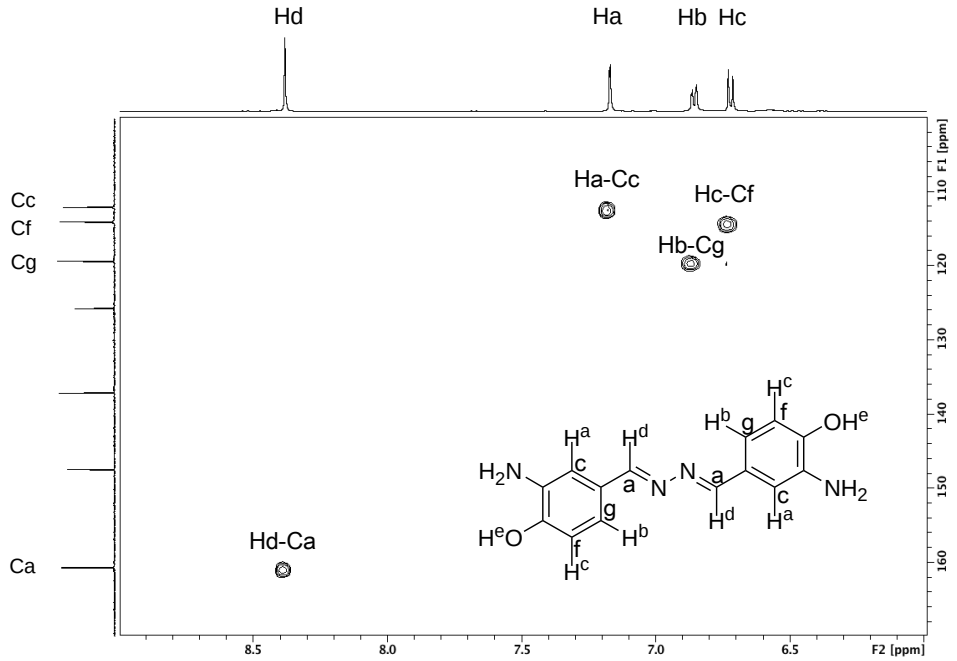

Figure 4-16. HSQC spectrum of 3,4-AHBZL.

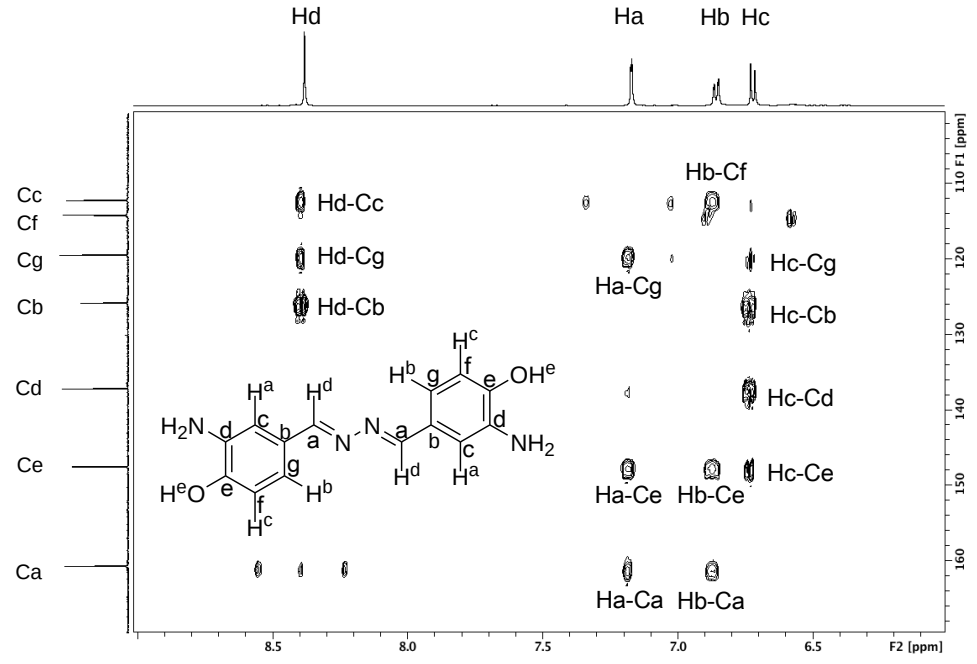

Figure 4-17. HMBC spectrum of 3,4-AHBZL.

4.2.4 Syntheses of PBO precursors

PBO precursor synthesis from 3,4-AHBZL and TC

A typical preparation of 3,4-AHBZL-TC poly(hydroxyl amide) (PHA) precursor proceeds as follows. Under a nitrogen atmosphere, 3,4-AHBZL (0.20 g) was dissolved in DMAc solution (0.5 ml) and then cooled to 0 ^{o}C. TC (0.15 g) was also dissolved in DMAc solution (0.5 ml) under a nitrogen atmosphere at room temperature. TC DMAc solution was slowly added to the solution of 3,4-AHBZL. After addition of TC, the mixture was stirred at room temperature for 48h. The solution was poured into 20 ml of methanol to produce a precipitate, which was filtered. The obtained solid was dried at room temperature overnight in a vacuum that produced an ocher color powder. yield: 0.24 g (82%). IR (in cm^{-1}): 1635 ($\nu_{C=O}$), 1537(δ_{N-H}) (Figure 4-18 (a)). ^{1}H-NMR (400 MHz, DMSO-d_6, δ, ppm): 10.57 (s, 2H, OH, H^{f}), 9.78 (s, 2H, amide, H^{e}), 8.64 (s, 2H, CH=N, H^{d}), 8.27 (m, 2H, aryl-H^{a}), 8.14 (s, 4H, aryl-H^{α}), 7.58 (m, 2H, aryl-H^{b}), 7.06 (d, 2H, aryl-H^{c}) (Figure 4-18 (c)).

Scheme 4-3. Synthesis of 3,4-AHBZL-TC PHA

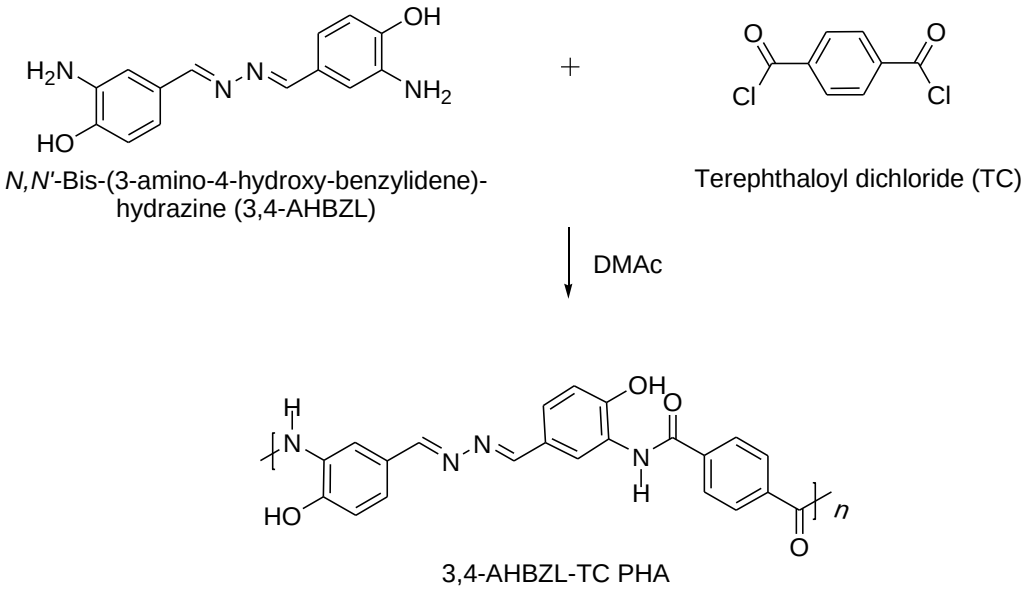

N,N'-Bis-(3-amino-4-hydroxy-benzylidene)-hydrazine (3,4-AHBZL)

Terephthaloyl dichloride (TC)

3,4-AHBZL-TC PHA

PBO precursor synthesis from 3,4-AHBZL and IC

A typical preparation of 3,4-AHBZL-IC poly(hydroxyl amide) (PHA) precursor proceeds as follows. Under a nitrogen atmosphere, 3,4-AHBZL (0.2 g) was dissolved in DMAc solution (0.5 ml) and then cooled to 0 ^{o}C. IC (0.15 g) was also dissolved in DMAc solution (0.5 ml) under a nitrogen atmosphere at room temperature. IC DMAc solution was slowly added to the solution of 3,4-AHBZL. After addition of IC, the mixture was stirred at room temperature for 48h. The solution was poured into 20 ml of methanol to produce a precipitate, which was filtered. The obtained solid was dried at room temperature overnight in a vacuum that produced an occur color powder. yield: 0.19 g (65%). IR (in cm^{-1}): 1646 ($\nu_{C=O}$), 1530 (δ_{N-H}) (Figure 4-19 (a)). ^{1}H-NMR (400 MHz, DMSO-d_6, δ, ppm): 10.54 (s, 2H, OH, H^{f}), 9.80 (s, 2H, amide, H^{e}), 8.69 (m, 1H, aryl-H^{β}), 8.60 (s, 2H, CH=N, H^{d}), 8.28 (s, 2H, aryl-H^{a}), 8.19 (m, 2H, aryl- H^{β}), 7.70 (m, 2H, aryl-H^{b}), 7.57 (m,1H, aryl-H^{β}), 7.06 (d, 2H, aryl- H^{c}) (Figure 4-19 (c)).

Scheme 4-4. Synthesis of 3,4-AHBZL-IC PHA

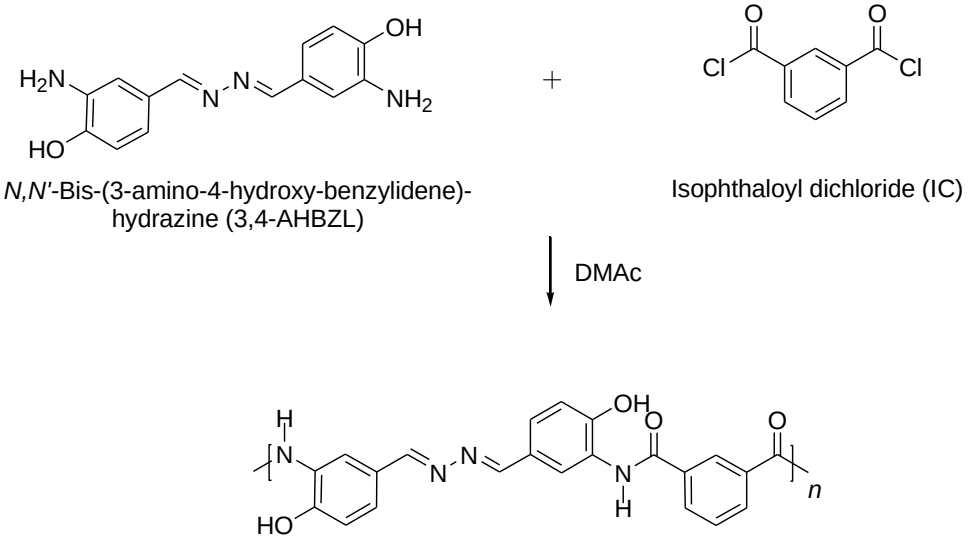

N,N'-Bis-(3-amino-4-hydroxy-benzylidene)-hydrazine (3,4-AHBZL)

Isophthaloyl dichloride (IC)

3,4-AHBZL-IC PHA

PBO precursor synthesis from 3,4-AHBZL and FC

2,5-Furandicarbonyl chloride (FC) was prepared wrote below [157]. 0.12 g of 2,5-Furandicarboxylic acid (FA), 1.1 ml of $SOCl_2$ was introduced into a round bottom flask fitted with a condenser and a magnetic stirrer, and the mixture was refluxed at 80 ^oC for 3h with constant stirring. After the reaction, the bottom was cooled to room temperature. The excess of $SOCl_2$ was removed under vacuum at room temperature and collected in a trap cooled with liquid nitrogen and concentrated sodium hydroxide trap. This product was directly used for PBO precursor synthesis.

Scheme 4-5. Synthesis of FC

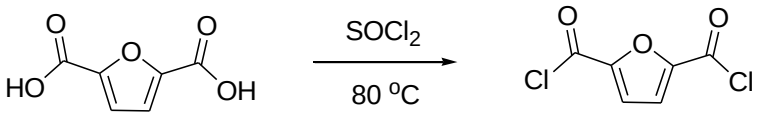

2,5-Furandicarboxylic acid (FA) 2,5-Furandicarbonyl chloride (FC)

A typical preparation of 3,4-AHBZL-FC poly(hydroxyl amide) (PHA) precursor proceeds as follows. Under a nitrogen atmosphere, 3,4-AHBZL (0.2 g) was dissolved in DMAc solution (0.5 ml). FC prepared above was also dissolved in DMAc solution (0.5 ml) under a nitrogen atmosphere and then cooled to 0 ^oC. 3,4-AHBZL DMAc solution was slowly added to the cooling FC solution. After addition of the solution of 3,4-AHBZL DMAc, the mixture was stirred at room temperature for 48h. The solution was poured into 20 ml of methanol to produce a

precipitate, which was filtered. The obtained solid was dried at room temperature overnight in a vacuum that produced an occur color powder. yield: 0.23 g (79%). IR (in cm^{-1}): 1653 ($\nu_{C=O}$), 1531 (δ_{N-H}) (Figure 4-20 (a)). ^{1}H-NMR (400 MHz, DMSO-d_6, δ, ppm): ^{1}H-NMR (400 MHz, DMSO-d_6, δ, ppm): 10.72 (s, 2H, OH, H^f), 9.86 (s, 2H, amide, H^e), 8.62 (s, 2H, CH=N, H^d), 8.20 (m, 2H, aryl-H^a), 7.60 (m, 2H, aryl-H^a), 7.42 (s, 2H, furan-H^γ), 7.07 (d, 2H, aryl-H^c) (Figure 4-20 (c)).

Scheme 4-6. Synthesis of 3,4-AHBZL-FC PHA

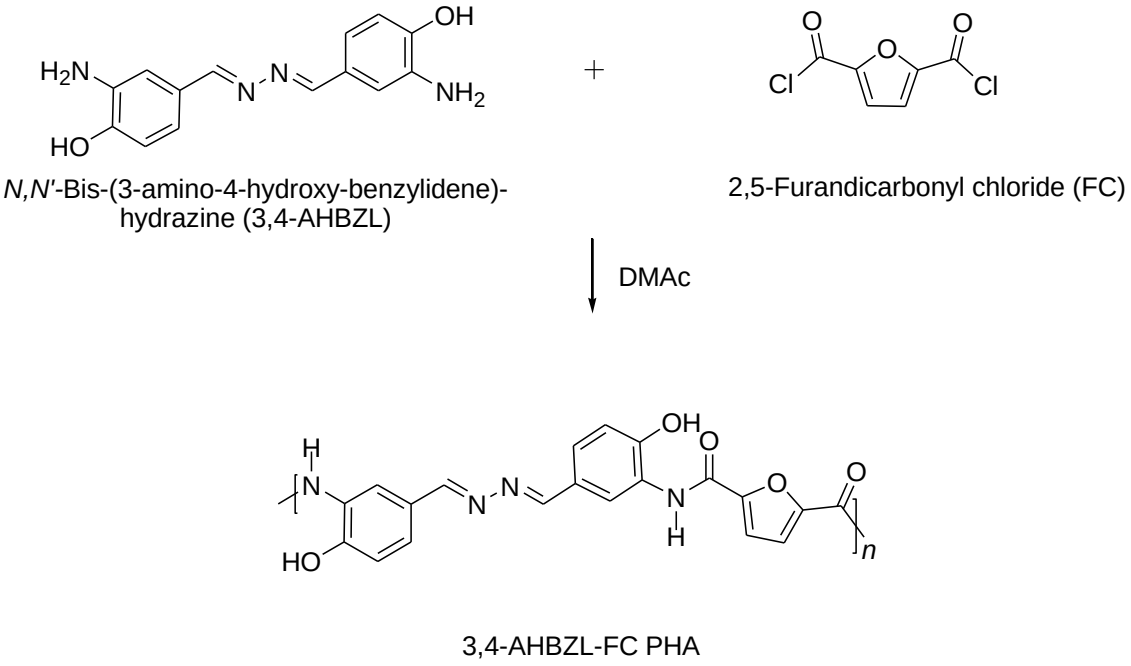

N,N′-Bis-(3-amino-4-hydroxy-benzylidene)-hydrazine (3,4-AHBZL)

2,5-Furandicarbonyl chloride (FC)

3,4-AHBZL-FC PHA

.

4.2.5 Syntheses of PBOs

Preparation of 3,4-AHBZL-TC PBO film from 3,4-AHBZL-TC PHA

100 mg of 3,4-AHBZL-TC PHA in 2 ml of DMAc filtered through a 0.5 μm PTFE membrane filter was cast on a glass substrate. The obtained film was dried at 60 ^{o}C for 1h and then at 100 ^{o}C for 1h. The film was peeled off the glass substrate by immersing the substrate in water. The obtained film was dried at 80 ^{o}C for 4h under vacuum and subsequently heated in a vacuum at 200 ^{o}C for 1h, 250 ^{o}C for 1h, 300 ^{o}C for 24h.

Scheme 4-7. Synthesis of 3,4-AHBZL-TC PBO

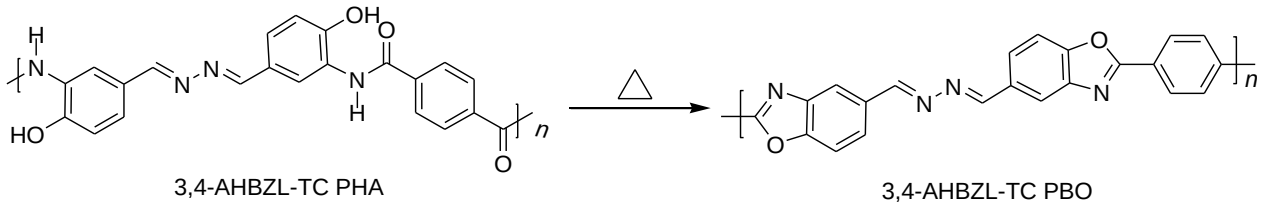

Preparation of 3,4-AHBZL-IC PBO film from 3,4-AHBZL-IC PHA

100 mg of 3,4-AHBZL-IC PHA in 2 ml of DMAc filtered through a 0.5 μm PTFE membrane filter was cast on a glass substrate. The obtained film was dried at 60 ^{o}C for 1h and then at 100 ^{o}C for 1h. The film was peeled off the glass substrate by immersing the substrate in water. The obtained film was dried at 80 ^{o}C for 4h under vacuum and subsequently heated in a vacuum at 200 ^{o}C for 1h, 250 ^{o}C for 24h.

Scheme 4-8. Synthesis of 3,4-AHBZL-IC PBO

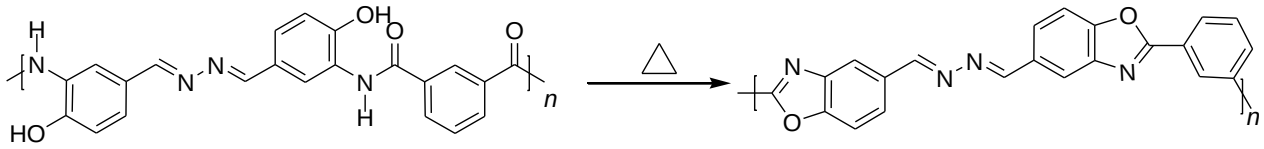

3,4-AHBZL-IC PHA　　3,4-AHBZL-IC PBO

Preparation of 3,4-AHBZL-FC PBO film from 3,4-AHBZL-FC PHA

100 mg of 3,4-AHBZL-FC PHA in 2 ml of DMAc filtered through a 0.5 μm PTFE membrane filter was cast on a glass substrate. The obtained film was dried at 60 ^{o}C for 1h and then at 100 ^{o}C for 1h. The film was peeled off the glass substrate by immersing the substrate in water. The obtained film was dried at 80 ^{o}C for 4h under vacuum and subsequently heated in a vacuum at 200 ^{o}C for 1h, 250 ^{o}C for 24h.

Scheme 4-9. Synthesis of 3,4-AHBZL-FC PBO

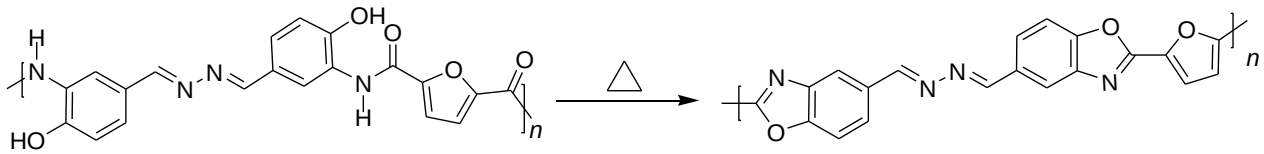

3,4-AHBZL-FC PHA　　3,4-AHBZL-FC PBO

4.2.6 Measurements

Fourier transform infrared spectra (FT-IR) of 3,4-NHBZL, 3,4-AHBZL, and its polymer were recorded on a Perkin-Elmer Spectrum One spectrometer using a diamond-attenuated total reflection (ATR) accessory. ^{1}H and ^{13}C, HSQC, HMBC NMR spectra were measured in a DMSO-d_6 solution by an NMR spectrometer (Bruker, Avance III) at 500MHz. ^{1}H and ^{13}C, HSQC, HMBC. NMR spectra chemical shifts in parts per million (ppm) were recorded downfield from 2.5 ppm and 39.5 ppm using DMSO as an internal reference.^{13}C-NMR spectra were recorded at an NMR spectrometer (Bruker, Avance III) at 500 MHz at a frequency of 125 MHz by using complete decoupling or DEPT (distortionless enhanced by polarization transfer) mode.

Fourier transform ion cyclotron resonance mass spectra (FT-ICR MS) with an electrospray ionization system (ESI) were recorded on a Solari X, Bruker Daltonics Inc. A methanol solution of 3,4-AHBZL was prepared as a specimen.

4.2.7 Molecular weight measurement

Number- and weight-average molecular weights (M_n and M_w) were determined by JASCO gel permeation chromatograph (GPC) system equipped with KD-803 and KD-807 (Shodex) as the column at 40 ^{o}C, and calibrated with pullulan standards at a flow rate of 1.0 ml/min by eluant as DMF.

4.2.8 Thermal Analysis

Thermal degradation was analyzed by thermogravimetric analysis (TGA; SSC/5200 SII Seiko Instruments Inc.) by heating from 50 to 750 ^{o}C at a rate of 10 ^{o}C/min under a nitrogen atmosphere.

4.2.9 Photoluminescence of solutions

Photoluminescence excitation and emission spectra of the PBO solutions were obtained with a spectrophotometer. The polymer concentration in concentrated sulfuric acid was 5 mg/l.

4.3 Results and discussion

4.3.1 Syntheses and characterization of PBO precursors (prePBOs)

The monomer 3,4-NHBZL was synthesized by the reaction of 3,4-NHBAL with hydrazine. After that the monomer 3,4-AHBZL was reduced by the hydrogenation reaction from nitro group of 3,4-NHBZL. Similar to polyimides, most PBOs are insoluble in common organic solvents. [152] In this study, the author chose two step reaction about synthesis of a soluble PBO precursor followed by the fabrication of PBO films according to Nakashima's method. [153-155] The precursor of PBO, 3,4-AHBZL-TC PHA, 3,4-AHBZL-IC PHA, and 3,4-AHBZL-FC PHA were synthesized by the condensation reaction of 3,4-AHBZL with TC, IC, FC as shown in Scheme 4-3, 4-4, 4-6. The obtained polymer powders were characterized by FT-IR spectroscopy. As shown in Figure 4-18 (a), 4-19 (a), and 4-20 (a), characteristic peaks of the amide bonding (1635 and 1537 cm^{-1}, 1646 and 1530 cm^{-1}, 1653 and 1532 cm^{-1}, C=O stretching mode and N-H bending mode, respectively) due to the prePBO were observed, which clearly indicated the progress of the polycondensation reaction. It is important to note that the 3,4-AHBZL-TC PHA, 3,4-AHBZL-IC PHA, and 3,4-AHBZL-FC PHA exhibited an excellent solubility in common organic solvents such as DMF and DMAc. The good solubility of the 3,4-AHBZL-TC PHA, 3,4-AHBZL-IC PHA, and 3,4-AHBZL-FC PHA allowed author to characterize it using GPC in DMF and ^{1}H-NMR in DMSO-d_6 as the solvent. The GPC and ^{1}H-NMR results were shown below. The molecular

weights of the 3,4-AHBZL-TC PHA, 3,4-AHBZL-IC PHA, and 3,4-AHBZL-FC PHA were measured in DMF by GPC with a pullulan standard. It showed M_n = 6200, 9900, 62000, M_w = 18000, 35000, 190000, and M_w/M_n = 2.9, 3.5, 3.0, respectively. The thermogravimetric analysis (TGA) of the 3,4-AHBZL-TC PHA, 3,4-AHBZL-IC PHA, and 3,4-AHBZL-FC PHA were conducted at a heating rate of 10 $^oC\ min^{-1}$ under flowing nitrogen, and as shown by the black line in Figure 4-18 (b), 4-19 (b), 4-20 (b), the 10% weight loss was observed at around 221, 250 and 300 ^oC. The ^{1}H-NMR spectra of 3,4-AHBZL-TC PHA, 3,4-AHBZL-IC PHA, and 3,4-AHBZL-FC PHA were presented in Figure 4-18 (c), 4-19 (c), 4-20 (c) with a good assignment of each resonance. The peaks due to the hydroxyl, amide, and imine protons are observed at 10.57 (broad), 9.78 (singlet), 8.64 (singlet) in Figure 4-18(c), 10.54 (broad), 9.80 (singlet), 8.60 (singlet) in Figure 4-19 (c), and 10.72 (broad), 9.86 (singlet), 8.62 (singlet) in Figure 4-20 (c), respectively. These results indicated that the prePBO reaction was proceeded in each polymer.

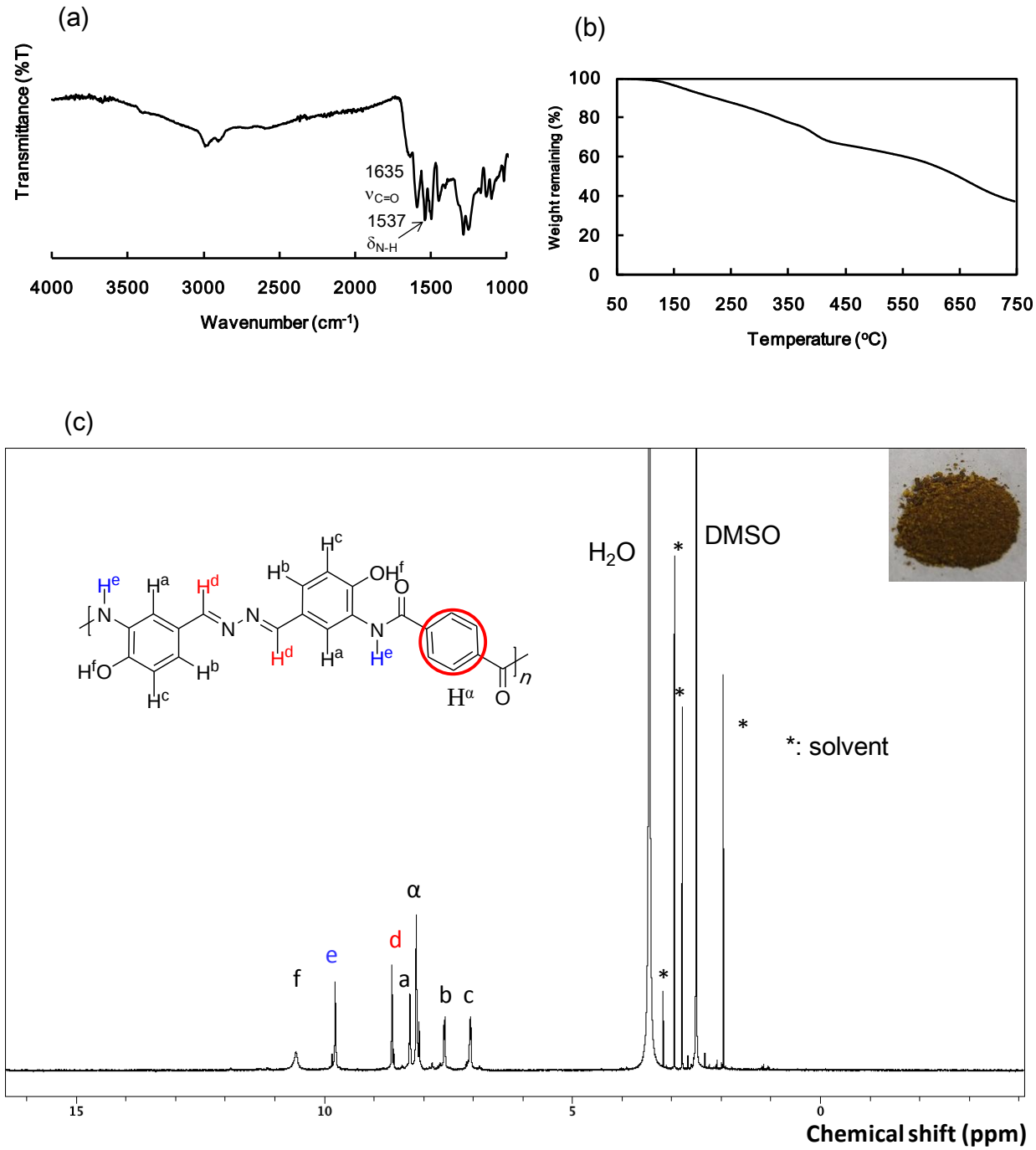

Figure 4-18. (a) FT-IR spectrum of 3,4-AHBZL-TC PHA. (b) TGA curve of 3,4-AHBZL-TC PHA (10 ^{o}C min^{-1} in N_2). (c) ^{1}H-NMR spectrum of 3,4-AHBZL-TC PHA. Inset photo: The powder of 3,4-AHBZL-TC PHA.

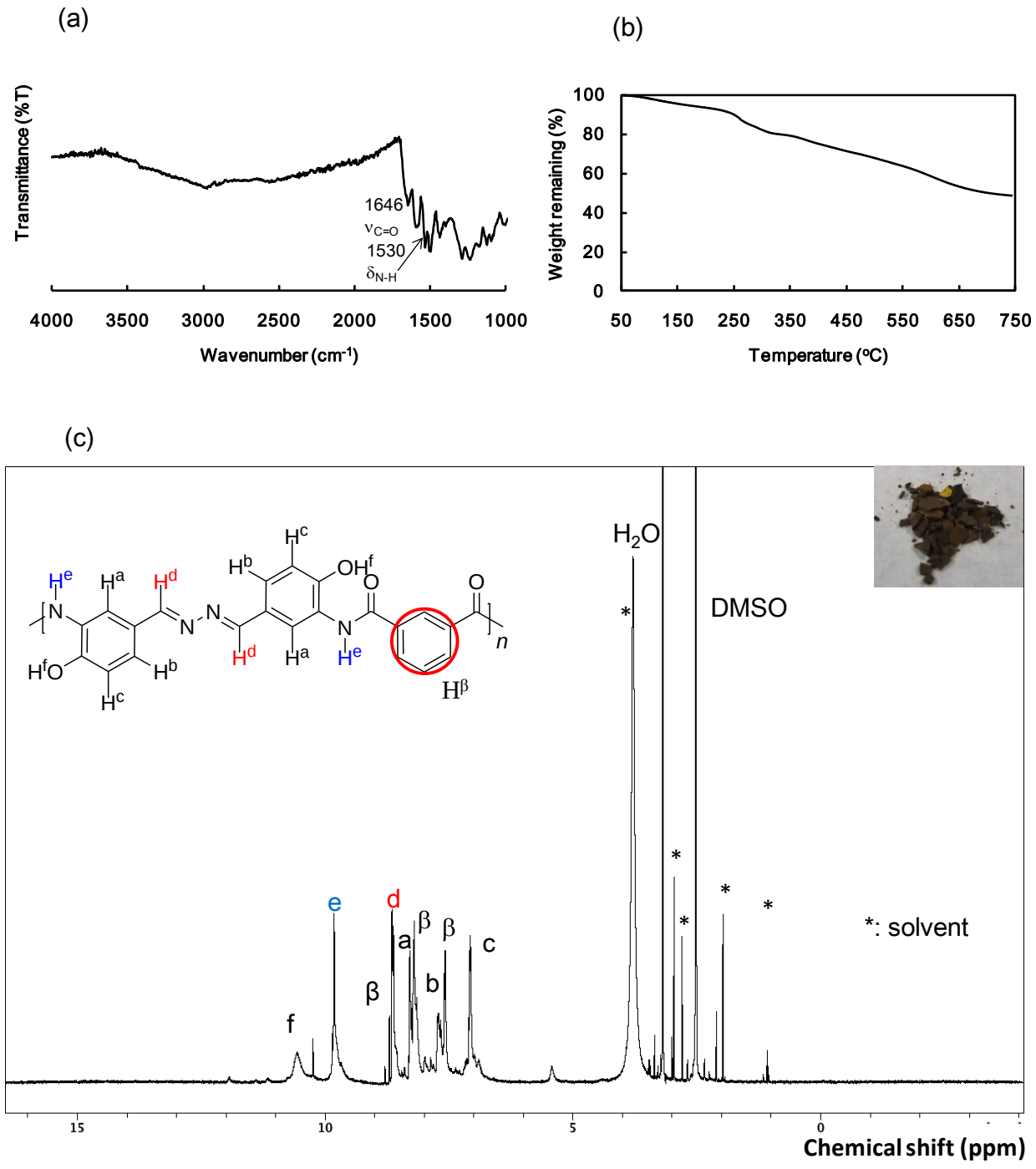

Figure 4-19. (a) FT-IR spectrum of 3,4-AHBZL-IC PHA. (b) TGA curve of 3,4-AHBZL-IC PHA (10 ^{o}C min^{-1} in N_2). (c) ^{1}H-NMR spectrum of 3,4-AHBZL-IC PHA. Inset photo: The powder of 3,4-AHBZL-IC PHA.

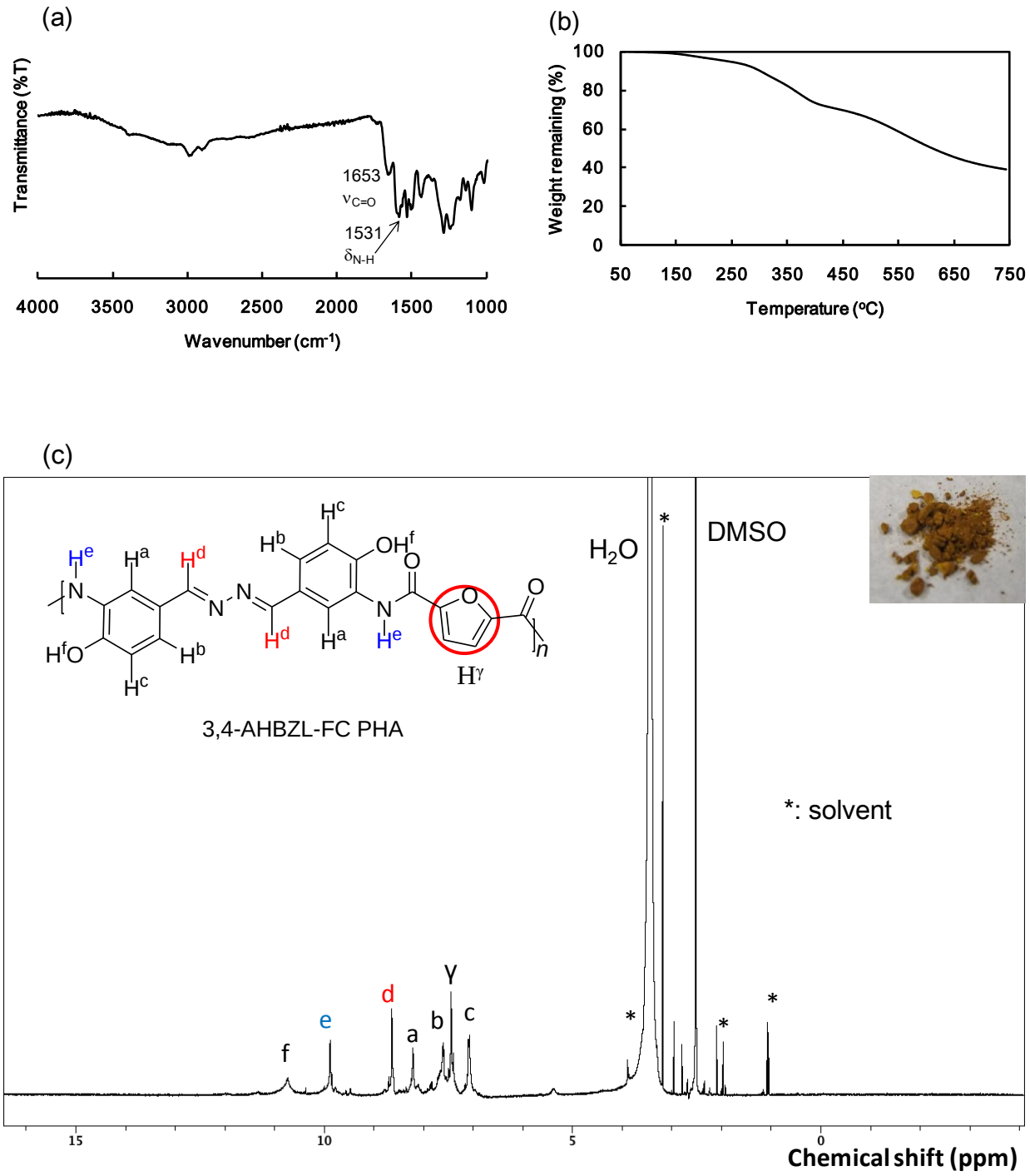

Figure 4-20. (a) FT-IR spectrum of 3,4-AHBZL-FC PHA. (b) TGA curve of 3,4-AHBZL-FC PHA (10 ^{o}C min^{-1} in N_2). (c) ^{1}H-NMR spectrum of 3,4-AHBZL-FC PHA. Inset photo: The powder of 3,4-AHBZL-FC PHA.

4.3.2 Preparation and characterization of prePBO films and PBO films

One of the advantages of 3,4-AHBZL-TC PHA, 3,4-AHBZL-IC PHA, and 3,4-AHBZL-FC PHA are the high processability due to its good solubility. The good solubility can allow the author to fabricate its films from the solution-cast method. A DMAc solution of the 3,4-AHBZL-TC PHA, 3,4-AHBZL-IC PHA, and 3,4-AHBZL-FC PHA were cast on a glass substrate, and then the obtained film was peeled off the glass substrate by immersing it in water as described in the Experimental Section. As shown in Figure 4-21 (a), 4-22 (a), and 4-23 (a), the obtained free-standing films were bright orange color. The obtained films were heated at 80 ^{o}C for 4h under vacuum and subsequently heated in a vacuum at 200 ^{o}C for 1h, 250 ^{o}C for 24h of 3,4-AHBZL-IC PHA, 3,4-AHBZL-FC PHA. In 3,4-AHBZL-TC PHA film case, final two steps were changed at 250 ^{o}C for 1h, 300 ^{o}C for 24h under vacuum. After heating, the author observed the films were changing dark brown color. The formation of the PBO films from prePBO films upon heating was monitored by FT-IR (Figure 4-21 (c), 4-22 (c), and 4-23 (c)). It was revealed that the C=O peaks at 1643, 1648, 1648 cm^{-1} (amide) decreased during heating and C=N peaks at 1616, 1623, 1631 cm^{-1} appeared in 3,4-AHBZL-TC PHA film, 3,4-AHBZL-IC PHA film and 3,4-AHBZL-FC PHA film. The thermogravimetric analysis (TGA) of each films about the 3,4-AHBZL-TC PHA, 3,4-AHBZL-IC PHA, 3,4-AHBZL-FC PHA, 3,4-AHBZL-TC PBO, 3,4-AHBZL-IC PBO, and 3,4-AHBZL-FC PBO were conducted at a heating rate of 10 ^{o}C min^{-1} under flowing nitrogen, and as shown by the black line in Figure 4-21 (b), 4-22 (b), and 4-23 (b), the 10% weight loss was observed at around 355, 261 and 303 ^{o}C in prePBO and 552, 375 and 378 ^{o}C in PBO. All of the PBOs exhibited good thermal resistance; especially 3,4-AHBZL-TC PBO exhibited the highest thermal stability with a T_{10} of 552 ^{o}C.

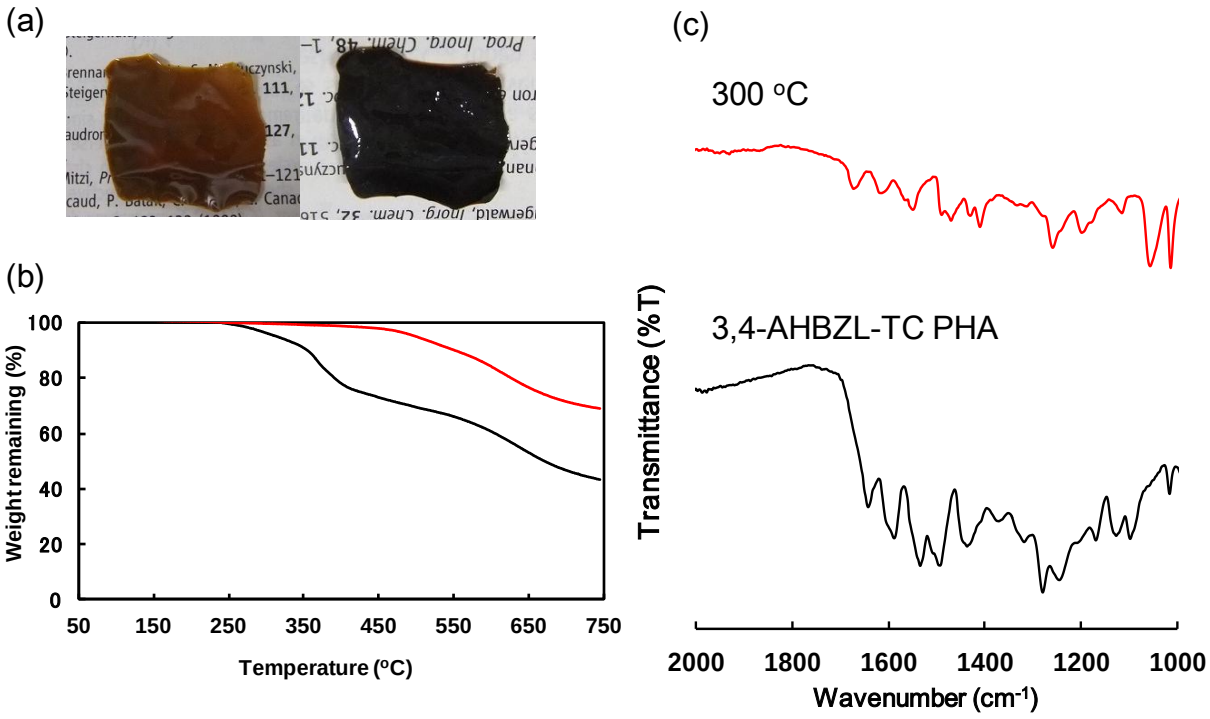

Figure 4-21. Photographs of free-standing 3,4-AHBZL-TC PHA (left) and 3,4-AHBZL-TC PBO (right) films. (b) TGA curves of the 3,4-AHBZL-TC PHA film (black line) and 3,4-AHBZL-TC PBO film (red line). (c) FT-IR spectra of 3,4-AHBZL-TC PHA film (black line) and after heating at 300 ^{o}C (red line) are displayed as a comparison.

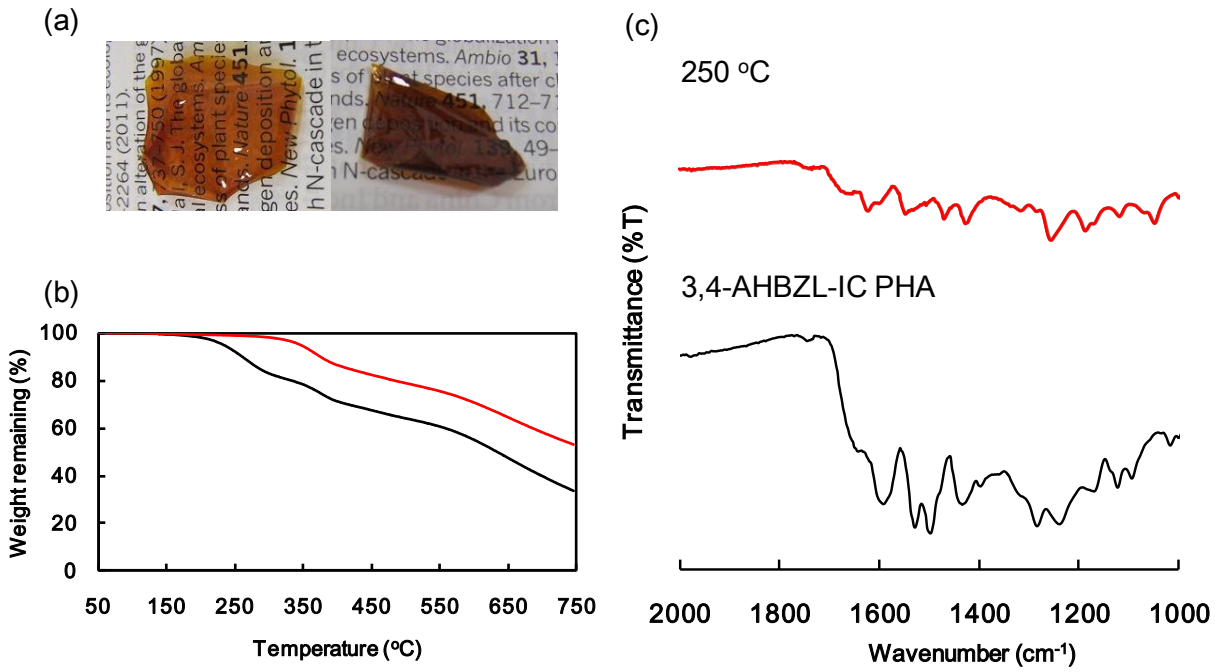

Figure 4-22. Photographs of free-standing 3,4-AHBZL-IC PHA (left) and 3,4-AHBZL-IC PBO (right) films. (b) TGA curves of the 3,4-AHBZL-IC PHA film (black line) and 3,4-AHBZL-IC PBO film (red line). (c) FT-IR spectra of 3,4-AHBZL-IC PHA film (black line) and after heating at 250 ^{o}C (red line) are displayed as a comparison.

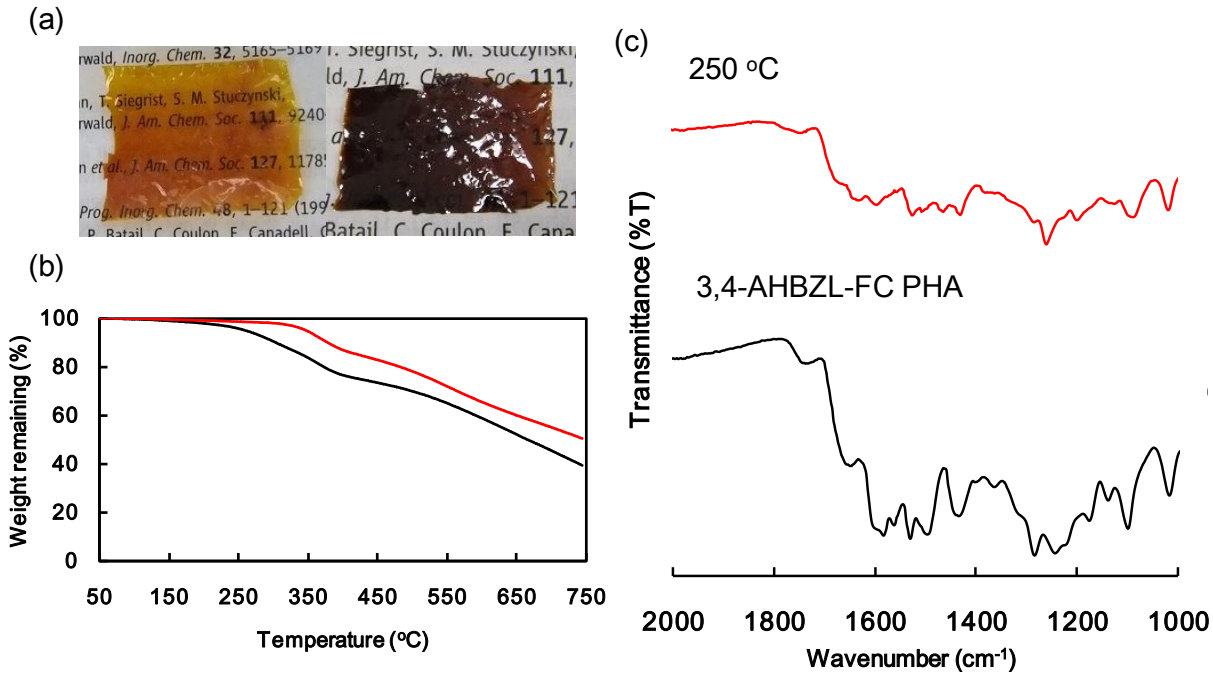

Figure 4-23. Photographs of free-standing 3,4-AHBZL-FC PHA (left) and 3,4-AHBZL-FC PBO (right) films. (b) TGA curves of the 3,4-AHBZL-FC PHA film (black line) and 3,4-AHBZL-FC PBO film (red line). (c) FT-IR spectra of 3,4-AHBZL-FC PHA film (black line) and after heating at 250 ^{o}C (red line) are displayed as a comparison.

4.3.3 Photoluminescence of solutions

The photograph shown in Figure 4-24 demonstrated the visual photoluminescence of the (i) 3,4-AHBZL-TC PBO, (ii) 3,4-AHBZL-IC PBO, (iii) 3,4-AHBZL-FC PBO in a concentrated sulfuric acid at a concentration of 5 mg/L. Those solutions were transparent and faint yellow, but emitted blue light depending on each PBOs when ultraviolet (UV) light (λ = 365 nm) was irradiated. In order to quantify these colors, the author recorded the photoluminescence spectra. Figure 4-25 shows the photoluminescence excitation spectra (left), and emission spectra (right), and Table 4-1 shows the photoluminescence excitation λ_{max} (ex), and emission λ_{max} (em) of (i) 3,4-AHBZL-TC PBO, (ii) 3,4-AHBZL-IC PBO, and (iii) 3,4-AHBZL-FC PBO. From Figure 4-

25 and Table 4-1 can see each PBOs show photoluminescence. This phenomenon implies that the 3,4-AHBZL-TC PBO, (ii) 3,4-AHBZL-IC PBO, and (iii) 3,4-AHBZL-FC PBO which having long π-conjugation units play the role of photoluminescence emission. As a consequence, these three kinds of PBOs have photoluminescence properties.

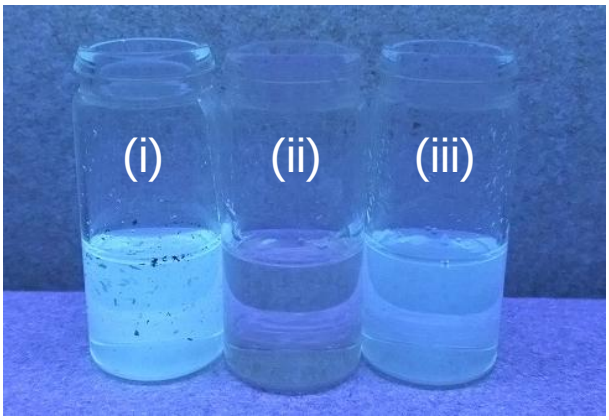

Figure 4-24. Digital photograph of an conc. sulfuric acid of (**i**) 3,4-AHBZL-TC PBO, (**ii**) 3,4-AHBZL-IC PBO, (**iii**) 3,4-AHBZL-FC PBO under 365 nm UV light excitation.

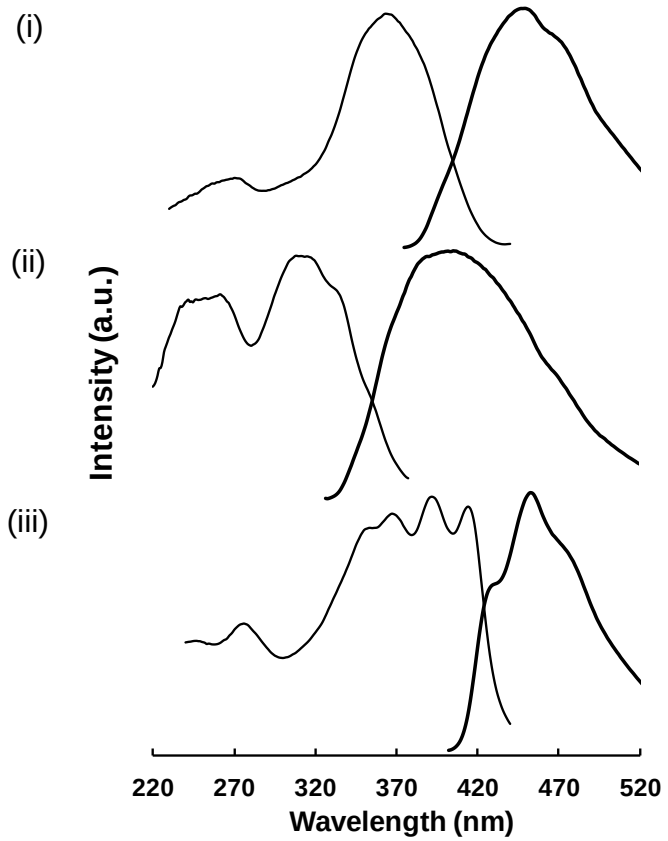

Figure 4-25. Photoluminescence excitation spectra (left), and emission spectra (right) of (i) 3,4-AHBZL-TC PBO, (ii) 3,4-AHBZL-IC PBO, and (iii) 3,4-AHBZL-FC PBO.

Table 4-1. Photoluminescence excitation λ_{max} (ex), and emission λ_{max} (em) of (i) 3,4-AHBZL-TC PBO, (ii) 3,4-AHBZL-IC PBO, (iii) 3,4-AHBZL-FC PBO.

Polymer	Excitation Max (nm)	Emission Max (nm)
(i) 3,4-AHBZL-TC PBO	365	435
(ii) 3,4-AHBZL-IC PBO	317	407
(iii) 3,4-AHBZL-FC PBO	392,414	453

4.4 Conclusion

The author prepared new prePBO and PBO series, 3,4-AHBZL-TC PHA, 3,4-AHBZL-IC PHA, 3,4-AHBZL-FC PHA and 3,4-AHBZL-TC PBO, 3,4-AHBZL-IC PBO, 3,4-AHBZL-FC PBO from π-conjugated novel 3,4-AHBA derivative symmetric monomer *N,N'*-Bis-(3-amino-4-hydroxy-benzylidene)-hydrazine (3,4-AHBZL). Polymerization of the 3,4-AHBZL and dichloride gave a soluble PBO precursors having an imine and phenolic OH group structure. The FT-IR and TGA measurements revealed the conversion of the prePBO to PBO upon heating at 250 ^{o}C for 24h under vacuum in 3,4-AHBZL-IC PHA, 3,4-AHBZL-FC PHA and 300 ^{o}C for 24h under vacuum in 3,4-AHZL-TC PHA. Especially 3,4-AHBZL-TC PBO film showed thermal resistivity of T_{10} 552 ^{o}C under nitrogen. Furthermore, 3,4-AHBZL-TC PBO, 3,4-AHBZL-IC PBO, and 3,4-AHBZL-FC PBO showed photoluminescence in a concentrated sulfuric acid under ultraviolet (UV) light with a wavelength of 365 nm. Here the author chose FC because it could prepare from 2,5-furandicarboxylic acid. Additionally 2,5-furandicarboxylic acid was nonpetroleum monomer which derived from hydroxymethylfurfural. Then the author prepared novel bio-based polybenzobisoxazole. Thus, the author prepared new, bio-based polybenzobisoxazole with photoemission properties derived from long rigid aromatic π-conjugated structures.

Chapter 5

Conclusion remarks

CHAPTER 5

Conclusive remarks

This thesis described the preparation of novel functional polymers derived from wholly aromatic amino acid, 3-amino-4-hydroxy benzoic acid (3,4-AHBA).

Chapter 2, the author prepared bio-based polyaniline, poly(3-amino-4-hydroxybenzoic acid) (poly(3,4-AHBA)), by electro-polymerization. Poly(3,4-AHBA) has higher solubility in common solvents, compared to polyaniline, due to the polar side groups such as carboxyl and hydroxyl. The polymers showed various chromic behaviors such as "Halochromism" and "Solvatochromism". From Halochromism, it showed color changes in poly(3,4-AHBA) solution around pH5-7. From the results of UV-vis spectra of the polymer solutions, it was suggested that the polymers including 3,4-AHBA units show self-doping effects by carboxylic acids. Further the polar solvent addition rendered the polymers undoped accompanying by the chromism. Thus the author first prepared novel functional bio-based polymers with chromism based on the π-conjugation structure change.

Chapter 3, the author prepared new functional bio-based liquid crystalline polyesters, poly{3-benzylidene amino-4-hydroxybenzoic acid (3,4-BAHBA)-*co*-*trans*-4-hydroxycinnamic acid (4HCA: *trans*-coumaric acid)} (P(3,4-BAHBA-*co*-4HCA)). When the 4HCA compositions of P(3,4-BAHBA-*co*-4HCA)s were above 55 mol%, the copolymers showed a nematic liquid crystalline phase due to the mesogenic effects of the continuous 4HCA units. X-ray analyses of the fibers indicated that the main chains were oriented perpendicularly to the shear direction, and the rigid benzylidene amino side chains were parallely oriented. The copolymers in an NMP solution showed photoluminescence under 365 nm, and the corresponding oriented films of P(3,4-BAHBA-*co*-4HCA)s with a 4HCA composition of 75 mol% emitted polarized light, as

confirmed by fluorescent spectroscopy equipped with paralleled and crossed polarizers. Furthermore, the oriented film showed polarized emissions and color change dependent on the angle of the analyzer rotation with the polarizer perpendicular to the shear direction. Thus, the author prepared new, rigid-rod oligomers with LC-related photoemission properties derived from aromatic structures in biomolecules available from microorganisms.

Chapter 4, the author prepared new functional π-conjugated PBOs and PBO precursor, 3,4-AHBZL-TC PHA, 3,4-AHBZL-IC PHA, 3,4-AHBZL-FC PHA and 3,4-AHBZL-TC PBO, 3,4-AHBZL-IC PBO, 3,4-AHBZL-FC PBO by 3,4-AHBA derivative symmetric monomer *N,N'*-Bis-(3-amino-4-hydroxy-benzylidene)-hydrazine (3,4-AHBZL). The new synthesis concept gave soluble PBO precursors having an imine and phenolic OH group. The FT-IR and TGA measurements revealed the conversion of the prePBO to PBO upon heating at 250 ^{o}C for 24h under vacuum in 3,4-AHBZL-IC PHA, 3,4-AHBZL-FC PHA and 300 ^{o}C for 24h under vacuum in 3,4-AHZL-TC PHA. Especially 3,4-AHBZL-TC PBO film showed thermal resistivity of T_{10} 552 ^{o}C under nitrogen. Furthermore, these three kinds of PBOs showed photoluminescence in a concentrated sulfuric acid under ultraviolet (UV) light with a wavelength of 365 nm. Thus, the author prepared new, bio-based polybenzobisoxazoles with photoemission properties derived from long rigid aromatic π-conjugated structures.

From these works, the author designed new π-conjugated polymer systems from 3,4-AHBA as a renewable resource. 3,4-AHBA is very simple structure which can create new materials and possible mass-availability from *S. griseus*. Normally the nature compound had very difficult structure and difficult to create new materials. However, it could play an important part in environmental problems and new design from nature. From this study the author hopes the biomass resource can play an important role as a chemical breakthrough to replace not only petroleum-based polymers but also apply for liquid crystalline materials, photo functional advanced materials, super engineering plastics, and so on.

REFERENCES

1. P. T. Anastas, John C. Warner, *Green Chemistry: Theory and Practice*, Oxford University Press, New York, USA, **1988**.
2. J. R. Mihelcic, J. C. Crittenden, M. J. Small, D. R. Shonnard, D. R. Hokanson, Q. Huichen, S. H. Sorby, V. James, J. W. Sutherland, J. L. Schnoor, *Environmental Science and Technology* **2003**, *37*, 5349..
3. R. L. Lankey, P. T. Anastas, *Ind. Eng. Chem. Res.* **2002**, *41*, 4498.
4. P. T. Anastas, R. L. Lankey, *Green Chemistry* **2000**, *6*, 289.
5. V. Polshettiwar, R. S. Varma, *Chemical Society Reviews* **2008**, *47*, 7982.
6. US EPA. Municipal solid waste. *United States Environmental Protection Agency*. (httep://www.epa.gov/epawaste/nonhaz/municipal/)
7. Y. Aheng, E. K. Yanful, A. S. Bassi, *Crit. Rev. Biotech.* **2005**, *25*, 243.
8. L. Averous, E. Pollet, *Environmental Silicate Nano-Biocomposites*, Springer-Verlag, London, **2012**.
9. R. A. Gross, B. Kalra, *Science* **2002**, *297*, 803.
10. F. Wang, S. J. Lee, *Appl. Environ. Microbiol.* **1997**, *63*, 3703.
11. Y. Tokiwa, C. U. Ugwa, *J. Biotechnol.* **2007**, *132*, 264.
12. Y. Tokiwa, B. P. Calabia, *Can. J. Chem.* **2008**, *86*, 548.
13. M. Vert, *Biomacromolecules* **2005**, *6*, 538.
14. I. Taniguchi, Y. Kimura, *Biopolymers* **2001**, *3b*, 431.
15. B. Saulnier, S. Ponsart, J. Coudane, H. Garreau, M. Vert, *Macromol. Biosci.* **2004**, *4*, 232.
16. M. Yamamoto, U. Witt, G. Skupin, D. Beimborn, R. –J. Mueller, *Biopolymers* **2002**, *4*, 299.

17. V. Nagarajan, M. Singh, H. Kane, M. Khalili, M. J. Bramucci, *Polym. Environ.* **2006**, *14*, 281.

18. K. Okano, A. Kondo, H. Noda, *Eco Ind.* **2006**, *11*, 43.

19. Y. Imai, R. Yokota, *Saishin Polyimides*, NTS Press, Tokyo **2002**.

20. A. W. Chow, S. P. Bitler, P. E. Penwell, D. J. Osborne, J. F. Wolfe, *Macromolecules* **1989**, *22*, 3514.

21. H. Suzuki, Y. Ohnishi, Y. Furusho, S. Sakuda, S. Horinouchi, *J. Biol. Chem.* **2006**, *281*, 36944.

22. S. Horinouchi, *Biosci, Biotechnol, Biochem.* **2007**, *71*, 283.

23. A. Noguchi, T. Kitamura, H. Onaka, S. Horinouchi, Y. Ohnishi, *Nat. Chem. Biol.* **2010**, *6*, 641.

24. A. Noguchi, S. Horinouchi, Y. Ohnishi, *J. Antibiot.* **2011**, *64*, 93.

25. H. Suzuki, Y. Furusho, T. Higashi, Y. Ohnishi, S. Horinouchi, *J. Biol. Chem.* **2006**, *281*, 824.

26. H. Suzuki, Y. Ohnishi, S. Horinouchi, *J. Antibiot.* **2007**, *60*, 380.

27. T. Kaneko, Green Polymerization Methods: Renewable Starting Materials, Catalysis and Waste Reduction, ed. by R. T. Mathers, M. A. R. Meier, Wiley-VCH Verlag, Weinheim **2011**, Ch. 12.

28. Y. Ohnishi, J. Ishikawa, H. Hara, H. Suzuki, M. Ikenoya, H. Ikeda, A. Yamashita, M. Hattori, S. Horinouchi, *J. BACTERIOL*, **2008**, *19*, 4050.

29. S. Horinouchi, Y. Ohnishi, K. Yoshino, S. Yanagiya, Y. Kitagawa, I. Inohara, Jpn. Kokai Tokkyo Koho 283163, **2004**.

30. J. Fritzsche, *J. Prake. Chem. (Leipzig)* **1840**, *20*, 454.

31. J. C. Chiang, A. G. MacDiarmid, *Synth. Met*. **1986**, *13*, 193.

32. F. Wudl, N. P. Balsara, O. R. Angus. Jr., R. L. Lu, P. M. Allemand, D. J. Vachon, M. Nowak, Z. X. Liu, A. J. Heeger, *J. Am. Chem. Soc.* **1987**, *109*, 3677.

33. A.G. MacDiarmid, S. L. Mu, M. L. D. Somasiri, W. Wu, *Mol. Cryst. Liq. Cryst.* **1985**, *121*, 187.

34. N. Oyama, T. Ohsaka, *Synth. Met.* **1987**, *18*, 191.

35. P. K. H. Ho, J. –S. Kim, J. H. Burroughes, H. Becker, S. F. Y. Li, T. M. Brown, F. Cacialli, R. H. Friend, *Nature* **2000**, *404*, 481.

36. V. Gupta, N. Miura, *Mater. Lett.* **2006**, *60*, 1466.

37. S. Singh, P. R. Solanki, M. K. Pandey, B. D. Malhotra, *Sens. Actuators B Chem.* **2006**, *115*, 34.

38. M. P. T. Sotomayor, M. -A. De Paoli, W. A. Oliveira, *Anal. Chim. Acta* **1997**, *353*, 275.

39. E. Pringsheim, E. Terpetschnig, O. S. Wolfbeis, *Anal. Chim. Acta* **1997**, *357*, 247.

40. M. Kaneko, H. Nakamura, *J. Chem. Soc., Chem. Commun.* **1985**, *6*, 346.

41. A. G. MacDiarmid, L.S. Yang, W. S. Huang, B. D. Humphry, *Synth. Met.* **1987**, *18*, 393.

42. E. M. Genies, P. Hany, C. J. Santier, *J. Appl. Electrochem.* **1988**, *18*, 285.

43. M. Mizumoto, M. Namba, S. Nishimura, H. Miyadera, M. Koseki, Y. Kobayashi, *Synth. Met.* **1989**, *28*, 639.

44. E. W. Paul, A. J. Rico, M. S. Wrighton, *J. Phys. Chem.* **1985**, *89*, 1441.

45. W. S. Huang, M. A. Lecorre, M. Tissier, *J. Vac. Sci. Technol*. **1991**, *B9*, 3428.

46. S. –A. Chen, Y. Fang, *Synth. Met.* **1993**, *60*, 215.

47. A. Kitani, J. Yano, K. Sasaki, *J. Electroanal. Chem.* **1986**, *209*, 227.

48. B. P. Jelle, G. Hagen, *J. Electrochem. Soc.* **1993**, *140*, 3560.

49. M. A. Rodrigues, M.-A. De Paoli, M. Mastragostino, *Electrochim. Acta* **1991**, *36*, 2143.

50. E. Edelson, *Pop. Sci.* **1990,** June**,** 90.

51. K. Kaneto, W. Takashima, Y. –G. Min, A. G. MacDiarmid, *Synth. Met.* **1995**, *71*, 2211.

52. K. Kaneto, M. Kaneko, W. Takashima, *Jpn. J. Appl. Phys.* **1995**, *34*, L837.

53. W. Takashima, M. Fukui, M. Kaneko, K. Kaneko, *Jpn. J. Appl. Phys.* **1995**, *34*, 3786.

54. W. Takashima, K. Kaneto, A. G. MacDiarmid, *Synth. Met.* **1995**, *71*, 2265.

55. A. S. Wood, *Mod. Plast.* **1991**, August, 47.

56. A. J. Epstein, J. Yue, U.S. Patent 5,237,991, **1991**.

57. S. P. Armes, J. F. Miller, *Synth. Met.* **1988**, *22*, 385.

58. A. F. Diaz, J. A. Logan, *J. Electrocanl. Chem.* **1980**, *111*, 111.

59. J. A. Conklin, S. C. Huang, S. M. Huang, T. Wen, R. B. Kaner, *Macromolecules* **1995**, *28*, 6522.

60. Y. Furukawa, F. Ueda, Y. Hyodo, I. Harada, *Macromolecules* **1988**, *21*, 1297.

61. W. Y. Zheng, K. Levon, *Macromolecules* **1994**, *27*, 7754.

62. D. M. Chao, X. F. Lu, J. Y. Chen, X. G. Zhao, L. F. Wang, W. J. Zhang, Y. Wei, *J. Polym. Sci., Part A: Polym. Chem.* **2006**, *44*, 477.

63. E. Pringsheim, E.Terpetschnig, O. S. Wolfbeis, *Anal. Chim. Acta* **1997**, *357*, 247.

64. G. L. Yuan, N. Kuramoto, *Macromolecules* **2003**, *36*, 7939.

65. M. M. Ayad, N. A. Salahuddin, A. K. Abou-Seif, M. O. Alghaysh, *Polym, Adv. Technol.* **2008**, *19*, 1142.

66. W. J. Bae, K. H. Kim. Y.H. Park, W. H. Jo, *Chem. Commun.* **2003**, *22*, 2768.

67. T. J. Scheffer, *J. Appl. Phys. Lett.* **1984**, *45*, 1021.

68. D. Broer, J. Lub, G. N. Mol, *Nature* **1995**, *378*, 467.

69. R. A. M. Hikmet, H. Keperman, *Nature* **1998**, *392*, 476.

70. K. S. Yim, G. G. Fuller, A. Datko, C. D. Eisenbach, *Macromolecules* **2001**, *34*, 6972.

71. C. Pujolle-Robic, L. Noirez, *Nature* **2001**, *409*, 167.

72. T. Kaneko, K. Yamaoka, J. P. Gong, Y. Osada, *Macromolecules* **2004**, *37*, 5385.

73. J. Igne's-mullol, A. K. Schwartz, *Nature* **2001**, *410*, 348.

74. Y. Kawanishi, T. Tamaki, T. Seki, M. Sakuragi, Y. Suzuki, K. Ichimura, K. Aoki, *Langmuir* **1991**, *7*, 1314.

75. Y. Lansac, M. A. Glaser, N. A. Clark, O. D. Lavrentovich, *Nature* **1999**, *398*, 54.

76. K. Ichimura, S. K. Oh, M. Nakagawa, *Science* **2000**, *288*, 1624.

77. P. J. Dollings, M. Hird, *Introduction to Liquid Crystals*, Tayor & Francis: London, UK, **1997**.

78. S. Chandroasekhar, *Liquid Crystals*, 2nd ed., Cambridge University Press, Cambridge, UK, **1992**.

79. C. Robinson, *Tetrahedron* **1961**, *13*, 219.

80. F. Livolant, *J. Phys. Fr.* **1989**, *50*, 1729.

81. M. Spencer, W. Fuller, M. H. F. Wilkins, G. L. Brown, *Nature* **1962**, *194*, 1014.

82. M. F. Perutz, A. M. Liquori, F. Eirich, *Nature* **1951**, *167*, 929.

83. C. M. Coppin, P. C. Leavis, *Biophys. J.* **1992**, *63*, 794.

84. M. M. Giraud-Guille, *Int. Rev. Cytol.* **1996**, *166*, 59.

85. S. Suto, T. Umeda, *Angew. Makromol. Chem.* **1999**, *264*, 60.

86. W. D. Hoff, P. Dux, K. Hard, B. Devreese, I. M. Nugteren-Roodzant, W. Crielaard, R. Boelens, R. Kaptein, J. van Beeumen, K. J. Hellingwerf, *Biochemistry* **1994**, *33*, 13959.

87. F. Wightman, M. D. Chisholm, A. C. Neish, *Photochemistry* **1961**, *1*, 30.

88. T. Kaneko, M. Matsusaki, T. T. Hang, M. Akashi, *Macromol. Rapid Commun.* **2004**, *25*, 673.

89. M. Matsusaki, H. T. Tran, T. Kaneko, M. Akashi, *Biomaterials* **2005**, *26*, 6263.

90. T. Kaneko, T. T. Hang, M. Matsusaki, M. Akashi, *Chem. Mater.* **2006**, *18*, 6220.

91. T. Kaneko, H. T. Tran, M. Matsusaki, D. J. Shi, M. Akashi, *Nat. Mater.* **2006,** *5***,** 966.

92. T. Kaneko, D. Kaneko, S. Q. Wang, *Plant Biotechnol.* **2010**, *27*, 243.

93. S. Q. Wang, S. Tateyama, D. Kaneko, S. Ohki, T. Kaneko, *Polym. Degrad. Stabil.* **2011**, *96*, 2048.

94. M. Chauzer, S. Tateyama, T. Ishikura, K. Matsumoto, D. Kaneko, K. Ebitani, T. Kaneko, *Adv. Funct. Mater.* **2012**, *22*, 3438.

95. K. Kan, D. Kaneko, T. Kaneko, *Polymers* **2011**, *3*, 861.

96. Z. Steinberg, *Annu. Rev. Biophys. Bioeng.* **1978**, *7*, 113.

97. V. Barzda, L. Musthrdy, G. Garab, *Biochemistry* **1994**, *33*, 10837.

98. V. Barzda, A. Istokovics, I. Simidjiev, G. Garad, *Biochemistry* **1996**, *35*, 8981.

99. E. E. Gussakovsky, Y. Shahak, H. van Amerongen, V. Barzda, *Photosynth. Res.* **2000**, *65*, 83.

100. D. K. Milne, *Aust, J. Phys*., **1972**, *25*, 307.

101. J. L. Han, R. N. Manchester, R.X. Xu, G. J. Qiao, *Mon. Not. R. Astron. Soc.* **1998**, *300*, 373.

102. P. Laurent, J. Rodriguez, J. Wilms, M. Cadolle Bel, K. Pottschmidt, V. Ginberg, *Science* **2011**, *332*, 438.

103. X. Jin, C. Carfagna, L. Nicolais, R. Lanzetta, *Macromolecules* **1995**, *28*, 4785.

104. R. A. Gross, B. Kalra, *Science* **2002**, *297*, 803.

105. K. Yamaoka, T. Kaneko, J. P. Gong, Y. Osada, *Macromolecules* **2001**, *34*, 1470.

106. P. Dyreklev, M. Berggren, O. Inganäs, M. R. Andersson, O. Wennerström, T. Hjertberg, *Adv. Mater.* **1995**, *7*, 43.

107. M. Hamaguchi, K. Yoshino, *Appl. Phys. Lett.* **1995**, *67*, 3381.

108. M. Grell, D. D. C. Bradley, E. P. Woo, M. Inbasekaran, *Adv. Mater.* **1997**, *9*, 798.

109. M. Grell, W. Knoll, D. Lupo, A. Meisel, T. Mikeva, D. Neher, H. G. Nothofer, U. Scherf, A. Yasude, *Adv. Mater.* **1999**, *11*, 671.

110. K. S. Whitehead, M. Grell, D. D. C. Bradley, *Appl. Phys. Lett.* **2000**, *76*, 2946.

111. M. Oda, H.-G. Nothofer, G. Lieser, U. Scherf, S. C. J. Meskers, D. Neher, *Adv. Mater.* **2000**, *12*, 362.

112. T. Hassheider, S. A. Benning, H.-S. Kitzerow, M.-F. Achard, H. Bock, *Angew. Chem., Int. Ed.* **2001**, *40*, 2060.

113. M. O'Neill, S. M. Kelly, *Adv. Mater.* **2003**, *15*, 1135.

114. F. Würthner, C. Thalacker, S. Diele, C. Tschierske, *Chem. Eur. J.* **2001**, *7*, 2245.

115. Damm, G. Israel, T. Hegmann, C. Tschierske, *J. Mater. Chem.* **2006**, *16*, 1808.

116. S. Sivakova and S. J. Rowan, *Chem. Commun.*, **2003**, *19*, 2428.

117. G. Gustatsson, Y. Cao, G. M. Treacy, F. Klavetter, N. Colaneri, A. J. Heeger, *Nature* **1992**, *357*, 477.

118. M. Ozaki, M. Kasano, D. Ganzke, W. Haase, K. Yoshino, *Adv. Mater.* **2002**, *14*, 306.

119. M. H. Song, B. Park, K.-C. Shin, T. Ohta, Y. Tsunoda, H. Hoshi, Y. Takanishi, K. Ishikawa, J. Watanabe, S. Nishimura, T. Toyooka, Z. Zhu, T. M. Swager, H. Takezoe, *Adv. Mater.* **2004**, *16*, 779.

120. R. D. Xia, M. Campoy-Quiles, G. Heliotis, P. Stavrinou, K. S. Whitehead, D. D. C. Bradley, *Synth. Met.* **2005**, *155*, 274.

121. B. Martini, I. M. Craig, W. C. Molenkamp, H. Miyata, S. H. Tolbert, B. J. Schwartz, *Nat. Nanotechnol.* **2007**, *2*, 647.

122. Weder, C. Sarwa, A. Montali, C. Bastiaansen, P. Smith, *Science* **1998**, *279*, 835.

123. M. Irie, T. Fukaminato, T. Sasaki, N. Tamai, T. Kawai, *Nature* **2002**, *420*, 759.

124. T. Mutai, H. Satou, K. Araki, *Nat. Mater.* **2005**, *4*, 685.

125. Y. Sagara, T. Kato, *Angew. Chem. Int. Ed.* **2008**, *47*, 5175.

126. S. Yamane, Y. Sagara, T. Kato, *Chem. Commn.* **2009**, *24*, 3597.

127. X. Zhang, S. Rehm, M. M. Safont-Sempere, F. Würthner, *Nat. Chem.* **2009**, *1*, 623.

128. Y. Sagara, T. Kato, *Nat. Chem.* **2009**, *1*, 605.

129. Y. Sagara, T. Kato, *Angew. Chem. Int. Ed.* **2011**, *50*, 9128.

130. K. Tanabe, Y. Suzui, M. Hasegawa, T. Kato, *J. Am. Chem. Soc.* **2012**, *134*, 5652.

131. S. Yamane, Y. Sagara, T. Mutai, K. Araki, T. Kato, *J. Mater. Chem. C* **2013**, *1*, 2648.

132. J. L. Bredas, R. R. Chance, *Conjugated Polymeric Materials: Opportunities in Electronics Optoelectronics and Molecular Electronics*, Kluwer Academic Publishers, Dordrecht, **1990**.

133. S. R. Marder, J. E. Sohn, G. D. Stucky, *Materials for Nonlinear Optics: Chemical Perspectives*, American Chemical Society, Washington, DC **1991**.

134. J. H. Burroughes, D. D. C. Bradley, A. R. Brown, R. N. Marks, K. Mackay, R. H. Friend, P. L. Burn, A. B. Holmes, *Nature* **1990**, *347*, 539.

135. H. Shirakawa, E. J. Louis, A. G. MacDiarmid, C. K. Chiang, A. J. Heeger, *J. Chem. Soc., Chem. Commun.* **1977**, *16*, 578.

136. R. H. Friend, R. W. Gymer, A. B. Holmes, J. H. Burroughes, R. N. Marks, C. Taliani, D. D. C. Bradley, D. A. Dos Santos, J. L. Bredas, M. Logdlund, W. R. Salaneck *Nature* **1999**, *397*, 121.

137. H. E. Katz, Z. Bao, *J. Phys. Chem.* **2002**, *104*, 671.

138. J. F. Wolfe, F. E. Arnold, *Macromolecules* **1981**, *14*, 909.

139. J. F. Wolfe, B. H. Loo, F. E. Arnold, *Macromolecules* **1981**, *14*, 915.

140. D. B. Cotts, G. C. Berry, *Macromolecules* **1981**, *14*, 930.

141. S. G. Chu, S. Venkatraman, G. C. Berry, Y. Einaga, *Macromolecules* **1981**, *14*, 939.

142. E. W. Choe, S. N. Kim, *Macromolecules* **1981**, *14*, 920.

143. Y.-H. So, J. M. Zaleski, C. Murlick, A. Ellaboudy, *Macromolecules*, **1996**, *29*, 2783.

144. P. W. Morgan, *Macromolecules*, **1977**, *10*, 1381.

145. J. A. Osaheni, S. A. Jenekhe, *Chem. Mater.* **1995**, *7*, 672.

146. S. F. Wang, P. P. Wu, Z. W. Han, *Polymer* **2001**, *1*, 217.

147. S. F. Wang, P. P. Wu, Z. W. Han, *Macromolecules* **2003**, *12*, 4567.

148. S. F. Wang, P. Wu, Z. W. Han, *J. Mater. Sci.* **2004**, *39*, 2717.

149. S. F. Wang, H. Lei, P. Y. Guo, P. P. Wu, Z. W. Han, *Eur. Polym. J.* **2004**, *40*, 1163.

150. A. J. Lesser, P. J. Walsh, X. Hu, P. J. Cunniff, *J. Appl. Polym. Sci.* **2006**, *102*, 3517.

151. Y. Maruyama, Y. Oishi, M. Kakimoto, Y. Iami, *Macromolecules* **1988**, *21*, 2305.

152. S. L. –C. Hsu, K. –C. Chang, *Polymer* **2002**, *43*, 4097.

153. T. Fukumaru, T. Fujigaya, N. Nakashima, *Polym. Chem.* **2012**, *3*, 369.

154. T. Fukumaru, T. Fujigaya, N. Nakashima, *Macromolecules* **2012**, *45*, 4247.

155. T. Fukumaru, T. Fujigaya, N. Nakashima, *Macromolecules* **2013**, *46*, 4034.

156. C. E. Sroog, A. L. Endrey, S. V. Abramo, C. E. Berr, W. M. Edwards, K. L. Olivier, *J. Polym. Sci., Part A: Polym. Chem.* **1965**, *3*, 1373.

157. M. Ueda, N. Yamaji, Jpn. Kokai Tokkyo Koho 209139, **2010**.

ACHIEVEMENTS

List of Publications

1. K. Kan, D. Kaneko, T. Kaneko, Polarized Emission of Wholly Aromatic Bio-Based Copolyesters of a Liquid Crystalline Nature. *Polymers* **2011**, *3*, 861-874.
2. K. Kan, H. Yamamoto, D. Kaneko, S. Tateyama, T. Kaneko, Novel π-conjugated bio-based polymer, poly(3-amino-4-hydroybenzoic acid), and its solvatochromism. *Pure Appl. Chem.* (in press).
3. K. Kan, S. Tateyama, T. Kaneko, Polarimetry-controlled Fluorescent Color in Oriented LC Biopolyesters. *Macromol. Res.* (in press).
4. 闞凱, 金子達雄, 高性能・高機能植物分子由来プラスチックの開発, 植物由来ポリマー・複合材料の開発, サイエンス＆テクノロジー **2011**, 第 1 章・第 5 節, 36-47.

Other Publications

1. Q. T. Nguyen, M. Okajima, T. Mitsumata, K. Kan, H. T. Tran, T. Kaneko, Trivalent metal-mediated gelation of novel supergiant sulfated polysaccharides extracted from Aphanothece stagnina. *Colloid and Polymer Science* **2012**, *290*, 163-172.
2. S. Wang, D. Kaneko, K. Kan, X. Jin, T. Kaneko, Syntheses of hyperbranched LC biopolymers with strong adhesion from phenolic phytomonomers. *Pure Appl. Chem.* **2012,** *84*, 2559-2568.
3. H. D. Hieu, S. Tateyama, S. Wang, K. Kan, K. Yasaki, T. Kaneko, Development of high performance bioplastics from aromatic biomolecules. *Vietnam J. Chem.* **2012**, *50*, 135-141.
4. S. Tateyama, S. Wang, M. Chauzar, K. Yasaki, K. Kan, T. Kaneko, Innovative molecular designs of high-performance but degradable bioplastics. *J. Mater. Life Soc.* **2013**, *25*, 52-55.

International conferences

1. K. Kan, D. Kaneko, T. Kaneko, Polarized Emission of Liquid Crystalline Polyesters Derived from Wholly Aromatic Amino Acids, 7th International Symposium on Advanced Materials in Asia-Pacific, G4-10, Ishikawa, Japan, (September 2010)
2. K. Kan, D. Kaneko, T. Kaneko, Development of Highly Thermostable and Functional Polymers from Naturally-occurring Aromatic Amino Acid, The International Chemical Congress of Pacific Basin Societies, 1149, Hawaii, USA, (December 2010)
3. K. Kan, D. Kaneko, T. Kaneko, Thermotropic bio-based polymers derived from wholly aromatic amino acid and their polarized photoluminescence, IUPAC 7th International Conference on Novel Materials and their Synthesis (NMS-VII) & 21st International Symposium on Fine Chemistry and Functional Polymers (FCFP-XXI), P33, Shanghai, China, (October 2011)
4. K. Kan, S. Tateyama, T. Kaneko, Biomimetic Design of Liquid Crystalline Copolymers from Phenolic Microbial Monomers and its Polarized Emission, Thirteenth International Symposium on Biomimetic Materials Processing (BMMP-13), P-12, Takayama, Japan, (January 2013)
5. K. Kan, S. Tateyama, T. Kaneko, Polarimetry-Induced Anomalous Fluorescence Behavior for LC Bio-based Polyarylates, The 4th International Conference on Biobased Polymers (ICBP2013), POS4-02, Seoul, Korea, (September 2013)
6. K. Kan, S. Tateyama, T. Kaneko, Synthesis of wholly aromatic bio-based liquid crystalline Copolyesters and their polarized emission, International Symposium on Advanced Materials Science 2013, P-13, Ishikawa, Japan (October 2013)

ACKNOWLEDGMENTS

This study was performed at School of Materials Science, Japan Advanced Institute of Science and Technology (JAIST), from 2008 to 2014. This study was financially supported by a Grant-in-Aid for Comprehensive Support Programs for Creation of Regional Innovation Science and Technology Incubation Program in Advanced Regions "Practical Application Research" (Kaneko project) and Grant-in-Aid for Scientific Research (B) (No. 23350112) of MEXT.

I would like to express my deepest and sincere gratitude to Associate Professor Tatsuo Kaneko of JAIST for his continuous guidance, helpful suggestions, and hearty encouragement throughout this work.

Especially, I would like to express my grateful appreciation to Assistant Professor Daisaku Kaneko of Kyushu Institute of Technology, Assistant Professor Seiji Tateyama, and Dr. Akio Miyasato of JAIST for their continuous guidance, helpful suggestions, technical support, and encouragement during this work.

I also would like to express my gratitude and thanks to my minor research supervisor, Prof. Yasuo Ohnishi, Dr. Akio Noguchi, Dr. Ryuhei Nomoto, Department of Biotechnology, Graduate School of Agriculture and Life Sciences, University of Tokyo who gave me the great opportunity to study extraction of bio-based monomer (3-amino-4-hydroxybenzaldehyde: 3,4-AHBAL) from *Streptomyces griseus*. I learn many bio-logical experiments through this laboratory and knowledge. They give me many generous support, continuous encouragement, direct expert guidance and ambitious through 3,4-AHBAL breakthrough.

I specially thank my sub-supervisor Prof. Shinya Ohki in JAIST for his kind support about my experience of NMR knowledge through my research assistant in JAIST and guiding my minor research thesis.

I would like to express my appreciation to my referees, Prof. Noriyoshi Matsumi, Prof. Minoru Terano, Masayuki Yamaguchi of JAIST, Assoc. Prof. Masatoshi Tokita of Tokyo Institute of Technology for their assistance to complete my thesis.

I specially thank Dr. Maiko Okajima for her kindness, concern about not only my research but also my living and study in JAIST.

I also would like to deeply thank all the members in Kaneko Laboratory who offered kind assistance and mach helpful suggestions.

I especially should pay my gratitude to Dr. Siqian Wang, Dr. Katsuaki Yasaki, Dr. Nguyen Thi Le Quyen, Mr. Masatoshi Nakamura, Mr. Hiroyuki Yamamoto, Mr. Shogo Kinugawa, Ms. Sharma Rupali, Mr. Asif Mohammad Ali, Mr. Amit Kumar, Mr. Hieu Duc Nguyen, Mr. Xin Jin, Ms. Phruetchika Suvannasara for giving me much support cooperative daily researches, and Dr. Yuriko Kakihana, Dr. Ervithasuporn Vuthichai, Dr. Xin Wang in Kawakami laboratory, Dr. Panitha Phulkerd in Yamaguchi laboratory for helping my researches and knowledge.

Finally I would like to express my gratitude to my parents, Liying Kan, and Zhaoyun Bian, my brother, Shin Kan, my grandparents, Xuetian Kan, Xiaoran Lu, and my aunt Fengling Kan for their continuous support ,encouragement, giving me hope and ambitious through my life.

March 2014

JAIST

Kai Kan